Identification, classification and quantification of the developing postanal cortex of Monodelphis domestica using an isotropic fractionator method

Baričević, Zrinko

UNIVERSITY OF RIJEKA
DEPARTMENT OF BIOTECHNOLOGY

Zrinko Baričević

Identification, classification and quantification of the developing postanal cortex of *Monodelphis domestica* using an isotropic fractionator method

Doctoral Thesis

Mentor: Assoc. Prof. Jelena Ban

Co-mentor: Prof. Miranda Mladinić Pejatović

Rijeka, 2023

SVEUČILIŠTE U RIJECI

ODJEL ZA BIOTEHNOLOGIJU

Zrinko Baričević

Identifikacija, klasifikacija i kvantifikacija razvojnih stadija postnatalnog korteksa *Monodelphis domestica* pomoću metode izotropne frakcionacije

Doktorski rad

Mentorica: izv. prof. dr. sc. Jelena Ban

Komentorica: prof. dr. sc. Miranda Mladinić Pejatović

Rijeka, 2023.

Mentor: Associate Professor Jelena Ban, PhD

Doctoral thesis was defended on _____, at the University of Rijeka, Department of Biotechnology, in front of the Evaluation Committee:

1. Associate Professor Nicholas J. Bradshaw, PhD
2. Associate Professor Rozi Andretić Waldowski, PhD
3. Associate Professor Silva Katušić Hećimović, PhD

Acknowledgments

I learned a lot in the time it took me to construct, investigate and write this thesis. From my mentor and co-mentor, I learned the benefits and costs of an academic position, respectively. From my mother, I constantly re-learned that perseverance and patience always triumph over any obstacle, no matter how big it seems at first. From my father, I learned that it is more than alright to not know everything, but a shame not to learn it. From my aunt and uncle, I learned that kindness towards someone makes them your family.

Lastly, from my best friend, partner for life and fiancée, I am still learning to put my needs before those of others, at least some of the time.

Thank you all, this work wouldn't have been possible without each and every one of you, and many others!

Funding

This experimental work has been conducted on equipment financed by the European Regional Development Fund (ERDF) within the project ‘‘Research Infrastructure for Campus-based Laboratories at the University of Rijeka’’ (RC.2.2.06-0001), the Croatian Science Foundation (Hrvatska Zaklada za Znanost; CSF) grant IP-2016-06-7060, the financial support from the University of Rijeka (Uniri-prirod-18-290 (2019-2023), “Identification and quantification of neural stem cells with the new method of optimized homogenization”).

Abstract

One of the less understood branches of modern neurobiology is the (in)ability of adult mammals to regenerate their central nervous system (CNS) after injury. This is possible in species such as octopuses and lizards but is lacking in mammals as it becomes lost during development. *Monodelphis domestica,* the grey South American short-tailed opossum is one of the few mammals that can fully and functionally regenerate their CNS after injury in the first two postnatal weeks, whereas most other species from the mammalian class lose their regenerative capacity soon after birth. Opossum are born very immature and continue to develop latched to the mother's belly, which therefore makes them excellent candidates for neuroregenerative and neurodegenerative research.

Corticogenesis of the opossum brain is mostly postnatal, but in contrast to rodents has not been sufficiently explored. To better understand the process of corticogenesis and transition of heterogenous neural stem cells (NSC) into neurons, a specific method is required for precise quantification of their number and characterization of their expression profile.

For this purpose, the isotropic fractionator (IFR) method has been modified and optimized for work with opossum tissues and under inverted fluorescent microscope, and used to identify, quantify, and classify cortical cell lines of the developing opossum brain. Data gained on fixed and homogenized cortical tissue samples has been compared with the recently established primary dissociated opossum cortical cell cultures, which also exhibit regenerative potential during different developing periods *in vitro*. Additionally, the robustness and precision of the IFR has been validated for opossum tissue by comparing the results with immunohistochemically labelled cortical tissue slices and primary dissociated opossum cortical cell cultures.

Three timepoints of interest have been chosen for research of postnatal development of the opossum cortex. The timepoints have been previously examined on the opossum spinal cord, which gave us the cerebral timepoints in conjunction with the knowledge that the maturation process of developing spinal cords starts in cervical and ends in lumbar regions. The timepoints chosen are: postnatal day 5-6 (P5-6), where the regeneration is still possible; P17-

18, where the regenerative properties cease, but the brain is still not fully developed; and P30, where all the cortical structures are present, with a variety of cell lines.

We successfully developed IFR for opossum tissues at various postnatal ages and for the inverted microscope, both as a one-day and two-day protocol variants. Additionally, we showed that many of the existing antibodies can be efficiently used on opossum due to the high protein homology between opossum and the immunogen/referent animal for which the antibodies were developed.

Keywords: *Monodelphis domestica*, immunocytochemistry, cortex, development, regeneration, fluorescence microscopy, isotropic fractionator method

Sažetak

Jedna od najslabije istraženih grana moderne neurobiologije je (ne)mogućnost odraslih sisavaca da regeneriraju središnji živčani sustav (SŽS) nakon ozljede. Regeneracija je moguća u nižih vrsta kao što su hobotnice i gušteri, ali je rijetka u sisavaca, te se gubi tokom razvoja. *Monodelphis domestica*, sivi južnoamerički kratkorepi oposum je jedan od rijetkih sisavaca koji postnatalno mogu potpuno regenerirati SŽS nakon ozljede, zadržavajući svu njegovu funkcionalnost. Takva regeneracija se može dogoditi unutar prva dva postnatalna tjedna, dok većina ostalih sisavaca gubi mogućnost regeneracija odmah nakon poroda. Oposumi se rađaju jako nerazvijeni i nastavljaju rast i razvoj pričvršćeni majci na trbuhu. Zbog tih osobina su izvrsni kandidati za istraživanja neuroregeneracie i neurodegeneracije.

Kortikogeneza mozga oposuma odvija se većinom postnatalno, ali za razliku od glodavaca nije dostatno istražena. Kako bi se bolje razumio proces kortikogeneze i tranzicija heterogenih neuralnih matičnih stanica u neurone, potrebna je metoda s kojom se može dobiti precizna kvantifikacija njihovog broja i karakterizacija njihove ekspresije proteina.

Metoda izotropne frakcionacije (IFR) je u tu svrhu modificirana, te je optimizirana za rad s tkivima oposuma pod invertnim fluorescentnim mikroskopom. Koristi se za identifikaciju, kvantifikaciju i klasifikaciju staničnih linija u korteksu oposuma u razvoju. Podatci dobiveni na fiksiranim i homogeniziranim uzorcima tkiva korteksa su uspoređeni sa primarnim disociranim staničnim kulturama korteksa oposuma, nedavno uspostavljenima u našem laboratoriju. One također pokazuju regenerativne sposobnosti u različitim *in vitro* razvojnim periodima. Robustnost i preciznost IFR metode je također validirana usporedbom rezultata sa imunohistokemijskim prerezima tkiva korteksa i primarnim disociranim staničnim kulturama korteksa oposuma.

Izabrali smo tri razvojna trenutka za istraživanje postnatalnog razvoja korteksa oposuma. Ti razvojni trenutci su detektirani u istraživanjima leđne moždine oposuma *in vivo* i *in vitro*, s posebnim naglaskon na to da maturacija SŽS počinje u cervikalnoj, a završava u lumbarnoj regiji. Odabrani razvojni trenutci su postnatalni dan 5-6 (P5-6), kada je regeneracija SŽS još uvijek moguća; P17-18, kada regenerativne sposobnosti prestaju, ali mozak oposuma i dalje nije razvijen do kraja; te P30, kada je prisutna definirana kortikalna struktura.

Uspješno smo razvili metodu IFR za tkiva oposuma različitih starosti za invertni mikroskop, kao protokol za jedan i dva dana. Dodatno smo pokazali kako se mnoga postojeća antitijela mogu koristiti na oposumima zbog visoke homologije između proteina u oposuma i imunogene/referentne životinje za koju su antitijela napravljena.

Ključne riječi: *Monodelphis domestica*, imunohistokemija, korteks, razvoj, regeneracija, fluorescentna mikroskopija, metoda izotropne frakcionacije

Table of Content

1. Introduction

1.1. Mammalian corticogenesis

The mammalian cerebral cortex is by far the most complex structure throughout the entirety of eukaryotic species. It processes information of all sensory inputs and, combining them with previously acquired and stored information, gives rise to motor functions and behavioural patterns, including the most complex ones – imagination, art and thinking. Notably, *Homo sapiens* have the largest brain-to-body weight ratio of all mammals, where differences in brain size vary largely due to variations in the cerebral cortex [1–3].

The cerebral cortex develops into six layers regionally organized in functionally specialized areas, housing varied classes of neurons and non-neuronal cells. After the closure of the neural tube during embryonic development (embryonic day (E) 12 in rats), the three primary vesicles (forebrain, midbrain, and hindbrain) divide into secondary vesicles, with telencephalon giving rise to the cerebral cortex. In its first emergence around E14 it is comprised of proliferative neuroepithelial cells, the apical radial glia, lining the ventricular zone (VZ) (Figure 1)[4]. The VZ is a homogenous layer of radially oriented cells, bridging the ventricular lumen and the pial surface. The second structure appearing is the preplate (PP), emerging from, and forming above the VZ shortly after, followed by the subventricular zone (SVZ) forming between the two around E15. The SVZ, together with the VZ are at this point considered the neural nursery for all other layers, containing mitotic cells that generate neurons. These migrate radially into the PP around E16, splitting it into a superficial marginal zone (MZ) and the deeper subplate (SP), and forming the cortical plate (CP) between them. The intermediate zone (IZ) forms between the SVZ and the SP shortly afterwards. As the CP expands into progressively more superficial layers (E17-E21), it ultimately forms a cortex with six layers, where the spatial coordinates of the neurons correlate with their temporal onset, in regard to their laminar position. The process depletes the VZ to the point of becoming a single layer of ependymal cells lining the lateral ventricles. The same is true for the SVZ which disappears in all cortical regions except the lateral wall of the lateral ventricles, providing olfactory neurons throughout the whole life[4]. This process is known as adult neurogenesis.

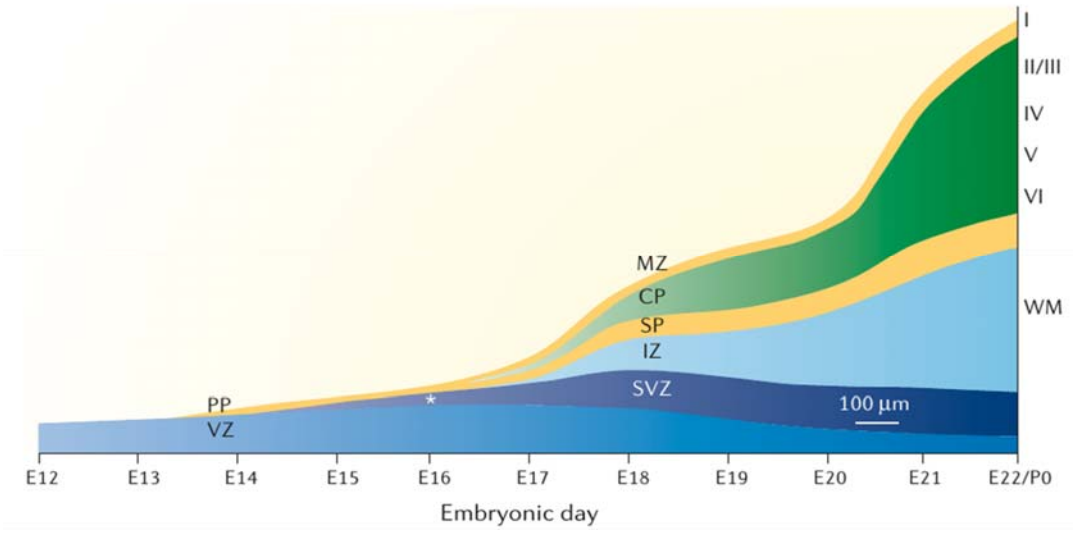

Figure 1: Histogenesis of the cerebral cortex. At embryonic day (E) 12, the only structure present is the VZ. Preplate starts emerging around E13.5, and the SVZ immediately afterwards, around E14.5, between the two layers. After E16, the neural nursery of SVZ and VZ gives rise to CP neurons who split the PP into MZ and SP, forming the CP between them. The structure is shortly after invaded by the elements of IZ. The asterisk represents the point of differentiation between SVZ and IZ. The cortical layers I-VI and white matter (WM) are depicted as the Y-axis, and the X-axis represents the embryonic days, from E12 to E22 or birth. White star indicates the invasion of neurons into the CP. PP – Preplate; VZ – Ventricular zone; MZ – Marginal zone; CP – Cortical plate; SP – Subplate; IZ – Intermediate zone; SVZ – Subventricular zone; I – VI – cortical layers; W/M – White Matter. Source: Krigstein et al., 2006.[4]

Cortical architecture of primates is characterized by the gyrencephalic cortex, the folding of the outermost cortical layers, as the increase in cortical size throughout evolution occurs in surface area rather than its thickness, resulting in a cortical sheet of high surface-to thickness ratio, which buckles and folds due to limited space inside the cranium. Although gyrification is assumed to be an exclusivly primate trait that correlates with increased brain size, it is rather a feature occurring in all major families of mammals, including rodents, who possess a six-layered cortical structure more similar to that of primates than that of many other mammals[2–4].

1.1.1. Cellular characterization and migration throughout corticogenesis

Neuroepithelial cells (NECs) are the first to emerge after the neural tube closure, around E12 in rats. As their cell cycle progression drives them in the direction from apical to basal, they become stratified and expand by symmetrical proliferation. Their later division becomes asymmetrical to generate radial glial cells (RGCs) emerging around E14, which form the VZ in the early embryonal development (Figure 2). This becomes possible due to changes in the gene expression pattern which limits and directs their differentiation potential[5]. The most abundant neurogenic period in rodents extends from E10.5 to E18.5, followed by a period of gliogenesis, which occurs mostly postnatally[1].

To populate the growing brain with neurons, RGCs rely on their asymmetrical division, leaving one daughter cell equivalent to the mother RGC, while the other eventually becomes a series of similar neurons destined for the same cerebral niche derived via symmetrical division of Intermediate progenitor cells (IPs). However, RGCs also produce neurons by immediate asymmetrical division in the later stages of neurogenesis, when the number of neurons is either to be finely tuned or maintained.

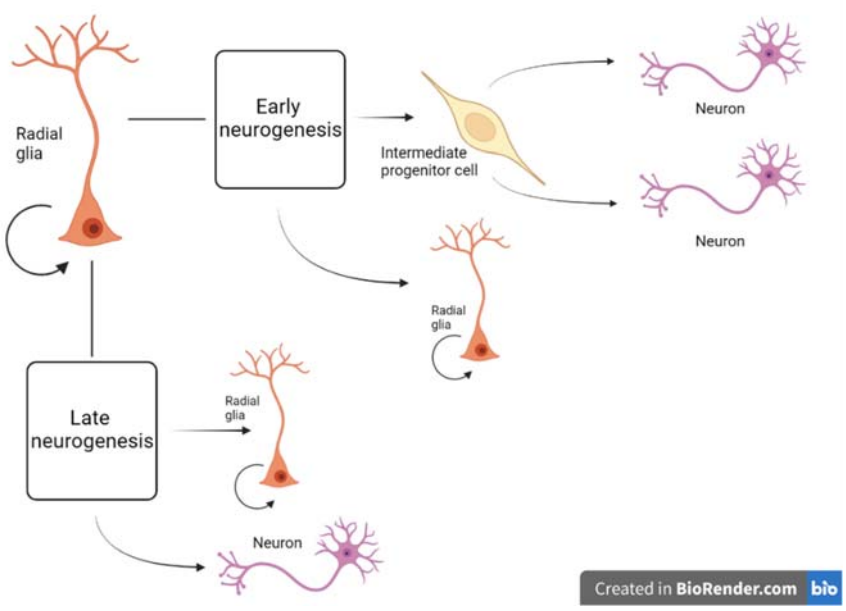

Figure 2: Schematic overview of radial glia division. In early neurogenesis, each RGC divides by asymmetrical division yielding one daughter radial glia and one intermediate progenitor (IP) cell. The IP divides symmetrically populating the early brain with neurons. This indirect expansion of neuronal pool better accommodates the demand for neurons in early neurogenesis. Additionally, late neurogenesis produces neurons via direct asymmetrical division of radial glia, where the daughter cells are one RGC, identical to the mother cell, and one neuron. Created in BioRender.

As the VZ starts forming, IPs generated by asymmetrical division of RGCs, delaminate from their layer of origin and invade the SVZ (around E15, Figure 1). The IPs' symmetrical division is crucial for gyrencephalic species to produce the mass of cortical neurons needed for the eventual gyrification. Migration starts to become a major challenge at this stage, as the correct positioning of neuronal progenitors becomes crucial for further development. Nesting of projection neurons inside the CP splits the growing tissue into MZ and SP. Migrating neuron precursors, the IPs, first rely on short somal translocations to move basally and integrate deeper into the cortex but are soon guided by the RGCs basal processes to traverse the deeper layers and form the granule cell layer (from around E17, Figure 1; Figure 3, number 2 and 3). IPs divide symmetrically into two identical projection neurons who populate the CP in distinct waves, forming six cortical layers of temporally successive neurons, in an inside-out manner[1]. Additionally, IPs are guided by astrocyte processes in early postnatal neurogenesis for long distance migration in a formed, but still developing brain.

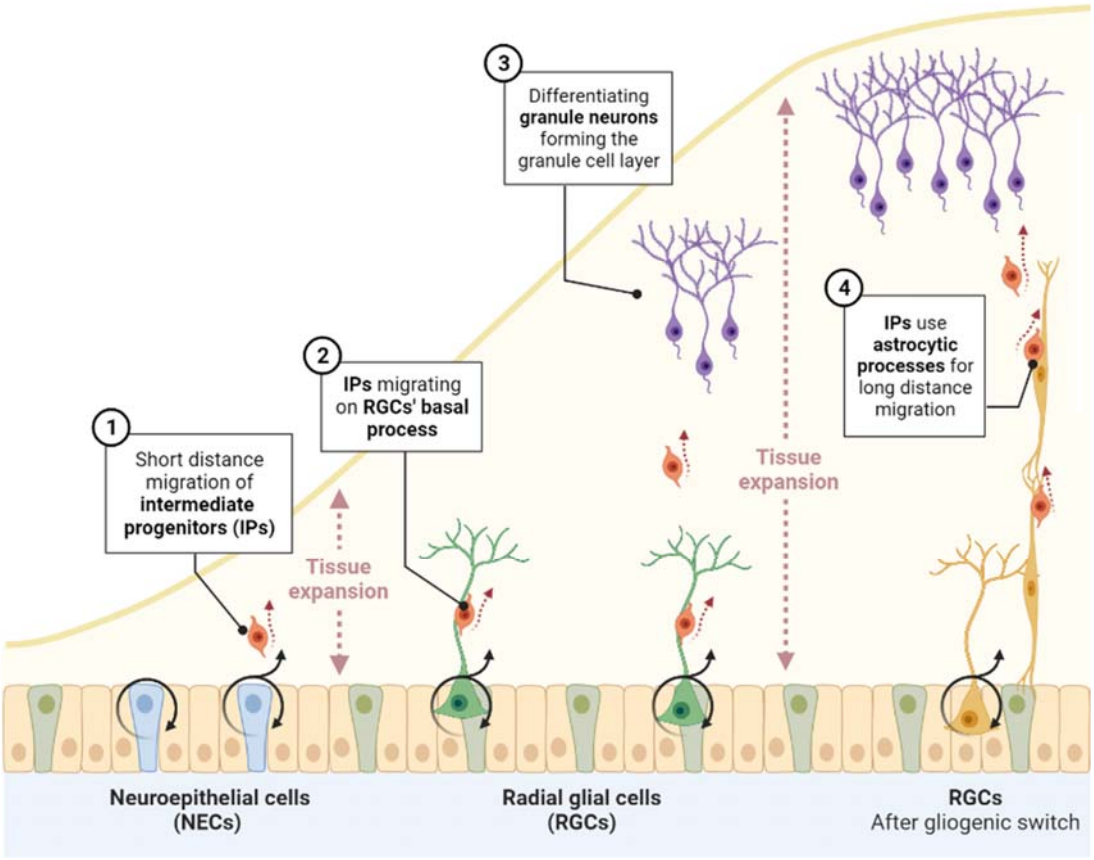

Figure 3: Cell migration in the developing cortex. Asymmetrical division of NECs yields RGCs who migrate short distance by chemotaxis and cellular proximity, forming the VZ. Later division of RGCs nets IPs who need to migrate into the SVZ, achieved with the help of RGCs' basal processes. Later on, they are also aided by astrocyte processes for long distance migration. The neurons emerging from the IPs populate the CP in distinct, inside-out waves, each one indicating a new layer of critical lamina. Created in BioRender by Alessia Caramello.

1.2. Mammalian postnatal development

1.2.1. Neurogenesis

The rat brain has a six-fold increase in its mass from birth to adulthood, owing to the addition of glial cells and increase in neuron size. At birth, more than 90% of cells in the rat brain are neurons[6]. A dormant period between P0 and P3 is followed by a period of rapid neuron number increase up to P7 in most cerebral structures, especially in the cortex. This net gain of nearly 50% of neurons is followed by their rapid loss during the second postnatal week, accounting for 60-70% of neurons lost throughout the whole brain, except the cerebellum and olfactory bulb. This phenomenon is referred to as neural pruning, where the redundant and unnecessary synapses and consequentially neurons are destroyed[6]. Changes in the neuronal number in most other cortical areas express no, or minor changes in the number of neurons between P25 and adulthood. However, the cerebral cortex continues to add new neurons, resulting in a minor increase in the number of neurons in the adult rat brain, compared to P25[6].

1.2.2. Astrocytogenesis and oligocytogenesis

Gliogenesis follows neurogenesis and is almost exclusively a postnatal trait in rats and mice. The ratio of neuronal and non-neuronal (i.e. glial) cells in the rat brain varies drastically between birth and adulthood[6]. The rat brain contains only 6% non-neuronal cells at birth, compared to 50% in adulthood, comparable to the mouse[7]. After the first postnatal week, the number of non-neuronal cells in all cortical structures drastically rises due to the addition of astrocytes and the infiltration of a relatively small number of microglia. It stops abruptly at the end of the third postnatal week and is followed by a period of net loss of about 50% of all non-neuronal cells between P17 and P25. The second period of non-neuronal cell addition continues from P25, marking the addition of oligodendrocytes[6]. The CNS generates several populations (and subpopulations) of cells, all stemming from neuroepithelial cells (Figure 4).

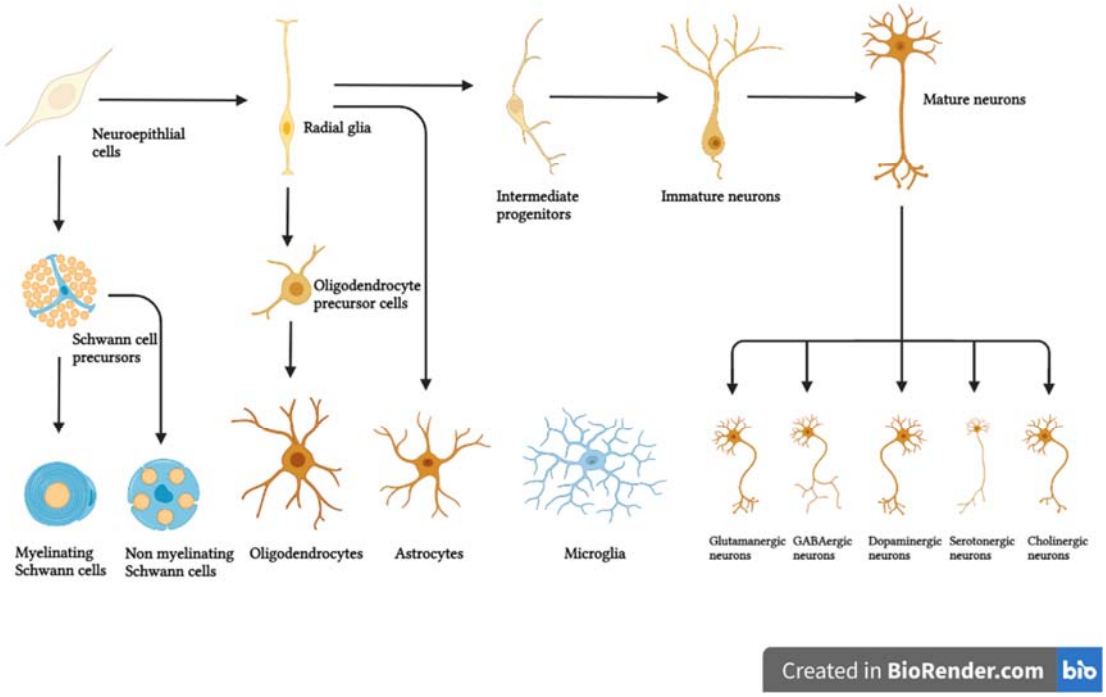

Figure 4: Neural lineages. The neuroepithelial cells give rise to all three distinct populations of neural cells: oligodendrocytes and astrocytes via radial glia, and neurons via morphogenically and chemically increasingly mature, yet distinct neuronal cells. Mature neurons are then separated into glutaminergic, GABAergic, dopaminergic, serotonergic, and cholinergic neurons. Microglia infiltrates neural ranks from the immune system. Created in BioRender, according to Abcam's "Neural lineage markers at a glance" poster[8].

1.3. Marsupials and the *Monodelphis domestica*

Living mammals comprise three major lineages: Prototheria, Eutheria and Metatheria. The Prototheria, which contains only the platypus and the four species of echidna as their living representatives, have diverged from their common ancestor some 230 million years ago (Figure 5). Not far after, some 180 million years ago, the Metatherian and Eutherian branch diverged from their most recent common ancestors[9]. Their relative proximity in the evolutionary tree makes metatherians the most appropriate outgroup for researching the preservation of, and innovation in genetic changes occurring in eutherian mammals post their divergence[9,10].

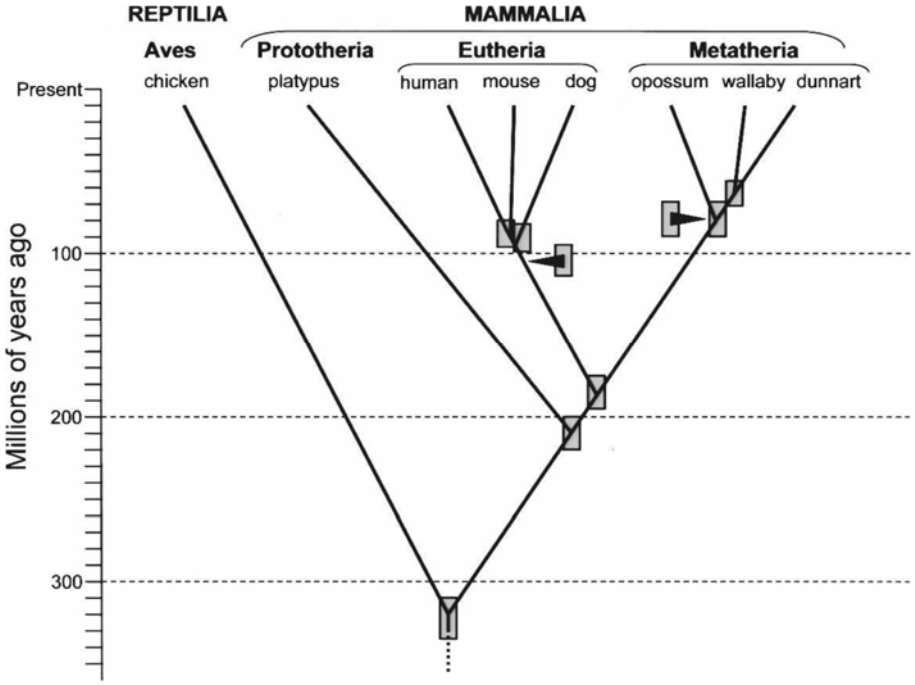

Figure 5: The evolutionary tree of mammalian divergence. The mammalian branch diverged around 330 million years ago, and further split 230 million years ago into the Prototherian branch. 180 million years ago the remainder of the Mammalia split into Eutheria and Metatheria. Shaded boxes indicate the approximate ranges for divergence dates [9].

Marsupials, who belong to the metatherian clade (in contrast to eutherians) distinguish from most other mammals by the immaturity of their young at birth[11]. They diverged from the rest of the mammalian evolutionary tree some 180 million years ago by developing a characteristic pouch allowing for pup maturation after birth, and present their closest outgroup[10]. All marsupials, including *Monodelphis domestica* are born extremely underdeveloped, in an embryonic-like state, and spend their first days inside the pouch (or just attached to their mothers' teats in the case of the pouchless opossums). This provides an unique opportunity for research of CNS regeneration and embryonic development in postnatal animals, without invasive surgeries of gravid females, which is the case in other animal models (mice, rats and others)[12].

The South American grey short-tailed opossum, *Monodelphis domestica* is native to Brazil and adjacent countries. It is a small (up to 120 g) nocturnal animal with large litters containing 6 to 13 pups less than 1 cm in length at birth (Figure 6). The young are born after only 14 days of gestation, equivalent to rat embryo of 12 days (E 12), mouse embryo E11.5 or human embryo of 6 weeks[7,13–15] in terms of developmental stage. The newborns have developed jaws and forelimbs and have an operational gut. However, their hind legs, immune system, and visual and olfactory senses are underdeveloped (Figure 7).

Figure 6: Monodelphis domestica. Adult females (A) are docile and adapt to domestication relatively well. They carry their young attached with forelimbs and jaws to mother's teats (B). Photos: Larry Wadsworth, TAMU Media Resources.

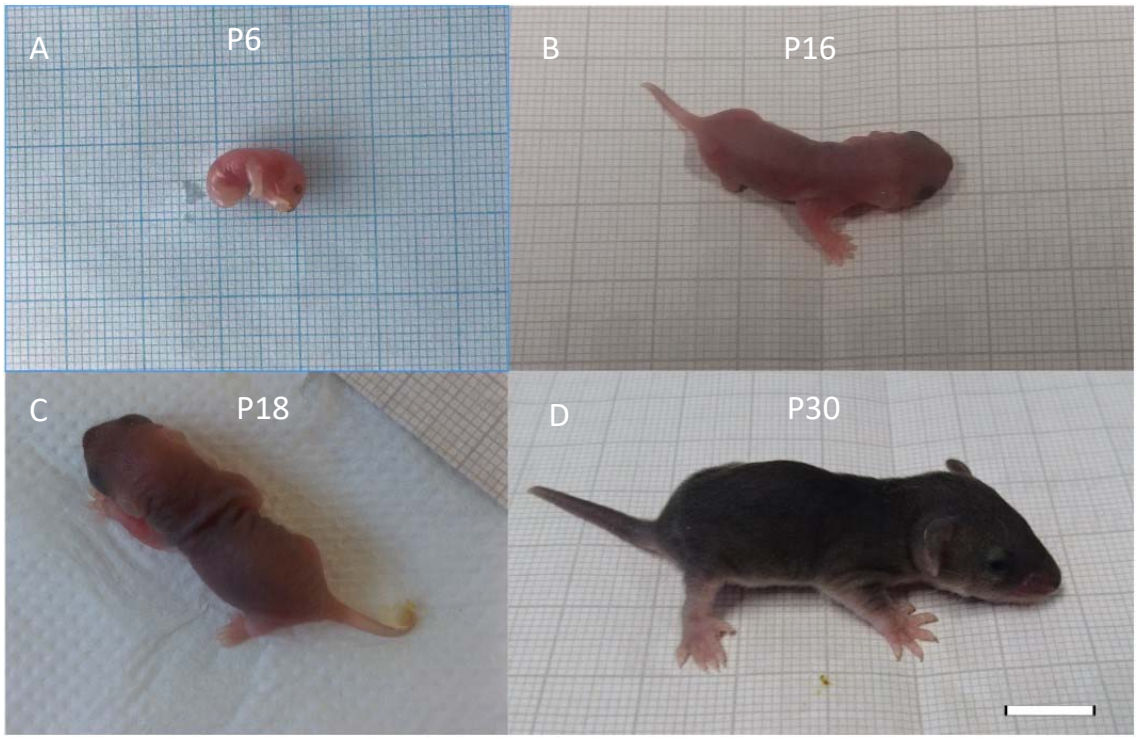

Figure 7: Monodelphis domestica at various postnatal ages: P6 (A), P16 (B), P18 (C) and P30 (D). Newborn pups display a visible lack of development across the body, especially the hind legs. All the limbs are developed at P16, while at P30 a layer of fur covers the young opossum. Scale bar: 1 cm.

1.3.1. Genetic similarities between *Monodelphis domestica* and other mammals

The *M. domestica* genome was sequenced in 2007 by Mikkelsen and coworkers[10]. However, the gene expression in organ development across mammalian species remained largely uncharacterized. Only recently transcriptome analysis allowed extensive comparison of gene expression between species and revealed the developmental analogues of opossum and other mammals such as mice, which showed their exact developmental correlation (Figure 8). It has been shown that a newborn opossum (postnatal day 0, P0) is comparable to the mouse E11.5, whereas P0 in mice correlates to P14 of opossum[7].

The opossum genome contains 18, 000 – 20, 000 protein-coding genes, with the majority having a eutherian homologue. Their autosomes outsize even the largest chromosome

sequenced in any amniote (human chromosome 1) and range from 257 to 748 Mb. In contrast, their X chromosome is only 76 Mb long, which is the shortest among any sequenced eutherian[10]. Their chromosomal organization is well conserved, aligning even between distant American and Australian lineages.

The sequence composition of any amniote experiences a gradual decline in total cytosine-guanine (C+G) content as evolution progresses[16]. However, the C+G content is also positively related with the local recombination rate. Those opposing mutational processes can be explained as the function of a general GC to AT mutation bias in the first process, with methylated cytosines in CpG dinucleotides being very prone to deamination processes, thus mutating into its counterpart. The second process is governed by the AT to GC mismatch repair during recombination. This means that higher recombination rates positively correlate to increase in G+C content, despite the evolutionary progress. With the opossum genome having only 37.7% G+C content (in contrast to the average of 41.3% in humans, dogs and mice), and only 0.9% CpG dinucleotide content (in contrast to the average of 2% in humans, dogs and mice), the model predicts a very low recombination rate for the autosomes, consistent with the data[9,10]. However, the opossum X chromosome has a higher C+G and CpG content (40.9% and 1.4%, respectively), exceeding any other sequenced amniote, pointing to a much higher recombination rate in the X chromosome, despite its small size.

The relatively large size of the opossum genome can be attributed to transposable elements. More than 52% of its genome consists of such elements, in contrast to other amniotes (34-43%). Those elements are mostly non-long terminal repeats and retrotransposons[9, 10].

Despite all the differences above the synteny between human and opossum genome is still 93%. Furthermore, 82% of opossum genes have distinct human orthologues, including T-cell lineage markers such as CD4 and CD8. Most of the remaining genes (14%) have been identified as homologues as well, but without definitive orthologous groups. 3% of opossum genes have no clear homologue, and are either evolutionary pseudogenes or open reading frames, and only eight functional genes in opossum have no homologues in humans, including CPD-photolyase, malate synthase and inosine/uridine hydrolase, all ancient genes still present in the opossum[9,10].

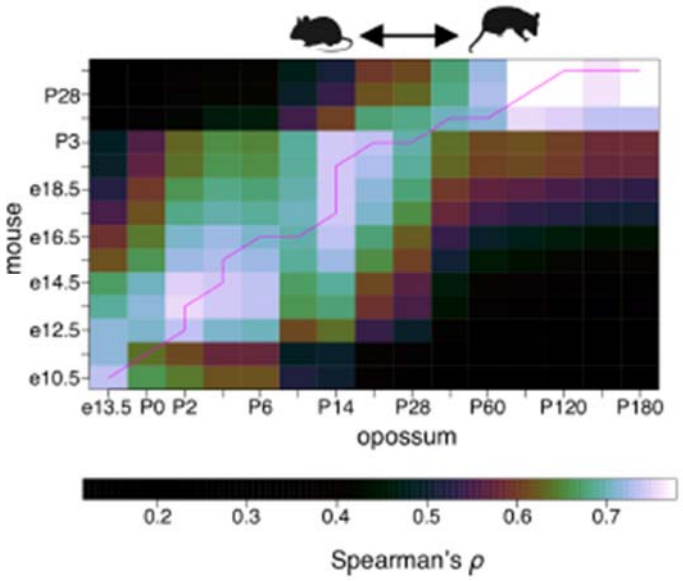

Figure 8: Developmental correspondence between mouse and opossum. Stage transcriptome correlation combining all somatic organs was used to determine the best alignment (pink line) between temporal points (y-axis for mouse, x-axis for opossum. E – embryonic, p - postnatal). Colour indicates the Spearman's probability value (similarity) between the animals' developmental stages[7].

1.3.2. Embryonic development of the *Monodelphis domestica*

The embryonic stages of opossum development are still poorly researched, mainly due to its small size and the overall underdevelopment of the whole organism. The newborn opossum pup is less than 1 cm in length and weighs less than 200 mg[13]. In addition to their embryonic-like appearance, all of their tissues are very soft, which makes their extirpation and handling difficult. As the gestation period is only 14 days long, the majority of the development, in both the organs and the CNS, is accomplished postnatally[12–14,17]. At P0 the opossum has developed forelimbs, jaw, and a functional gut. It can breathe and suckle milk, but little else[13]. However, the neocortex is comprised of only two layers, with most of the cortical architecture missing, with the cerebellum being absent as well. The longitudinal overview of P0 CNS reveals different stages of its development, with overall cell population in cervical regions showing more developed markers than those in the lumbar regions[13].

1.3.3. Postnatal development of the *Monodelphis domestica*

The CNS, together with most other organs in the opossum, develops mostly postnatally. Temporal onset of certain genetical traits can give insight into different stages of organ development across species. Cardoso-Moreira *et al.* offer a comprehensive cross-species genetic analysis, also between mice and opossum. The development of opossum organs happens mostly postnatally, with the main exception being the heart. Other organs, especially ovaries and testis develop much later in opossum postnatal development[7]. Overview of the postnatal development of individual organs is shown in Figure 9. The opossum's postnatal development largely mirrors that of rat and mice, only more prolonged, with several key rat embryonic steps occurring postnatally in the opossum (Figure 10).

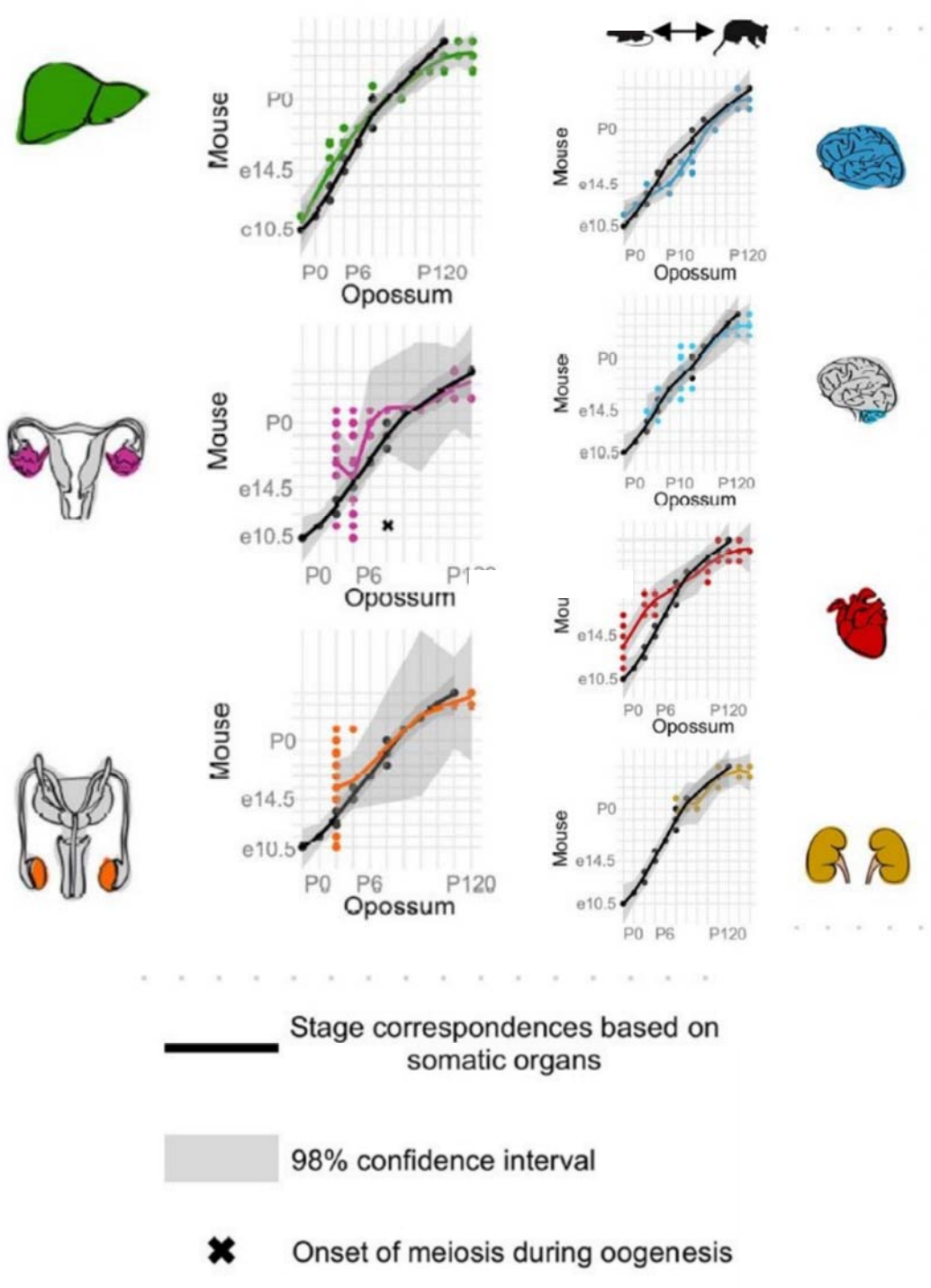

Figure 9: Organ-specific stage correspondence between mice and opossum. Coloured lines indicate the stage correspondence between mice (y-axis) and opossum (x-axis) whereas the black lines represent stage correspondence based on somatic organs. Each coloured dot represents a set of repeated measures for a specific age. Grey area is the 98% confidence interval. X marks the onset of meiosis during oogenesis. Green organ: liver; pink: ovaries; orange: testis; blue: whole brain; partial blue: cerebellum; red: heart; yellow: kidneys[7].

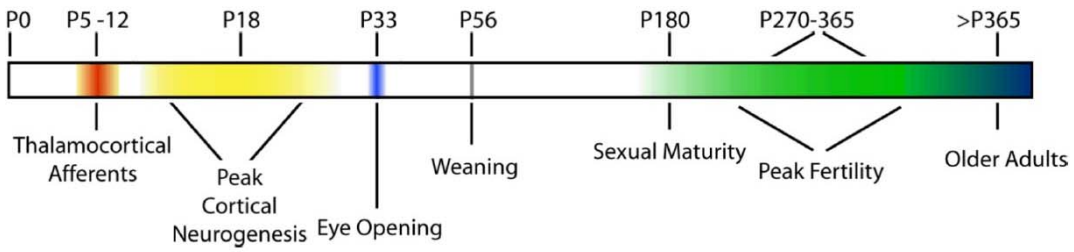

Figure 10: Timeline of opossums' postnatal development, Seelke et al.[17]. P-postnatal day.

1.3.4. Corticogenesis of *Monodelphis domestica*

The corticogenesis of the embryonic opossum is still not fully researched. The development of the hexalaminar cortex is similar to that of the eutherian species, but no research has been done in the embryonic period. This is partly due to the opossum cortex being mostly developed postnatally. At P0, the cortex still has a two-layered "embryonic" architecture, with no indication of a cortical plate, which first appears at P3 as a distinct layer in the telecephalic lateral wall [12,14,18]. In the more ventral regions of the lateral wall, it appears as a single cell layer which grows by P5 into a regular, evenly spread plate. At the same time the subplate appears beneath the cortical plate, and the intermediate zone follows soon after[12]. However, Calretinin$^+$ cells, markers of subplate and Cajal-Retzius cells in mice, are present from P1 in the marginal-lateral part of the cortical telencephalon. By P7, the subplate becomes a distinct layer, housing the most mature neurons. The marginal zone appears around P5 and grows in size, but not in depth, by P9, forming a sheet only several cells thick. The subventricular zone is at this point morphologically indistinguishable from VZ, lacking the characteristic proliferative cells. However, the SVZ still exists as a thin sheet, starting from P9[14,19]. The appearance of proliferative cells in SVZ is visible after P14, and becomes prominent from P24, with ample phosphohistone H3-immunoreactive mitotic cells (H3$^+$). By P20, the SP becomes the widest layer in the telencephalic wall, closely followed by the IZ, all to the detriment of the VZ, which diminishes greatly between P15 and P25. At P20, the MZ remains a layer containing a few cells, unchanged by the perturbance in the inner layers. By P60, the

development of the opossum cortex has the appearance of the adult structure, with all 6 layers present. The histogenesis of the opossum cortex has been summarized in Figure 11.

The development of marsupial hexalaminar cortex is similar to that of other mammals, however, they do not generate basal progenitors. Rather, apical progenitor neurons almost exclusively generate neocortical projection neurons[12].

Peak cortical neurogenesis has been reported around P18, after which it decreases in subcortical structures[17]. The cellular density of the cortex decreases in the period between P35 and P60 but remains constant in the older age groups. Accordingly, the number of neurons in the cortex remains constant from P35 onwards, but the declining percentage of neurons reveals the influx of non-neuronal cells after P18. As in other mammals, gliogenesis closely follows neurogenesis, and while the cortical neurogenesis is at its highest, a steady income of glial cells is emerging in this period. The gliogenic period is highly prolonged in opossum, and extends into adulthood (up to P180)[17]. Oligodendrocytogenesis is the last stage of opossum cortex development and is present from P40 onwards[12]. Accordingly, Seelke *et al*. proposed the onset of cortex convolutions around the postnatal day 5 (P5), peak of cortical neurogenesis at P18, eye opening around P33, and weaning after P56 (Figure 10) [17].

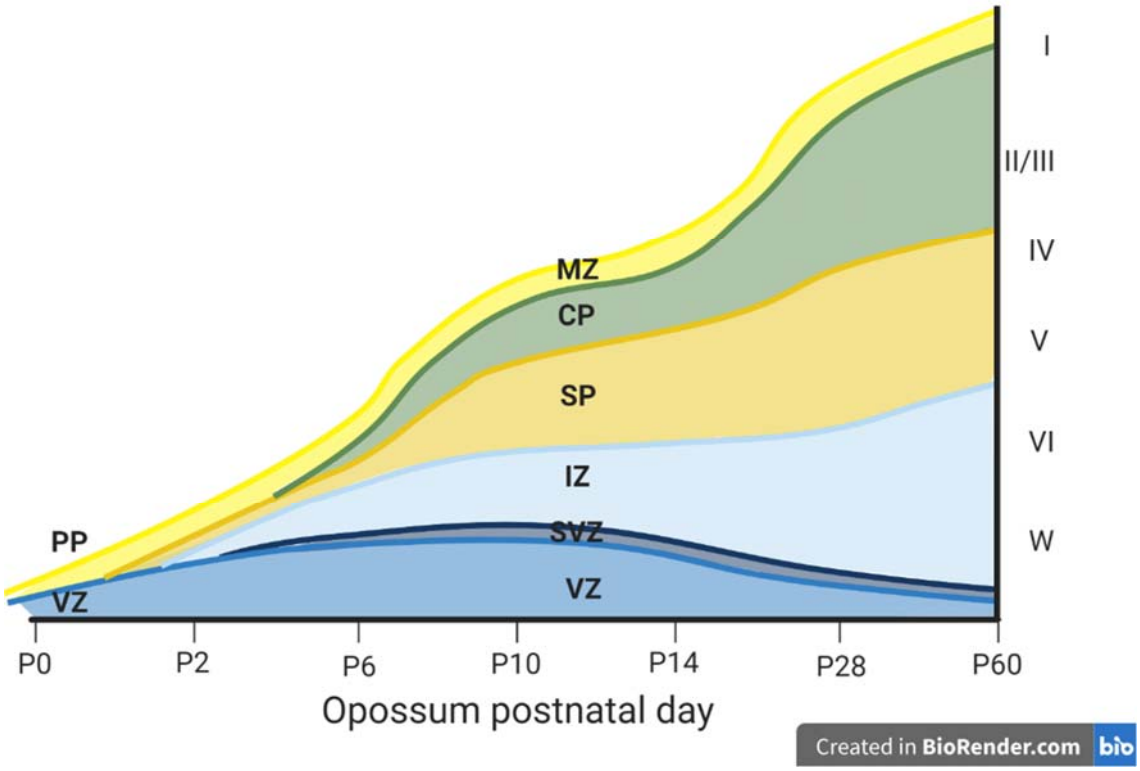

Figure 11: Histogenesis of the opossum cortex. The graph was created in BioRender according to Saunders et al., coupled with data from Cardoso-Moreira et al., and templated after Krigstein et al.[4,7,14] . The scheme provides an approximation of cortical structures' appearance and relative size in opossum. Both the VZ and PP are present at P0, forming a two-layered "embryonic" architecture. CP appears around P3, and MZ and SP around P5, with Calretinin$^+$ cells being present from P0. The SVZ is morphologically indistinguishable from VZ up until P14. By P60 the cortex gains its hexalaminar structure. P - Postnatal day; PP - Preplate; VZ - Ventricular zone; SVZ - Subventricular zone; IZ – Intermediate zone; SP – Subplate; CP – Cortical plate; MZ – Marginal zone; I – VI – cortical layers; W – White matter.

1.3.5. Regenerative capabilities of *Monodelphis domestica*

Regeneration of certain body parts, even the CNS is possible in many invertebrates and lower vertebrates. Higher vertebrates and humans do not possess this trait, or it is very limited. CNS injuries, as well as neurodegenerative diseases pose lifelong complications, whereas injuries of the peripheral nervous system are almost entirely repairable[20,21]. Although the overall understanding of the underlying molecular mechanisms of regeneration in mammals is rapidly expanding, it is still uncertain which traits allow one CNS to regenerate while inhibiting another, and how they can be manipulated to promote regeneration in humans[22].

Opossum have the ability to regenerate the CNS during the first two postnatal weeks after spinal cord injury. It has been chosen as the ideal animal model as it provides several prominent features important in the research of regeneration[23,24]. The most important ones are the closeness to the eutherian lineage, their synteny with the human genome, and their availability due to their short reproductive cycle and their absence of a pouch. As they exhibit *in utero* features up until P14[7], opossum represent a unique opportunity to study CNS regeneration without invasive or lethal surgeries on gravid females, as is the case with mice and rats. This has the added benefit of being in line with the 3R rule of reduction, refinement and replacement[25]. Research has up until now been focused mainly on the regeneration of the spinal cord[20,26–31], while the regeneration of the brain lacks basic data such as the number of cells per developmental stage and their distribution.

1.3.6. Advantages and disadvantages of Monodelphis domestica as a laboratory animal

Opossums belong to the metatherian branch of the evolutionary tree, which makes them the closest outgroup to eutherian mammals, such as mice, rats, and humans (Figure 5). They diverged from the common ancestor some 180 million years ago, and are invaluable for studying genetic differences and drifts, as well as differentiation of species[10]. Moreover, *Monodelphis domestica* lost its pouch at some point after the divergence, a hallmark of the metatherian branch. Together with a very short gestation period, it allows for the availability of the opossum pups as they mature attached to the mothers' teats. The pups undergo embryonic processes *extra utero*, devoid of their protective pouch which shelters the early postnatal development of other metatherian species. The developing pups can simply be harvested without hurting the females, reducing the amount of unnecessary animal deaths, and applying the 3R principle (Reduce, Refine, Replace).

The opossum has also genetical advantages over other laboratory animals: the synteny between human and opossum genes is 93%. Additionally, 82% of opossum genes have a direct human orthologue, and a further 14% have a human homologue, higher than either mice or rats[9,32]. Opossum have also been used to investigate melanoma[33] and spinal cord injury[34,35].

There is an increasing need for diversity in analysis of neurogenesis in mammals, with great benefits to be gained from embracing diverse mammalian species as models[36,37].

There are also several downsides when using opossum as the laboratory animal of choice. They require a higher housing temperature (27-28 °C) than other laboratory animals, as their body temperature is 32 °C instead of 37 °C. They need a significantly higher humidity as well (at last 50-60% of room relative humidity). As the opossums' features mature postnatally and reach sexual maturity only at P180, it is also impossible to determine their sex before P10 without biochemical analysis (Figure 9)[17].

1.4. Expression markers of the CNS

To consistently serve as a suitable marker of a specific cell line, progeny, or population, it needs to be both persistent and consistent in a specified temporal and spatial confines. Failing to maintain these parameters in given confines could lead to erroneous assumptions about the nature and fate of the observed cell populations, diminishing the research's value. To assure their corollary, and understand their limitations, markers of interest are described in detail, in context of the postnatal cortex. An overview of the neural lineage markers is shown in Figure 12.

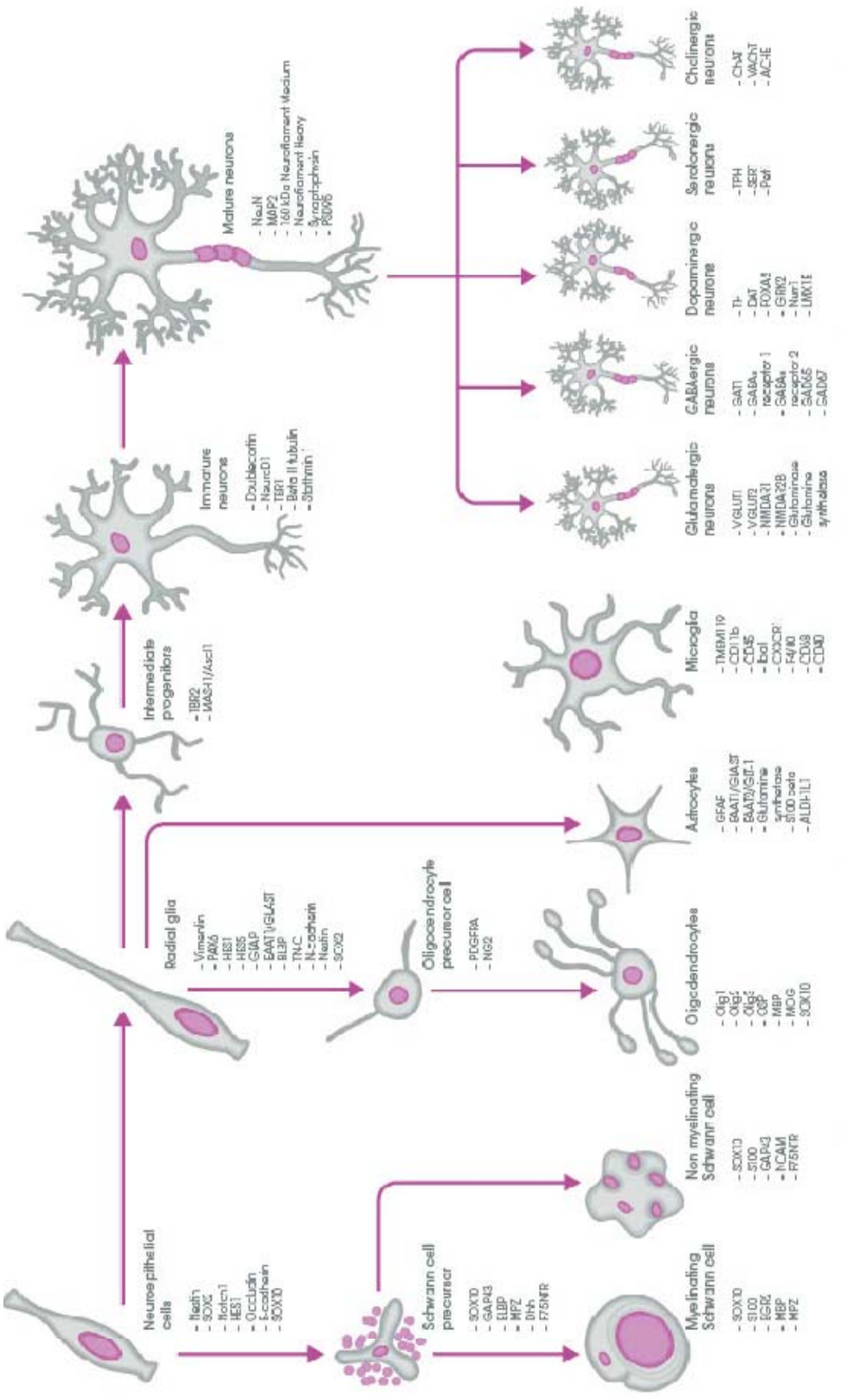

Figure 12: Schematic view of neural lineage markers. Downloaded with permission from https://www.abcam.com/neuroscience/neural-markers-guide

1.4.1. SOX2

SOX2 is a member of the Sex-determining region Y protein (SRY)-related HMG-box genes (SOX) genes, a regulatory gene group responsible for several crucial aspects of development. They are defined by and belong to a super-family of genes with the characteristic High Mobility Group (HMG) -box of the *SRY* gene, a DNA-binding domain present in most eukaryotes. The *SRY* gene (also called the Testis-determining factor) encodes for a transcription factor responsible for the initiation of male sex determination in placental mammals and marsupials, and the homology of *SOX* genes with the HMG box of SRY, together with functional assays, is what divides the *SOX* genes into subgroups. SOX2, together with SOX1 and SOX3 belongs to the SOXB1 subgroup[38–40] .

The well-defined characteristics of a neural progenitor/stem cell include their ability to proliferate, self-renew and give rise to differentiated progeny. Such cells are present during the development of the CNS and persist into the adulthood only in distinct populations[41]. They correlate with the expression of SOXB1 transcription factors who prevent neurogenesis by antagonizing Neurogenin (Ngn) and other proneural proteins. While they collectively maintain progenitor/stem cell state, each one has distinct functions. SOX2 is associated with multipotency of progenitor cells and their ability to proliferate through the upregulation of Notch1 as to be able to generate sufficient number of progenitor cells[42]. Yamanaka and Takahashi first showed the reprogramming potential differentiated somatic cells into an embryonic-like, i.e. pluripotent state by forced expression of several factors, including SOX2[43]. Having strong regulative potential in overall stemness is reflected in its role as a regulator of neuronal stem cell fate.

In humans, abnormal SOX2 function is associated with epilepsy, malformation of the hippocampal region and eye abnormalities. Deletion of SOX2 in mice creates similar effects, with reduction of overall connectivity between the retina and the thalamic dorso-lateral geniculate nucleus and between thalamus and the visual cerebral cortex[44,45]. SOX2 mutant cells express β-tubulin III in abundance, but fail to mature properly, expressing alternative lineage markers. Besides neural fate, SOX2 also plays a role in oligodendrocyte precursor cell maturation, and subsequent myelination in the postnatal brain. SOX2-deficient mice develop ataxia and tremors, together with severe motor function impairment, as a result of

undifferentiated oligodendrocytes. This is partly due to the lack of the usual negative control of miR145 microRNA, which is responsible for inhibition of several pro-differentiation factors[46,47].

The SOX family is defined as one of the most important developmental regulatory groups of transcription factors discovered to date. Their biological functions cover a wide array of regulatory mechanisms, one of them being the induction or suppression of progenitor cell properties, such as differentiation and proliferation by activating or repressing the expression of tissue-specific genes by having each SOX protein being responsible for a specific cell type and unique set of genes[39,44,48,49]. As a result, SOX2 is considered a reliable marker of the neural progenitor/stem cell pool.

1.4.2. SOX9

Another member of the SOX family is SOX9, a transcription factor of the SOXE subgroup, together with SOX8 and SOX10. As all other SOX proteins, it binds to a common consensus motif 5'-(A/T)(A/T)CAA(A/T)G-3'[49,50]. The ability of different SOX proteins to bind to this site in a non-competitive manner relates to the site's flanking sequences, with SOX9 preferring AG in the 5' flank and G or GG in the 3' flank. Furthermore, cooperative binding on adjacent DNA sites can also have a major impact on SOX protein activity, as well as on their binding preferences. SOX9 forms functional dimers with other members of the SOXE family (including itself), preferring tail-to-tail arrangements in neural crest cells[51,52]. SOX9 is co-expressed with SOX5 and SOX6 in developing chondrocytes, and all are required for chondrocyte differentiation in mice, with SOX5 and SOX6 being modulators of SOX9[53]. The same is true in developing oligodendrocytic lineages, where SOX5 and SOX6 are first co-expressed with SOX9 during specification, and later with SOX10, before terminal differentiation. SOX9 is the key regulator of chondrogenesis and sex determination. Moreover, it is present as a modulator of myocard by inhibiting MyoD-induced conversion of cells into myoblasts, preventing precocious differentiation into myotubes[39]. In brain development it suppresses neuronal cell fate, while promoting neural crest properties of astrocytes. SOX9 suppresses the expression

of PAX6, PAX7, Nkx6 and Irx3 neuronal markers and promotes astrocyte differentiation together with SOX10[38]. In oligodendrocyte specification and maturation SOX9 expression precedes the expression of SOX8 and SOX10 and is essential for the neuron-glia fate switch. It is important to emphasize both the overlap in function of the SOX protein family (SOX9-SOX10 during stem cell differentiation), as well as their possible complementary patterns (SOX2/SOX9 coexpression in multipotent lung epithelial cells)[42].

Most importantly for this research, SOX9 has been found to be a persistent and unambiguous marker of astrocytes in the adult mouse brain. The expression of other transcription factors in astrocytes has been found to be inconsistent, and not studied extensively. The only other cell lines SOX9 applies to are ependymal cells and cells in the neurogenic regions (SVZ, subgranular zone of the hippocampal dentate gyrus and the rostral migratory stream of the olfactory bulb), where it also labels neural progenitor cells. However, its expression does not diminish neither by age nor by the function of the cell[54]. Therefore, SOX9 is considered a reliable marker of astrocytes but it is also expressed in the progenitor cell pool in the neonatal brain, as well as in the neurogenic niches of the adult brain.

1.4.3. NeuN

The monoclonal antibody mAb A60, detected by Mullen *et al.* binds to a particular neuron-specific nuclear protein named NeuN[55]. From its discovery in 1992, it has served as the gold standard for labelling the terminally differentiated neuronal nuclei, with some exceptions, namely cerebellar Purkinje cells, mitral cells of the olfactory bulb and retinal photoreceptors. Its appearance correlates with the neuron's withdrawal from the cell cycle and the initiation of its terminal differentiation and its expression level indicative of the cells' physiological status[55,56].

It was later found that NeuN is the *Fox-3* gene product, a member of the RNA-binding protein Fox-1 family, also known as a hexaribonucleotide-binding protein 3 or D11Bwg0517e. It is situated exclusively in the postmitotic neurons, inversely proportional to the chromatin condensation. Its two isoforms of 46 and 48 kDa betray multiple phosphorilations, with the

48-kDa isoform being predominantly found in the cytoplasm, and the 46-kDa in the cell nucleus[57]. Its role has been determined as a splicing regulator after the cell's terminal differentiation. As a result, NeuN is considered a reliable marker of the mature neural cell pool.

1.4.4. Additional markers

Several other important markers have been tested and proven to work on opossum cortical tissue. All the markers listed fulfil the criteria of important, research-worthy targets with a potential to enrich the knowledge of opossum cerebral machinery.

1.4.4.1. BLBP

Brain lipid-binding protein (BLBP), also known as Fatty Acid Binding Protein 7 (FABP7) is involved in uptake and transport of fatty acids, with a consequential role of signal transduction and gene transcription. BLBP-KO mice show aberrant dendritic morphology and decreased spinal density than wild type mice, as well as perturbed synaptic plasticity and connectivity. Those mice were also observed to express behavioural symptoms similar to human neuropsychiatric disorders such as schizophrenia[58]. However, it is also present in the developing brain in radial glia population where it serves as a direct target of the Notch signalling cascade[59]. As a transcription factor it is located downstream of PAX6, with the role of neuroepithelial cell maintenance (neural progenitors and radial glia) during early cortical development of rat cortex[60,61]. More specifically, BLBP is required for radial glia fibre system establishment in the developing brain, which helps neuron migration and cortical layer separation[62]. Once migrated, BLBP also regulates dendritic morphology of situated neurons together with their synaptic activity.

1.4.4.2. PAX2

Paired Box protein 2 (PAX2) is a transcription factor required for the differentiation and maturation of GABAergic and glycinergic neurons in both the mouse and rat CNS. During embryonic development, PAX2 is associated with cortical segmentation, establishment of the human diencephalon and the polarity of the spinal cord[63,64]. It is continuously expressed from a perinatal age into adulthood and helps regulate the inhibitory transmitter effector genes, and so can be used as a marker of GABAergic neurons[65,66]. It is responsible for determining the neural identity of early neurons by steering them towards the GABAergic fate. PAX2 persists even into adulthood in the dorsal horn of the adult mouse, showing its importance in development, but also in the maintenance of the postmitotic neuron subset identity.

1.4.4.3. PAX6

PAX6 is a multifunctional regulating transcription factor highly conserved among vertebrates[67]. It is expressed in specific spatial and temporal patterns in the developing and the adult brain and is thought to be an upstream regulator for genes involved in CNS patterning, neuronal migration and their final placement[68,69]. It is also crucial for the development of the eyes, nose, pancreas, and the pituitary gland, as evidenced by $PAX6^{-/-}$ mice who either lack those organs or have them severely malformed. In CNS development, PAX6 is present from E8 in mice, where it is expressed in the forebrain, hindbrain and spinal cord[70,71]. It is present in the VZ for its whole duration, and the ependymal layer of the lateral ventricle, the ultimate fate of the shrinking VZ, also expresses PAX6. Radial glia and the neuroepithelial cells express PAX6 into their maturation, but not the intermediate progenitors, who originate from mitosis of radial glial cells that have lost their radial processes[68]. In the CNS PAX6 plays a key role in both embryonic and postnatal neurogenesis by recruiting neural progenitor cells for differentiation into mature neurons. It persists even into adulthood in the neurogenic niches, specifically in the subventricular zone of the lateral ventricle and in the dentate gyrus of the hippocampus.

1.4.4.4. NDE1 and NDEL1

Nuclear Distribution Element 1 (NDE1) and Nuclear Distribution Element-like 1 (NDEL1 or NudEL) are proteins that arose from a gene duplication event and are vital in cell mitosis and neurodevelopment. They are structurally similar, but exhibit distinct pathophysiological functions[72]. NDEL1 is a cytoskeletal regulator contributing to microtubule and intermediate filament dynamics as well as microtubule-based transport[73]. It also serves as a docking platform for various proteins, modulating enzymatic activities such as ATPase, GTPase, kinase and similar. Due to its ability to steer and modify cytoskeletal architecture, it plays a role in a variety of cellular processes, from neural migration and neurite outgrowth to mitosis and neurogenesis. NDEL1 is strongly expressed in the brain, starting from embryonic stages where neuronal progenitors start migrating and populating the outer cortical layers in the inside-out manner. In the maturing brain the expression of NDEL1 becomes even more progressively present, as it governs neurite outgrowth and their extension via the dynein-mediated transport of vimentin[73]. It is predominantly located in the cytoplasm of neurons, but is always present in the nucleus as well, and can be used as a marker of cells that have terminally undergone their differentiation towards the neural cell fate, both immature and mature[72].

1.4.4.5. OLIG2

OLIG2 is a basic helix-loop-helix (bHLH) transcription factor expressed exclusively in the CNS. It is first detectable at a very early embryonic date within the radial glia of the neural tube. Those cells ultimately give rise to motor neurons and oligodendrocytes[74]. In the spinal cord, OLIG2 exclusively promotes progenitors expressing platelet-derived growth factor receptor α (PDGFRα). Although it can be found both in a small subset of motor neurons and a specific subset of astrocytes, OLIG2 is the hallmark marker of oligodendrocyte cell lineage[75].

1.4.4.6. Ki67

Ki-67 is widely used as a clinical marker of cancer progression, as it is a marker of cell proliferation. It was discovered by Gerdes *et al*. in Kiel, Germany, as the 67th original clone of the Hodgkin lymphoma in a 96-well plate[76]. It promotes chromosomal mobility during cell

mitosis and after nuclear envelope disassembly by forming a steric and electrically charged barrier of Ki-67 polymeric structures around the chromosomal halves, preventing them from collapsing into a chromatin mass and ensuring their successful interaction with the mitotic spindle[77].

1.5. Isotropic fractionator

The first ever accurate count of neural and non-neural cells populating the human brain was described in 2009. Estimating the cell numbers in the CNS, especially the brain, was historically done via stereological techniques restricted to uniform and discrete structures of the neural architecture and could therefore not have been applied to the whole brain[78–80]. Estimates were obtained from cell densities of such uniform regions, giving rise to vast discrepancies in numbers[81]. Brain size across mammalian species varies by a factor of 100 000, corresponding to characteristics such as neuronal cell numbers, size of their bodies, axonal, and to a lesser extent dendritic furcation, extent of vascularization and extracellular matrix composition. Amalgamation of all neural regions' cell densities into singular value gave rise to speculative neural numbers ranging from 75 billion to 125 billion neurons in the human brain.

The Isotropic fractionator (IFR) method was invented to obtain more precise estimate of total number of both neuronal and non-neuronal cells from any brain or its dissectible region[82]. It relies on a single assumption – that each and every cell in the brain contains one and only one nucleus. The brain, or parts thereof are fixed and processed into an isotropic suspension of isolated nuclei without the surrounding cellular architecture, with defined volume and homogenous distribution. The total number of cell nuclei, and therefore the total number of cells in a brain, following the assumption that each cell has exactly one nucleus, can be expressed as the density of nuclei in any part (aliquot) of the homogenous suspension multiplied by the number of aliquots. To determine the number of a specific cellular subtype such as neuronal cells, the proportion of nuclei stained with its specific nuclear marker (such as NeuN) is multiplied with the total number of cells.

With this method, a much more precise number was proposed for both neural and non-neural cells of the human brain, amounting to 86 billion neurons and 85 billion non-neuronal cells[78,81]. Since then, this method has been validated and accepted multiple times on cerebral tissues of human, orangutan, gorilla, elephant, opossum, mouse, rat and other species[6,80,83,84].

2. Thesis aims and hypotheses

Quantification of cortical cells and its specific subpopulations of neurons and glial cells is a crucial information in the understanding of their function, both individually and systemically. It provides insight into the process of cortex development and maturation. Postnatal development of the opossum cortex has not been properly researched, and the data about the number of neuronal and non-neuronal cells is absent from the literature for the first two postnatal weeks (<P18), whereas the data about the ages P18 and further contains only the total number of cells and the number of neurons[12,17]. Moreover, this data has been obtained by only one research group, showing substantial differences between opossum and other marsupials[32].

The main aim of this research is to broaden the knowledge on opossum as the ideal animal model for the research of neuroregeneration. To do so we intend to classify different cell lines, their distribution and interaction within three developmental stages: in the period when regeneration is possible (P6), in the period when regeneration is already lacking (P18), and in the period when almost all the cell lines are present and developed (P30).

Another aim is to validate commercially available markers for specific cell lines on opossums of different developmental age, to validate IFR as a method suitable for inverted microscope configuration, detect the developmental cortical progression of the opossum, to compare with the other eutherians and to place the opossum more exactly on the evolutionary scale. We want to validate markers for specific age and cell populations of the opossum cortex, such as NeuN, SOX2, SOX9 and other. Once validated, we aim to obtain their relative and absolute numbers in each of the postnatal ages of interest.

The novelty of this research is in exploring SOX2 and SOX9 expression, never before investigated in the opossum, together with IFR method modified for inverted fluorescence microscopes, which has also never before been used on opossum younger than P18.

HYPOTHESES:

I. Commercially available cell markers can be applied to opossum due to their high homology with human and mice. These markers will help us segregate various cell lines of interest, whose distribution should follow mouse or rat model of corresponding age.
II. SOX2 will reliably and exclusively mark neural stem/progenitor cells in all postnatal ages considered.
III. SOX9 will have expression overlap in progenitor cells with SOX2 and will additionally mark differentiated astrocytes in P16-18 and P30 age groups.
IV. IFR can be adapted to work with inverted microscopes.
V. It is possible to discern both relative and absolute numbers of specific cell lines in different developmental stages of the opossum cortex.
VI. The fluctuations of cell lines between different developmental stages are indicative of the opossum's maturation and allow evolutionary studies and comparisons.

3. Materials and Methods

3.1. Materials

3.1.1. Tissue dissection

Dissection solution: 113 mM NaCl, 4.5 mM KCl, 1 mM $MgCl_2 \times 6H_2O$, 25 mM $NaHCO_3$, 1 mM NaH_2PO_4, 2 mM $CaCl_2 \times 2H_2O$, 11 mM glucose, 0.5% w/v penicillin/Streptomycin/Amphotericin B, pH 7.4 (all from Sigma–Aldrich, USA).

Tissue culture plates: Petri dish 35mm (Sarstedt, Germany)

Tissue fixation: 4% paraformaldehyde solution (Millipore, USA)

Dissection instruments: World Precision Instruments shears (Saratosa, USA), LOT: 0311B, Camel Dissection Instruments Junior 3013 shears and tweezers, dissection microscope (Omegon, Germany)

Ethanol (96%, Gram-mol, Croatia)

Inicidin Plus (Ecolab, Germany) diluted 1:100 (1%)

3.1.2. Isotropic Fractionatior

10x phosphate-buffered saline (PBS): 1.37 M NaCl, 27 mM KCl (Sigma Aldrich), 100 mM Na_2HPO_4 (Sigma Aldrich, Germany), 18 mM KH_2PO_4 (Sigma Aldrich), dH_2O, pH 7.4

Sodium Citrate buffer: 10 mM sodium citrate tribasic dihydrate (Sigma Aldrich), PBS, 0.1% (v/v) Tween® 20 (Carl Roth, Germany), pH 6.0

Blocking buffer: 5% (w/v) bovine serum album (BSA; Carl Roth) in PBS.

Tissue homogenizer Tenbroeck tissue grinder, Wheaton, USA; centrifuge Eppendorf Centrifuge 5424 R, Germany; Micro centrifuge Mikro 120, Hettich Zentrifugen, Germany; Dissection microscope Olympus SZX12, cat. No. 1E12964, Japan; Dry Bath Incubator Kisker Biotech GmbH & Co. KG, Germany.

3.1.3. Immunofluorescence

Fixation buffer: 4% paraformaldehyde (PFA; Sigma Aldrich), pH 6.9

Tissue storage solution: 30% (w/v) sucrose (Sigma Aldrich) in 1x PBS with 0.1% Triton X-100 (all from Sigma–Aldrich)

Table 1: List of primary antibodies. The protein sequence similarity between opossum and immunogen was compared using the Universal Protein Resource (UniProt) for each primary antibody used.

Antibody	Host and isotype	Dilution	Immunogen	Cat. No.
Anti - SOX2 [9-9-3]	Mouse monoclonal IgG1	1:625	Synthetic peptide conjugated to KLH, derived from the C-terminus of the human SOX2	Abcam ab79351
Anti-NeuN [EPR12763]	Rabbit monoclonal	1:500	Synthetic peptide within human NeuN aa 1-100 (Cysteine residue)	Abcam ab177487
Anti - SOX9 [EPR14335-78]	Rabbit monoclonal IgG	1:500	Recombinant human SOX9 aa fragment (inner sequence, 150-300)	Abcam ab185966
Anti - Ki67	Rabbit polyclonal IgG	1:100 1:250 1:500	Synthetic peptide conjugated to KLH, derived from human Ki76 (1200-1300)	Abcam ab15580
Anti - Ki67	Mouse monoclonal IgM	1:500	Nuclear preparation of HeLa cells, clone PP-67.	Sigma-Aldrich P6834
Anti - NeuN [EPR12763]	Mouse monoclonal	1:500	Purified cells nuclei from mouse brain, clone A60	Milipore MAB377
Anti – GFAP	Mouse monoclonal IgG1	1:400	GFAP derived from pig spinal cord, clone G-A-5	Sigma-Aldrich G3893
Anti- PAX2	Rabbit monoclonal	1:200	Synthetic peptide within Human PAX2 aa 1-100.	Abcam ab79389
Anti-PAX6	Rabbit polyclonal	1:500	Synthetic peptide corresponding to Mouse PAX6 aa 267-285. Sequence: REEKLRNQRRQASNTPSHI	Abcam ab5790
Anti-BLBP	Rabbit polyclonal	1:500	Synthetic peptide corresponding to Mouse BLBP aa 1-100conjugated to keyhole limpet haemocyanin.	Abcam ab32423
Anti-OLIG2 [EPR2673]	Rabbit monoclonal	1:500	Synthetic peptide within Human OLIG2 aa 250-350. The exact sequence is proprietary.	Abcam ab109186)

Table 2: List of secondary antibodies.

Fluorophore	Host and isotype	Dilution	Company	Cat. No. And RRID
Goat anti-Rabbit IgG (H+L) Highly Cross-Adsorbed Secondary Antibody, Alexa Fluor™ Plus 555	goat anti-mouse	1:400	Thermo Fisher Scientific	Cat# A32732
Goat anti-Mouse IgG (H+L) Highly Cross-Adsorbed Secondary Antibody, Alexa Fluor™ Plus 488	goat anti-mouse	1:400	Thermo Fisher Scientific	Cat# A32723
Goat anti-rabbit Alexa Fluor 555 Goat anti-Rabbit IgG (H+L) Highly Cross-Adsorbed Secondary Antibody, Alexa Fluor™ Plus 555	goat anti-rabbit	1:400	Thermo Fisher Scientific	Cat# A32732
Goat anti-Mouse IgG1 Cross-Adsorbed Secondary Antibody, Alexa Fluor™ 488	goat anti-mouse immunoglobulin (Ig) G1	1:300	Themo Fisher Scientific	Cat# A-21121
Goat anti-Mouse IgG2a Cross-Adsorbed Secondary Antibody, Alexa Fluor™ 555	goat anti-mouse immunoglobulin (Ig) G2a	1:300	Thermo Fisher Scientific	Cat# A-21137

Nuclear staining: 2 µg/mL 2'-(4-Ethoxyphenyl)-5-(4-methyl-1-piperazinyl)-2,5'-bi-1H-benzimidazole trihydrochloride (Hoechst 33342, Merck KGaA, Germany) diluted in PBS.

12- and 15-mm coverslips (Thermo Fischer Scientific, USA) were mounted on a glass slide using the Mounting medium (Vectashield, Vector Laboratories, USA) and sealed with nail polish.

3.1.4. Haemocytometer

Haemocytometer Bright-Line (Hausser Scientific, USA)

Ethanol (96%, Gram-mol, Croatia)

Olympus IX73 inverted fluorescent microscope (Olympus, Japan) equipped with differential interference contrast (DIC, IX3-FDICT) and fluorescence optics. Mirror units: U-FUNA: EX360–370, DM410, EM420–460; U-FBWA: EX460–495, DM505, EM510-550; U-FGW: EX530–550, DM570, EM575IF (Olympus). Objective: 20x dry, LUCPlanFLN long working distance objective (6.60-7.80 mm), numerical aperture 0.45. Fluorescence images were acquired with Olympus XM10 monochrome camera.

3.1.5. Primary Dissociated Neuronal Cultures

Primary dissociated neuronal cultures were acquired from previously established work in our lab[34].

10x Krebs solution, pH 7.5: 113 mM NaCl, 4.5 mM KCl, 1 mM $MgCl_2$ x $6H_2O$, 25 mM $NaHCO_3$, 1 mM NaH_2PO_4, 1 mM $CaCl_2x2H_2O$, 11 mM glucose, 0.5% (v/v) Penicillin / Streptomycin / Amphotericin B Solution (all from Sigma Aldrich), dH2O

Hanks' Balanced Salt Solution (HBSS), pH 7.5: HBSS, 10 mM HEPES (PAN-Biotech, Germany), 3.5 g/L glucose, 0.3 g/L BSA, 1% (v/v) Penicillin-Streptomycin (PAN-Biotech)

Enzyme solutions: 0.5% (v/v) and 2.5% (v/v) Trypsin-EDTA solution in HBSS (Santa Cruz Biotechnology (SCBT), USA), collagenase type I (Sigma Aldrich)

Triturating solution: 10 µg/mL Deoxyribonuclease I from bovine pancreas Type IV (DNAse I; Sigma Aldrich), 1 mg/mL trypsin inhibitor (SCBT, USA), 1% (w/v) BSA, HBSS

BSA cushion: 5% (w/v) BSA in HBSS

Substrates that promote cell adhesion: poly-L-lysine, poly-D-lysine, poly-L-ornithine hydrobromide, Laminin from Engelbreth-Holm-Swarm murine sarcoma (all from Sigma Aldrich)

Plating medium: Dulbecco's minimum essential medium with stable glutamine (DMEM; PAN-Biotech) supplemented with 10% (v/v) of foetal bovine serum (FBS; PAN-Biotech) and 1% (v/v) Penicillin-Streptomycin

Neuronal medium: Neurobasal™ Medium (Thermo Fisher Scientific), B-27™ Supplement (50X), serum free (Thermo Fisher Scientific), 1 mM stable glutamine (PAN-Biotech), 1% (v/v) Penicillin-Streptomycin

3.1.6. Tissue Slices

Tissue slices were prepared using a protocol previously established in our laboratory[35,85].

Freezing medium: Killik O.C.T. Compound embedding medium for cryostat (Bio Optica Milano s.p.a.), UDI: 080339762W01030799Y5 IVD in Classe A, Reg. UE 2017/746

Cryostat: SuperFrost Cryostat, Thermo Fischer Scientific. The slices were collected onto SuperFrost microscopy glasses (Thermo Fischer Scientific).

Slice wash: 0.1% Tween® 20 (Carl Roth, Germany) in 1xPBS (Sigma-Aldrich)

Blocking solution: 3% Normal Goat Serum, (NGS; PAN Biotech, USA), 3% BSA (Carl Roth), 0.3% TritonX-100 i 10xPBS (Sigma Aldrich)

Fixation buffer: 4% paraformaldehyde (PFA; Sigma Aldrich), pH 6.9

Tissue storage solution: 30% (w/v) sucrose (Sigma Aldrich) in 1x PBS with 0.1% Triton X-100 (all from Sigma–Aldrich)

3.2. Methods

3.2.1. Animals

South American grey short-tailed opossum (*Monodelphis domestica*) pups of both sexes, postnatal days 5-6, 16-18 and 30 were obtained from the Department of Biotechnology's *Monodelphis domestica* colony located in the University of Trieste's vivarium, following the guidelines of the Italian Animal Welfare Act. Their use was approved by the Local Veterinary Service, the Ethics Committee board, and the National Ministry of Health (Permit Number: 1FF80.N.9Q3), as per the European Union guidelines for animal care (d.1.116/92;86/609/C.E.). The animals were housed in standard laboratory cages in a temperature- and humidity-controlled environment (27–28 C; 50–60% humidity) with a 12/12 h light/dark cycle and *ad libitum* access to food and water. All efforts had been made to minimize the number of animals used, as well as minimize their suffering, and were adhering to the European Directive 2010/63/EU for animal experiments.

3.2.2. Data analysis

Statistical analysis was performed using online statistical tools (https://www.calculator.net/), as well as GraphPad Prism 8.4 software (GraphPad Software Inc., San Diego, California, USA). Three or more data groups were used for each measurement, and data are represented as mean ± standard error. Data were compared using Student's t-test, based on the assumption that all data are sampled from populations with the same standard deviations. The p value was adjusted for multiple comparisons, and the accepted level of significance was $p < 0.05$. Decimal format used to report p values follows the recommended New England Journal of Medicine style (Table 3).

Table 3: New England Journal of Medicine defined accepted levels of statistical significance.

p value	Wording	Summary
< 0.001	Very significant	***
0.001 – 0.01	Very significant	**
0.01 – 0.05	Significant	*
≥ 0.05	Not significant	Ns

3.2.3. Dissection for IFR

All animals were quickly decapitated, and all efforts were made to minimize their suffering. The dissection instruments were previously sanitized with 70% ethanol and 1% Inicidin Plus. Dissections were performed in Petri dishes containing the dissection solution, under the dissection microscope (Omegon, Germany). Both left and right hemispheres from each animal were used while olfactory bulbs and remaining subcortical structures were discarded. Meninges were removed as well, and the prepared cortical halves fixed by immersion in 4% paraformaldehyde solution (PFA) for at least 24 hours at 4 °C.

3.2.4. The isotropic fractionatior

IFR has been established by Suzane Herculano-Houzel and Roberto Lent in 2005[82]. The method uses paraformaldehyde solution to reinforce the cell nuclei so that they do not get damaged in the process of tissue homogenization, whereas the rest of the cell gets destroyed. The cell suspension acquired after homogenization is equivalent in cell distribution and ratio in every one of its fractions, so that each of them is representative of the whole suspension. The relative cell ratio inside any fraction is equivalent to the relative cell ratio of any other fraction, including the whole homogenate.

3.2.4.1. Fractionation

The original protocol had to be adapted for opossum tissues, given the different brain sizes between postnatal age groups. Cortices were extracted from 4% PFA after at least 24 hours and washed 3 times with 1 mL PBS. The cortices were transferred to a tissue homogenizer together with 1.5 mL of sodium citrate buffer and homogenized for 10 minutes until the smallest visible fragments are dissolved. The suspension was transferred to an empty 2 mL vial (vial 1), the grinder washed 4 times with 1 mL sodium citrate buffer and transferred to two additional 2 mL vials (vials 2 and 3). The vials were centrifuged for 10 minutes at 4000 g and +4 °C, the supernatant discarded and vials 2 and 3 each resuspended with 500 µL sodium citrate buffer. Their content was then transferred to vial 1 to capture all the homogenate. The final volume of the stock solution differed regarding the postnatal age due to the increasing size of the cortices and amounted to 500 µL for opossum P5-6, 1000 µL for P16-18 and 2000 µL for P30. These volumes ensured approximately the same concentration of cells per unit of volume.

3.2.4.2. Primary antibody incubation

Antigen retrieval was performed to ensure optimal antigen exposure for primary antibodies: 150 µL of the stock solution was centrifuged for 10 minutes at 4000 g and +4 °C, the supernatant discarded, and the sediment resuspended with 1000 µL sodium citrate buffer. The homogenate was then incubated for 15 minutes at 60 °C in a dry bath incubator.

The homogenate was centrifuged for 10 minutes at 4000 g and +4 °C, the supernatant removed and 1000 µL of 1% BSA in PBS added for 15 minutes to prevent unspecific binding.

The homogenate was centrifuged again for 10 minutes at 4000 g and +4 °C, the supernatant removed and 200 µL of PBS added. After a short spin-down, primary antibodies were added at their respective working concentrations, and left to incubate overnight at +4 °C.

3.2.4.3. Secondary antibody incubation

The homogenate was centrifuged for 10 minutes at 4000 g and +4 °C, the supernatant removed and 1000 µL of 1% BSA in PBS added for 15 minutes to discourage unspecific binding.

The homogenate was centrifuged again for 10 minutes at 4000 g and +4 °C, the supernatant removed and 200 µL of PBS added. After a short spin-down, secondary antibodies were added in desired concentrations and left to incubate for 1 hour in the dark at room temperature (RT), periodically agitating the homogenate by vortexing for an even spread of antibodies.

The homogenate was centrifuged again for 10 minutes at 4000 g and +4 °C, the supernatant removed and 500 µL of Hoechst solution in PBS added to incubate in the dark at RT for 20 minutes.

3.2.4.4. Immunofluorescence sample preparation

The homogenate was centrifuged for 10 minutes at 4000 g and +4 °C, the supernatant removed and 1000 µL of PBS added as a first wash.

The homogenate was centrifuged for 10 minutes at 4000 g and +4 °C, the supernatant removed and 500 µL of mQ H2O added as a second wash.

The homogenate was centrifuged for the last time for 10 minutes at 4000 g and +4 °C, the supernatant removed, and the pellet resuspended with 8 µL of Mounting medium and transferred to a microscopy glass slide previously cleaned with ethanol. Then it was sealed by covering it with a Φ18mm coverslip glass and lacquered with nail polish to prevent leaks. The whole procedure is summarized in Figure 13.

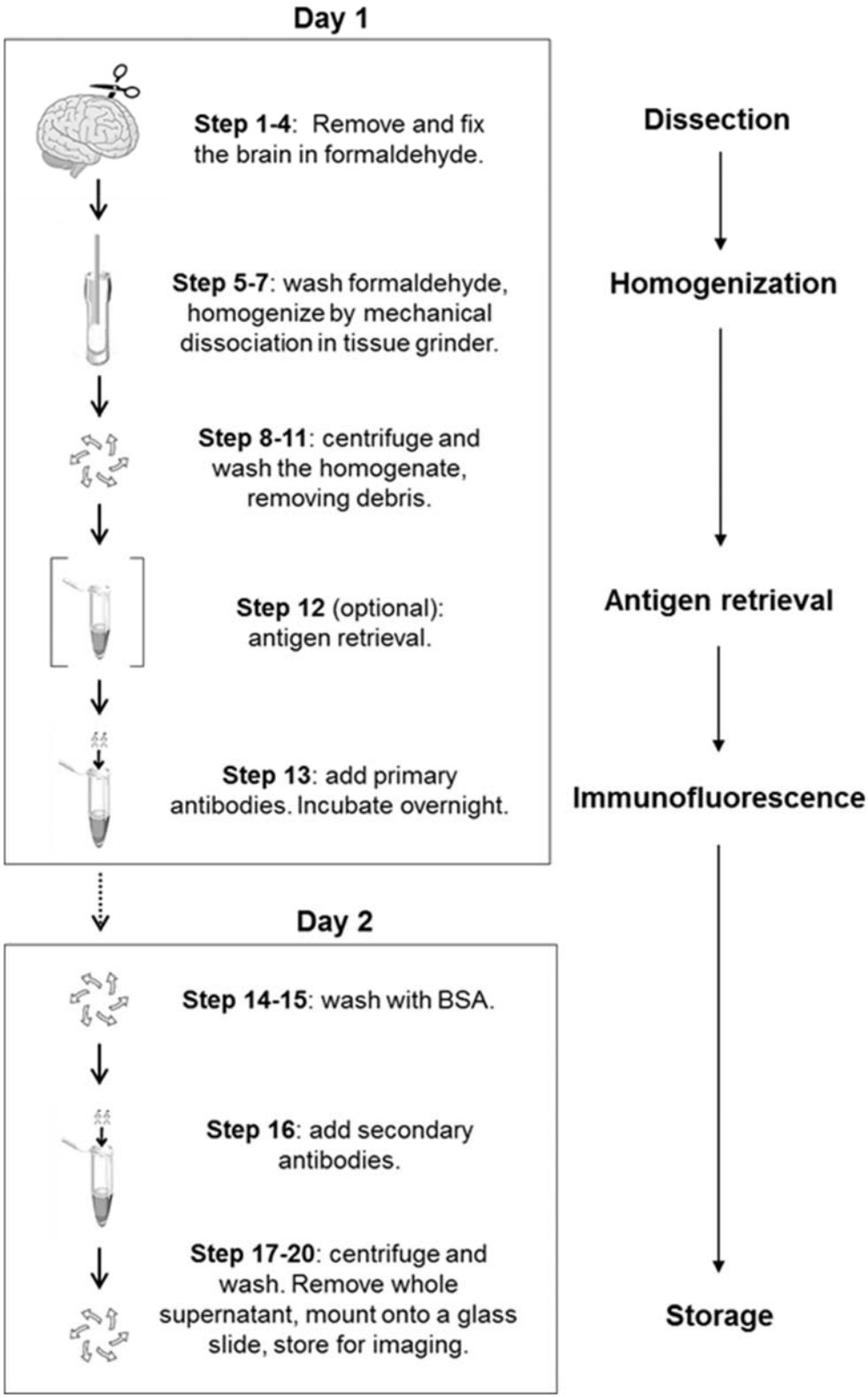

Figure 13: Schematic overview of the IFR protocol. The steps are described above in detail.

3.2.4.5. One-day protocol variation

It is possible to perform the whole IFR in a single day. To do so, all the steps from 3.2.2.2 are followed until the last step, where the primary antibodies are left to incubate at RT for 1 hour.

3.2.5. Immunoflorescence and acquisition of relative cell ratios

The fractionated and stained cell suspensions were analysed under Olympus IX83 inverted fluorescent microscope (Olympus, Tokyo, Japan) equipped with differential interference contrast (DIC, IX3-FDICT) and fluorescence optics (mirror units: U-FUNA: EX360–370, DM410, EM420–460; U-FBW: EX460–495, DM505, EM510IF; U-FGW: EX530–550, DM570, EM575IF (Olympus); and Cy5: EX620/60, DM660, EM700/75, (Chroma, Irvine, CA, USA)). Fluorescence images were acquired with Hamamatsu Orca R2 CCD camera (Hamamatsu Photonics, Hamamatsu, Japan) and CellSens software (Olympus, Japan), using different objectives (10x dry objective: UPLFLN 10x, N.A. 0.3; 20x dry objective: UPLFLN 20x, N.A. 0.50; 60x oil immersion objective: PLAPON 60XO, NA 1.42).

Another microscope used was the Olympus IX73 inverted fluorescent microscope (Olympus, Tokyo, Japan) equipped with differential interference contrast (DIC, IX3-FDICT) and fluorescence optics (mirror units: U-FUNA: EX360-370, DM410, EM420-460; U-FBW: EX460–495, DM505, EM510-550; U-FGW: EX530–550, DM570, EM575IF (Olympus). Fluorescence images were acquired with an Olympus XM-10 CCD camera (Olympus, Tokyo, Japan) and CellSens software (Olympus, Japan), using objectives with different magnifications (20x dry objective with long working distance of 6.60-7.80 mm: LUCPlanFLN 20x, N.A. 0.45 image size: 433.76 x 332.82 µm pixel size: 322.5 nm; 60x oil immersion objective: PlanApoN 60X, NA 1.42, image size 147.92 x 110.94 µm, pixel size: 107.5 nm).

Each sample acquired on the Olympus IX83 microscope was obtained by collecting at least 10 frames, with slice spacing of maximum 2 µm for 10x objective, 1.27 µm for 20x objective, and 0.24 µm for 60x objective. Maximum intensity projection was used for each image.

Image processing and analysis were performed with CellSens software and ImageJ/FIJI by W. Rasband (developed at the U.S. National Institutes of Health).

This method allowed us to calculate the precise ratio of cells in the cortex area for each postnatal day of interest.

3.2.6. Cell counting with haemocytometer (absolute cell count)

The absolute cell count was done with the Neubauer chamber of the Bright-Line haemocytometer (Sigma-Aldrich). The surface of the Neubauer chamber consists of an etched grid of 9 mm^2, further divided into a finer grid. The etched surface is 0.1 mm below the cover glass, giving each square millimetre a precise volume of 0.1 µL, allowing for precise and efficient scale-up of samples. The surface and the cover glass were cleaned with 70% ethanol prior to use. A droplet of immunostained homogenate was placed on the chamber with a cover glass to ensure the uniformity of the volume, and the homogenized nuclei were observed under the Olympus IX73 inverted fluorescent microscope[86]. This microscope was equipped with a long working distance objective (20x, 0.45NA) having a correction ring that can adjust the focus when very thick samples, such as a Neubauer chamber, are used. The long working distance of this objective (6.60 - 7.80 mm) allowed the correct focusing and visualization of cell nuclei stained with Hoechst 33342 on an inverted microscope. Cells in each of the four corner millimetre squares of the Neubauer chamber were counted, excluding the left and upper grid, but including the right and lower grid, to gain an average cell number in 0.1 µL of our cell homogenate. This number was multiplied by the number of fractions to calculate the absolute cell count in the whole homogenate.

The formula for determining the number of cells per cubic millimetre (or a microliter) is:

Number of cells per mm^3= number of cells per mm^2 x dilution x 10

This method allowed us to calculate the precise number of cells in the opossum brain for each postnatal day of interest.

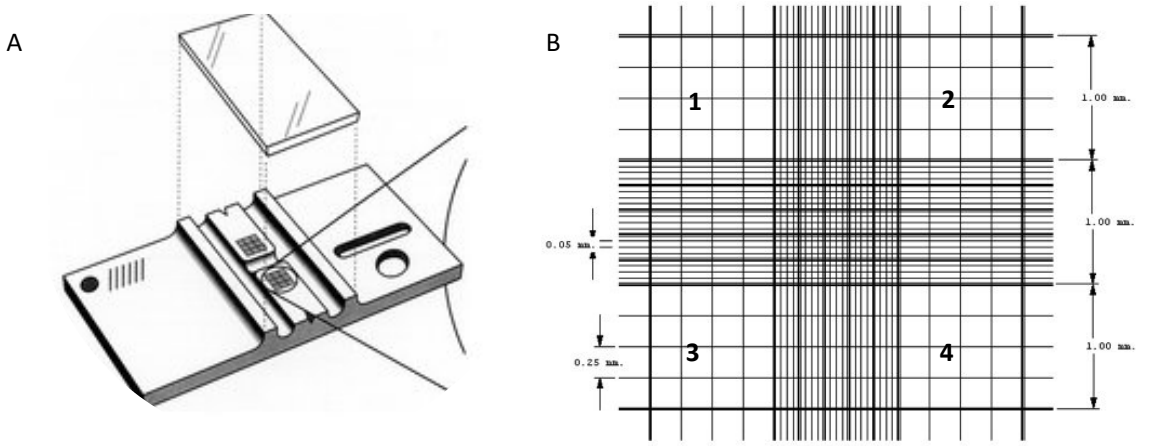

Figure 14: The schematic overview of the haemocytometer. The thick glass slide (A) holds a Neubauer chamber with two identical etched surfaces consisting of 9 square millimetres (B), further divided into a finer grid. The cover glass mounted from above gives each of the square millimetres a precise volume of 0.1 µL. The four corner squares (1, 2,3 and 4) amount to an average number of cells in every 0.1 µL of homogenous suspension. Pictures downloaded with permission from www.hasuserscientific.com.

3.2.7. Primary dissociated neuronal cultures

The dissociation protocol for opossum primary dissociated neuronal cultures was developed by Petrović *et al*., following the previously described procedures for rodents[34,87,88]. All the instrumentation was sterilized using 70% ethanol and 1% Inicidin (Gram-mol, Zagreb, Croatia, and Ecolab, Zagreb, Croatia, respectively). 12 mm coverslips were pretreated overnight at RT with 1M hydrochloric acid (Ru-Ve, Sv. Nedjelja, Croatia), and later washed with distilled water and absolute ethanol for 1 hour at RT, after which they were dry sterilized in the oven at 150 °C for 90 minutes. After placement in 24-well tissue culture plate (Sarstedt, Nümbrecht, Germany) they were coated with 50 µL of 50 µg/mL poly-L-ornithine (Sigma-Aldrich, St. Louis, Missouri, SAD) at 32°C overnight, then with 2 µg/mL laminin (Sigma-Aldrich), after removal of poly-L-ornithine. Isolation of opossum primary neurons was performed in ice-cold oxygenated dissection solution (Krebs solution), with the cortex hemispheres chopped, washed with PBS, and enzymatically digested with prewarmed trypsin in EDTA (0.5%-2.5% w/v trypsin, for 10 minutes. Santa Cruz Biotechnology, SCBT, Dallas, TX, USA). The sample was washed three times with PBS and triturated in a trituration solution by mechanical pipetting through a 1 mL filter tip for at least 30 times. The process was repeated three times before being layered on 5% w/v BSA in HBSS to remove the cell debris. Cells were centrifuged at 1000

rpm for 5 min at RT and resuspended in plating medium. To remove fibroblasts, cells were preplated and incubated at 32°C for 5 minutes on a 35 mm Petri dish (Sarstedt). Cells were counted on a haemocytometer and diluted to a density of 1 x 10^4 cells per well.

The neuronal primary cultures were maintained in an incubator at 32ºC with 5% CO_2 and 95% relative humidity, and their medium was replaced once weekly by exchanging half of the medium with fresh prewarmed neuronal medium.

3.2.8. Cortical tissue slices and immunostaining

Opossum cortices of P5-6, P17-18 and P30 were fixed in 4% PFA for at least 24 hours at 4 °C. They were washed twice in PBS and immersed in 30% sucrose/PBS solution at least 3 hours prior to slicing to prevent crystal formation and tissue deterioration after freezing. The cortices were submerged in Killik freezing medium (Bio Optica Milano s.p.a., Milano, Italy) and flash frozen at -80 °C. Once completely frozen, the cortices were transferred to cryostat at -30 °C and sliced frontally (coronally) to 16 mm thick slices and collected onto SuperFrost microscopy glass (Thermo Fischer Scientific, USA). The glass slips were air dried at RT for 30 minutes and stored at -20 °C or immediately used for fluorescent immunohistochemistry. To do so, the slices were surrounded with hydrophobic pen (Vector Laboratories, Inc, USA) and washed twice for 5 minutes with slice wash solution (0.1% Tween® 20 in 1xPBS – 1xPBS-T) after which antigen retrieval was performed by adding 10 mM sodium citrate and 0.05% Tween® 20 and incubating in a thermo block at +60 °C for 15 minutes. Unspecific blocking was done for 1 hour using Blocking solution.

Primary antibodies were added in the desired concentration and incubated over night at +4 °C in a wet chamber. After each incubation, the glasses were washed 3 times with 1xPBS-T. Secondary antibodies were added and incubated for two hours in a wet chamber at RT. 4’,6-diamidin-2-fenilindol (DAPI) was incubated for 20 minutes in a wet chamber at RT. The glasses were air dried, a coverslip glass was embedded with the help of mounting medium (Vectashield, Vector Laboratories, USA) and sealed with nail polish after which they were dried and transferred to either storage at -20 °C or to the Olympus IX83 microscope for imaging.

4. Results

4.1. Optimization of the IFR method

Optimization of the method was a fundamental part of this thesis since we had several parameters that we had to test for the first time. Firstly, IFR was used already on opossums (*Monodelphis domestica*) by Seelke *et al*.[17,89] but only for neuronal marker NeuN and DAPI (nuclear intercalator equivalent to Hoechst 33342) and only on opossums older than P18. The majority of studies using IFR were performed on adult brains. Secondly, to the best of our knowledge, several markers were not previously used on opossums and/or were not used with the IFR method (e.g., SOX2 and SOX9). Next, the IFR method is designed for use with upright fluorescence microscopes while we had only inverted configuration available. We also had to check for the compatibility between microscope filter and mirror units and fluorophores used in double or triple staining and further upgrade the Olympus IX73 microscope to be properly configured for cell counting with haemocytometers.

4.1.1. Opossum characterization at developing postnatal days

Due to lack of literature data, we investigated physical characteristics of opossum, mainly their size and weight throughout their developing postnatal days. The opossum grows quickly, and their length varies by a factor of 3 from postnatal day 3 to 18, whereas their weight varies by a factor of 7 in the same timeframe. Its mass further increases by a factor of 3.5 between P18 and P30, whereas the change in its size stops being as drastic and increases only by 40% (Table 4, Figure 7).

Table 4: Age, body weight and size of opossums from P3 to P30. At least 3 different pups from 3 different litters were used for each postnatal age.

Age	Body weight (g)	Body size (mm)
P3	0.22 ± 0.01	11.00 ± 0.82
P4	0.19± 0.02	11.50 ± 1.73
P5	0.22 ± 0.02	12.60 ± 0.42
P6	0.25 ± 0.03	13.50 ± 0.71
P16	1.43 ± 0.04	31.20 ± 2.05
P17	1.63 ± 0.05	33.33 ± 1.15
P18	1.71 ± 0.11	33.77 ± 0.94
P30	5.02 ± 0.13	47.75 ± 3.49

4.1.2. Isotropic fractionator method optimization

We developed and optimized the IFR for opossum tissues of different postnatal ages and sizes and introduced modifications to the original protocol which allowed its use on inverted microscope. Several parameters, such as volume, buffers, number of duration and washes, incubation times and others (including microscope configuration and upgrades) were tested for each of the ages of interest, before the optimal conditions were reached.

The following section explains all the tested modifications, while the final protocol is described in the Methods chapter.

Additionally, we tested different conditions and homogenization times due to different stiffness and prevalence of extracellular matrix in different postnatal ages, different fixation durations, centrifuge settings, antigen retrieval, washing steps, specificity of different antibodies, various concentrations of primary antibodies, their incubation period and mounting procedures.

To greatly improve both the accuracy and usefulness of this method, we introduced relative number counting, where different cell lines (e.g., neurons and astrocytes) were labelled with different antibodies. Their relative ratio was obtained by counting a percentage of cells

stained with cell line-specific antibody over a total number of cells in a fraction of the whole suspension (stained with Hoechst 33342). The ratios of various cell populations are identical inside each fraction, including the whole suspension - in other words, the whole cortex, due to the homogeneous nature of the suspension. The combination of both absolute and relative cell counting allowed us to accurately estimate the total number of each analysed cell line in the whole brain. To calculate the total number of a given cell population, its relative cell count (the percentage of those cells) was multiplied by the total number of cells inside the opossum cortex, acquired with the absolute cell count.

4.1.3. Dissection

Several dissection protocol variations have previously been tested in our laboratory to find the optimal ratio between speed and precision, keeping in mind different experiments and their needs. For the establishment of primary dissociated cortical neuron cultures, it was paramount to preserve neurons from dying between opossum sacrifice and cell dissociation and plating[34]. Different dissection media were tested, including Basal Medium Eagle (BME), Dulbecco's Modified Eagle Medium (DMEM) and ice-cold PBS, and the highest survival rate of neurons was achieved with Krebs solution[85]. On the other hand, dissection for cortical tissue slices immunostaining had to be fast and precise as well, without damaging the cortical hemispheres. We decided to keep the same dissection conditions for the IFR method in order to allow the highest neuronal survival possible prior to fixation. Moreover, keeping the same dissection protocol reduces experimental variability between different methods and allows more reliable comparison of the results obtained.

4.1.4. Fixation

The fixation was performed by immersing the dissected brain samples in solution composed of 4% PFA in PBS. For IHC analysis, overnight fixation is followed by further incubation in 30% sucrose in PBS. This treatment was omitted in IFR since it made the tissue too stiff and difficult to homogenize. Perfusion was also not necessary in any of the ages, due to their relatively small brain size (as is usually done with tissue samples thicker than 1 cm).

As previously mentioned, cortex mass and volume vary drastically between the three timepoints of interest, so several different solution volumes were established for different ages and experiment time points, to compensate for the change and to obtain samples with comparable densities of cell nuclei across different postnatal ages.

After the PFA immersion, the samples were kept at +4°C until fractionation, which in some cases was more than a month away, with the longest fixation being 223 days. However, to avoid overfixation, most of the experiments were performed within few days after fixation. Additionally, once undergone fractionation, the suspensions were also kept at +4°C, in some cases for longer than nine months.

Even if some papers suggest no more than 24 hours fixation period for SOX9 antibody[54], we noticed no changes in our case after longer fixations (Appendix 1). However, NeuN antibody worked better with antigen retrieval regardless of fixation duration, while SOX2 and SOX9 were working well independently of antigen retrieval step and fixation time.

4.1.5. Homogenization

Following fixation, the most characteristic part of the IFR method is the tissue processing, i.e., homogenization of fixed brain or its dissected subregions. Due to the small size of opossum brain samples, homogenization is performed through mechanical dissociation using a 15 mL glass Tenbroeck tissue homogenizer. Complete homogenization is achieved by grinding for 10 minutes, or until the smallest visible fragments are dissolved, if 10 minutes is insufficient[82]. When performed on fixed tissue, this procedure lyses the cell membrane but preserves the nuclear envelope intact. In this way, an isotropic suspension of isolated nuclei is created, in which cytoarchitectural heterogeneities have been literally dissolved[82].

In addition to mechanical dissociation, different solutions were used followed by several washing steps. Firstly, the brain tissue was homogenized in sodium citrate buffer which helps to remove and disintegrate cell structures (membrane, cytoskeleton, organelles, and cytoplasm) except for the cell nuclei. The original protocol suggests at least 1 ml of dissociation solution per every 100 mg of tissue sample.

The following volumes of citrate buffer in the initial homogenization step were tested and chosen as optimal in accordance with the increasing number of cells in each postnatal age: 0,5 mL for P5-6 opossum, 1 mL for P17-18 opossum and 2 mL for P30 opossum. Next, the homogenization times were proportionally increased for P18 and P30 opossum brains due their increased size, tissue stiffness and extracellular matrix content. Insufficient homogenization resulted in the presence of tissue aggregates of different size that made the cell staining and counting difficult.

The homogenate was afterwards transferred to a 2 mL tube. The grinding pestle and tube were each washed with 2 mL of sodium citrate buffer, and the washes were also collected in two separate 2 mL tubes for centrifugation (10 min at 4000 g, +4°C), preventing the loss of any nuclei. Once all the nuclei were collected in a pellet, the supernatant was pipetted carefully into a separate tube, incubated with Hoechst 33342, and checked later for the presence of nuclei, while the pellets were combined into a single tube. The absence of nuclear signal in the supernatant confirmed that the centrifugation parameters as well as sample handling were properly set.

All the following washing steps were performed by centrifugation (10 min at 4000 g at +4°C). We introduced 1% BSA in the washing buffer (PBS) for all the washing and incubation steps, which greatly reduced unspecific binding of antibodies.

After 3 washes, the isotropic suspension is ready for antibody incubation. Only a fraction with defined volume was used, keeping in mind the total volume in which the brain was resuspended. This fraction can be stored at +4°C for several weeks or months and can be used for additional/future immunostainings. During the sampling (collecting fractions with defined volume), the suspension was kept homogeneous by agitation on a vortex and pipetting up and down.

4.1.6. Primary antibody binding site comparison

As the opossum is not as widely used as mice and rats nor as widely available as a laboratory animal, no evidence of functional antibodies was present in the literature and no opossum-specific antibodies were developed and commercially available prior to this work, to our

knowledge. Therefore, we compared each immunogen and antibody-binding site (when available) between the opossum and the referent animal to select antibodies with the highest binding potential to the opossum protein homologue (Tables 1 and 5). The alignment was made with UniProt Align function between opossum and immunogen (as indicated in Table 1, most often immunogens were human or mouse proteins. https://www.uniprot.org/align). Given the proprietary nature of most immunogens, the whole protein sequence was aligned.

Table 5: Homology between referent organism and opossum proteins.

Antibody	Host and isotype	Homology
Anti - SOX2 [9-9-3]	Mouse monoclonal IgG1	91.7%
Anti-NeuN [EPR12763]	Rabbit monoclonal	54.64%
Anti - SOX9 [EPR14335-78]	Rabbit monoclonal IgG	83.23%
Anti - Ki67	Rabbit polyclonal IgG	55.97%
Anti - Ki67	Mouse monoclonal IgM	49.63%
Anti – β-Tubulin III (TUJ1)	Mouse monoclonal IgG_{2a}	99.8%
Anti- PAX2	Rabbit monoclonal	94.72%
Anti-PAX6	Rabbit polyclonal	100%
Anti-BLBP	Rabbit polyclonal	89.4%
Anti-OLIG2 [EPR2673]	Rabbit monoclonal	88.2%

As shown, most of the antibodies have a surprisingly high homology with opossums', some even higher than in mice and rats, such as anti-PAX6. Exceptions are NeuN, with 54.64% homology for rabbit, and Ki67, with 55.97% and 49.63% homology for rabbit and mouse,

respectively. However, opossum NeuN has been compared with the human variant as well, and has shown 94.21% homology, solidifying it as a primary candidate as the neural marker in opossum. Its expression patterns and abundance has been cross-referenced with literature, as well as with IHC on opossum cortical tissue slices. It is the only antibody previously used on opossums (older than P18) with IFR[17]. On the other hand, Ki67 had the lowest homology from the tested markers, and anti-Ki-67 antibody has been experimentally shown to bind to its opossum target with a lower specificity. Specific immunofluorescence staining for each of the mentioned markers will be shown separately in the following sections.

For every antibody used in this thesis, we have tested and introduced an antigen retrieval step. Among different temperature and incubation times tested, 15 min at +80°C was shown to work best. Antigen retrieval was necessary for the anti-NeuN antibody while SOX2 and SOX9 antibodies showed no difference.

To further evaluate the specificity of antibodies of interest, several other tests were performed. Additionally, each primary marker has been cross-checked on primary cortical cell cultures and IHC in our laboratory, but also it has been previously published in other papers[17,18,85,89–91]. Each individual staining will be discussed further in detail. In one test, the fluorophore switch had been made for each primary antibody, confirming the specific nuclear stain and the same percentage of cells, regardless of the fluorophore (i.e., secondary antibody conjugated with either Alexa Fluor 488 or Alexa Fluor 555). Next, the experiments where primary antibodies were omitted was done as well, demonstrating the low background fluorescence of secondary antibody or low autofluorescence of cell nuclei. Additionally, each primary antibody was examined alone before being used in double-staining experiments, to determine if its peak emission after the excitation with corresponding wavelengths interferes with other wavelengths. No such interferences were found. These tests are shown in Appendix 2 and Appendix 3, while staining of each individual antibodies are shown in Chapter 4.2.

4.1.7. One-day protocol validation

With cell nuclei stripped of their outer layers and the suspension evenly distributed, we tested and developed a one-day protocol for the IFR. The reasoning behind it was that the much smaller size of the object (the nucleus), and their singular distribution throughout the suspension could be more rapidly recognized by primary and secondary antibodies, meaning exponentially less time is needed for the antibodies to achieve the same intensity and level of binding.

The protocol follows the original two-day protocol, except for the primary antibodies' incubation time, where they are left to incubate at RT for 1 hour. This is enough to produce comparable results with the original two-day protocol in most cases. While anti-SOX2 and anti-SOX9 antibodies were shown to work equally well with incubation time of 1 hour instead of overnight staining, high intensity NeuN staining was more difficult to achieve with this method. Because NeuN was used in combination with SOX2 and SOX9 for many experiments, most of the results in this thesis are the result of overnight incubation of primary antibodies (a two-day protocol), as in the original IFR protocol.

4.2. Validation of primary antibodies

As no prior reference was available to confirm the equivalence in antibody binding and staining pattern between the more common laboratory animal species (mouse and rat) and opossum, each primary antibody was first tested using the IFR method to confirm their specific nuclear localization and staining intensity.

The antibody validation was performed for all three age groups and the representative images are shown below (Figure 15). To the best of our knowledge, while NeuN was used on dozens of different animal species, humans included, SOX2 has never been used as a marker with the IFR method, while SOX9 has been used on the adult mouse brain only[54]. Additional validations of mouse monoclonal NeuN antibody, proliferative marker Ki67, transcription factors PAX2 and PAX6 as well as other tested antibodies not previously used with the IFR method can be found in Appendix 3 and Appendix 4.

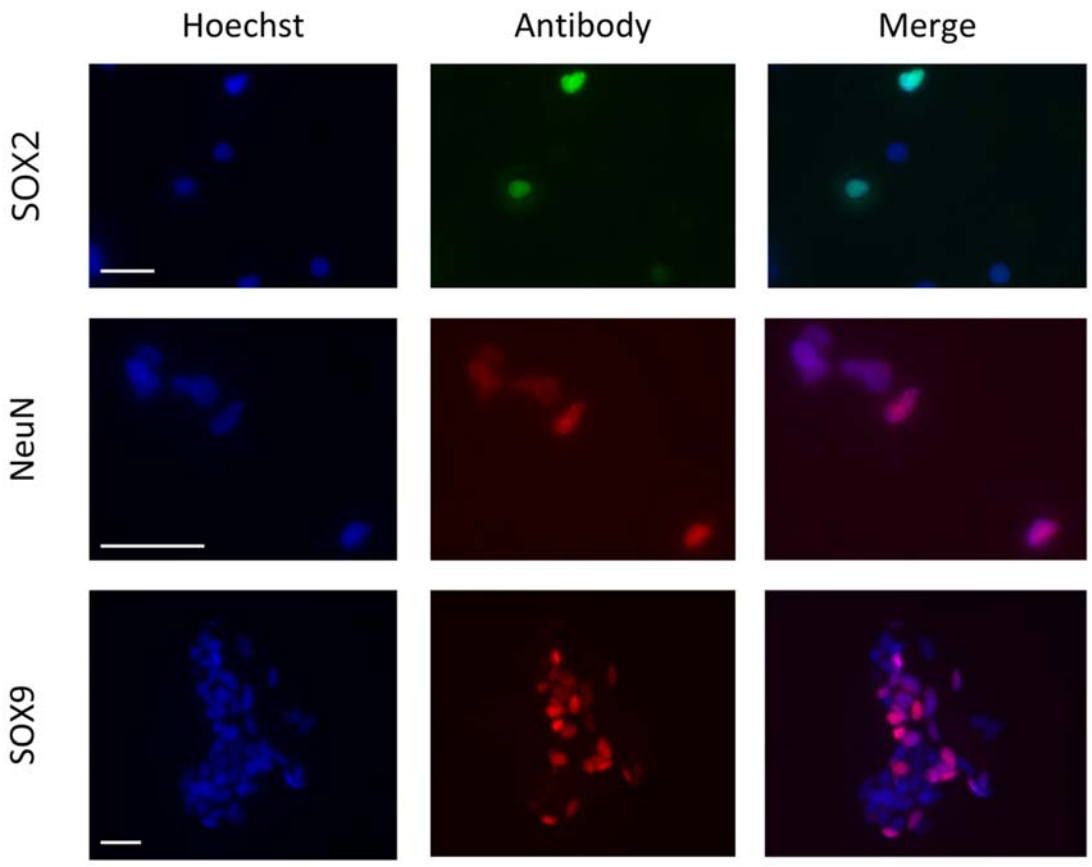

Figure 15: Primary antibody validation. Differently coloured cell nuclei in suspension reflect the true percentage of cell populations in the opossum brain. Left column indicates cells stained with Hoechst 33342, labelling all cell nuclei. Middle column indicates specific antibody staining of the same cell nuclei, from top to bottom: SOX2 (P30), NeuN (P6), SOX9 (P5), as indicated in each of their respective rows. Right column shows the result of a merged overlap of Hoechst 33342 staining and respective antibodies. Scale bars: 25 µm.

Additionally, to exclude that IFR method can interfere with staining, IHC on tissue slices using the same antibodies (and combinations in case of double-staining) were also performed (see Appendix 5).

4.3. Cellular composition in developing postnatal opossum cortex

4.3.1. Cellular composition in P5-6 cortex

We measured the relative and absolute number of cells in P5-6 opossum cortex. We also measured the combination of markers available to see how exclusive they are, and which (if any) cells were simultaneously marked with more than one marker (double-positive). To reduce differences due to the individual variability among opossum pups, at least two opossum litters were used in all measures, as well as at least three different animals from across those litters.

4.3.1.1. Absolute cell count of P5-6 opossum cortex

As previously described, IFR method requires a haemocytometer and an upright fluorescence microscope to count the total number of cells in a fraction and ultimately in the whole brain. Staining of cell nuclei with Hoechst 33342 and NeuN is used to count total cell and neuron numbers, respectively. Low resolution objective (typically 10x) is required, and samples are discarded after use. Since we were not equipped with an upright microscope, we used an inverted microscope equipped with 20x dry objective with long working distance. In this way, we managed to visualize fluorescently labelled cell nuclei with light passing from below through the semi-transparent chamber (haemocytometer). UV excitation for Hoechst 33342 allowed for correct focusing and counting as well as imaging (Figure 16). Due to the narrower field of view of the long working distance 20x objective, each corner square of the Neubauer chamber had to be captured between four separate pictures, amounting to a single corner square of the Neubauer chamber. All four corner squares are counted for each experiment and their number of cells normalized, with at least another experiment confirming the result (Figure 14). A sample counting is shown for each opossum age (Tables 6, 9 and 12). This also allowed us to obtain an additional control experiment – cell counting performed by different

users (Table 6). In the case of our experiments, the difference in the number of counted cells between two users was minimal. Table 6 shows one such example where the difference was 1.97%.

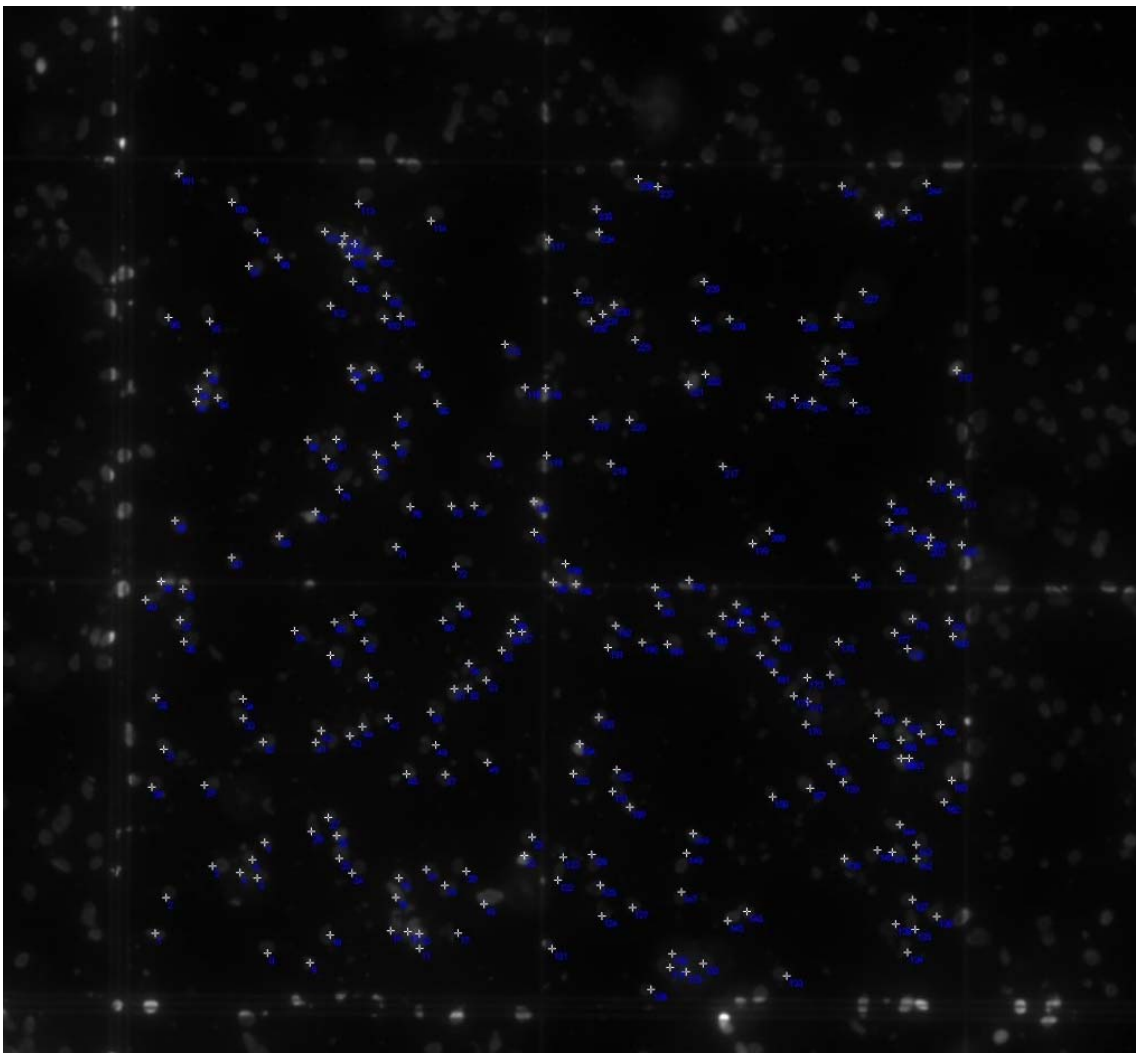

Figure 16: Absolute cell count using a haemocytometer in P5-6 opossum cortex. The field of view of the 20x objective allowed for acquisition of 0.25 mm^2 of the 1 mm^2 corner squares of the Neubauer chamber at a time (for a detailed description of absolute cell count acquisition, see Chapter 3.2.5). Each white plus represents a cell nucleus counted and numbered using the ImageJ Cell counter plugin and stained with Hoechst 33342. The white crosses are numbered in ImageJ and represent every cell counted in the 0.25 mm^2, while the brighter lines are the etched borders of the Neubauer chamber.

Table 6: Example of the difference in absolute cell counting of the same sample between two users. These counts were performed on multiple series of samples.

	Number of cells counted
User 1	1912
User 2	1875
Difference (in percentage)	37 (1.97%)

The drawback of this alternative approach is that the intensity of red nuclear staining with NeuN was too week to capture when the emitted light passes through the thick haemocytometer glass from below, and therefore we were not able to obtain total neuron number using a haemocytometer on an inverted microscope but had to calculate it from the relative percentage of cells stained with NeuN and mounted on a microscopy slide with coverslip.

Two separate fractions/experiments per opossum cortex, obtained from different litters, were made to strengthen the statistical significance of these results. Each experiment counted the number of cells in each of the four corner squares of the Neubauer chamber in the haemocytometer. All the counted squares were averaged. An example of such experiments is shown in Table 7. As per the formula for determining the number of cells in a suspension with a known volume, the average was multiplied by 5000 (for a detailed explanation, see Chapter 3.2.5).

Table 7: Example of the acquisition of the absolute number of cells from IFR experiments counted on a haemocytometer in P5-6 opossum cortex.

	Number of cells per square
Square 1	918
Square 2	1008
Square 3	1002
Square 4	1125
Average	1013.25
Total number (x5000)	5 066 250

According to our measurements performed on a series of independent IFR experiments, a P5-6 opossum cortex has, on average, approximately 5 203 750 ± 313, 786 cells.

This is, to our knowledge, the first counting of total cell number in P5-6 opossum cortex. This result should be validated and eventually confirmed by other laboratories. P5-6 opossums correspond to E16 mouse and E19 rat embryos, according to the transcriptome analysis by Cardoso-Moreira *et al.*, where developmental comparison between the opossum and other laboratory animals (rats and mice) was made[7]. However, no correlation can be drawn with other species due to a lack of data in all the other animals in this developmental period.

4.3.1.2. Relative cell count of P5-6 opossum cortex

The relative cell count was obtained by performing the IFR immunostaining protocol as previously described (see Chapter 4.1.2). The modification of the original protocol includes the final wash of cell suspension in deionized water which removes salts contained in PBS, and mounting of the nuclei sample on conventional microscopy slides using mounting medium and glass coverslip sealed with nail polish. These modifications to the original protocol offered several advantages:

- The addition of mounting medium prevents photobleaching and preserves fluorescence signal for a longer time.

- The samples are mounted on standard glass sample holders and can be stored for long term (weeks or months) and imaged several times on both upright or inverted fluorescence microscopes (including widefield and confocal microscopy).
- The use of oil immersion objectives with higher numerical aperture increases signal to noise ratio and image quality.
- Finally, the use of additional markers, i.e., cell-specific antibodies increase the versatility of this method (counting of different cell types, not just neurons).

The relative cell counting experiments were obtained from four different litters and six different animals from those litters. We first performed staining with single primary antibodies for each individual marker: SOX2 was used for identification of neural stem cells, NeuN for neurons and SOX9 for astrocytes. For each sample, Hoechst 33342 was used to mark cell nuclei to obtain percentage (relative number) of each cell type.

In total, 1387 Hoechst 33342-positive cells were counted within experiments using anti-SOX2 antibody, out of which 64.67% ± 9.9% were SOX2-positive cells. 645 cells were counted within experiments using anti-NeuN antibody, with 74.11% ± 2.93% being NeuN-positive, and 733 cells were counted within experiments using anti-SOX9 antibody, with 42.56% ± 17.56% being SOX9-positive (Table 8).

Table 8: Percentage of positive cells counted from IFR experiments involving respective markers in relation to total cells stained with Hoechst 33342 (n) for opossum P5-6.

Marker	Percentage in relation to Hoechst 33342 staining
SOX2	64.67% ± 9.9% (n=1387)
NeuN	74.11% ± 2.93% (n=645)
SOX9	42.56% ± 17.56% (n=733)

To our knowledge, this is the first quantification of relative ratio of SOX2-, NeuN- and SOX9-positive cells with IFR on P5-6 opossum cortex.

The composition of the P5-6 opossum cortex indicates the existence of a large majority of NeuN-positive cells, despite their embryo-like appearance, which should correspond to postmitotic neurons. This comes as no surprise, if we take into account the work of Cardoso-Moreira *et al*., characterizing several opossum organs as more mature than their age-correlated counterparts in rat and mice[7]. Moreover, even the opossum neonates are capable of clinging to their mothers' fur and suckling milk, indicating a presence of a rudimentary neural network at P1[9,13,14]. Finally, NeuN was already used on neonatal rat brains with the IFR method by Bandeira *et al*. who found more than 90% of the cells in the rat brain are neurons at birth. This work showed that NeuN is not just a marker of mature neurons in the adult brain, but that it can be used to label newborn/immature neurons during early postnatal brain development as well[6,35,85,89,92].

However, a surprising result was a large population of cells (>60%) in the P5-6 opossum cortex still positive for SOX2, which should correspond to neural progenitor/stem cell population (Figure 12)[93–95]. Their presence is also expected as this is a period of neurogenesis which includes both proliferation and differentiation: the cortical plate expands into an evenly spread layer; the subplate and the intermediate zone separate into distinct regions soon afterwards, with the subplate amassing the most mature neurons; and the marginal zone appears shortly before this period and grows in size[12].

A separate population of cells is also SOX9-positive, suggesting an early presence of astrocytes as well as neural progenitor/stem cells which are known to express glial markers, including SOX9[42,54]. This can also be partially explained by the early onset of neural differentiation in opossum due to their requirements for breathing, suckling milk and clinging to fur.

In this extremely dynamic period of cortical growth and development, differences happen in spans of hours. Therefore, it is no surprise that our counts were less consistent than expected, especially for SOX9. High standard errors for all measured cell populations reflect this developmental dynamic as the difference between two opossum only a day apart can be vast. A P5 opossum born at midnight, and another one born at noon might just be 12 hours apart and be labelled as born in the same day, but their cellular composition, together with their cortical architecture can be drastically different.

From the relative and absolute number of cells, we can also calculate the number of neurons (NeuN-positive) and non-neuronal cells (NeuN-negative) in opossum P5-6 cortex. The average opossum cortex of that age therefore has approximately 4.1 million neurons and 1.1 million non-neuronal cells.

4.3.1.3. Double-staining experiments in P5-6 opossum cortex

Since the percentages for single-stained cell type markers were higher than expected if they were exclusive (their sum should have been equal or less than 100%), we repeated the IFR experiments with double-staining to verify the coexpression of those markers. The following combinations were used: SOX2 in combination with NeuN and SOX2 in combination with SOX9. The combination of SOX9 and NeuN was not possible since both primary antibodies were of rabbit origin. Mouse monoclonal NeuN antibody (Table 5) was tested but was not working reliably (Table 1 and Figure 1 of Appendix 4). All experiments used Hoechst 33342 to stain cell nuclei.

Two different litters containing three different animals were used to see the interplay between SOX2 and NeuN. The fluorescently labelled cells mounted on microscope slide with coverslip (as described in Methods) were visualized using an inverted fluorescence microscope, imaged, and used for counting (Figure 17).

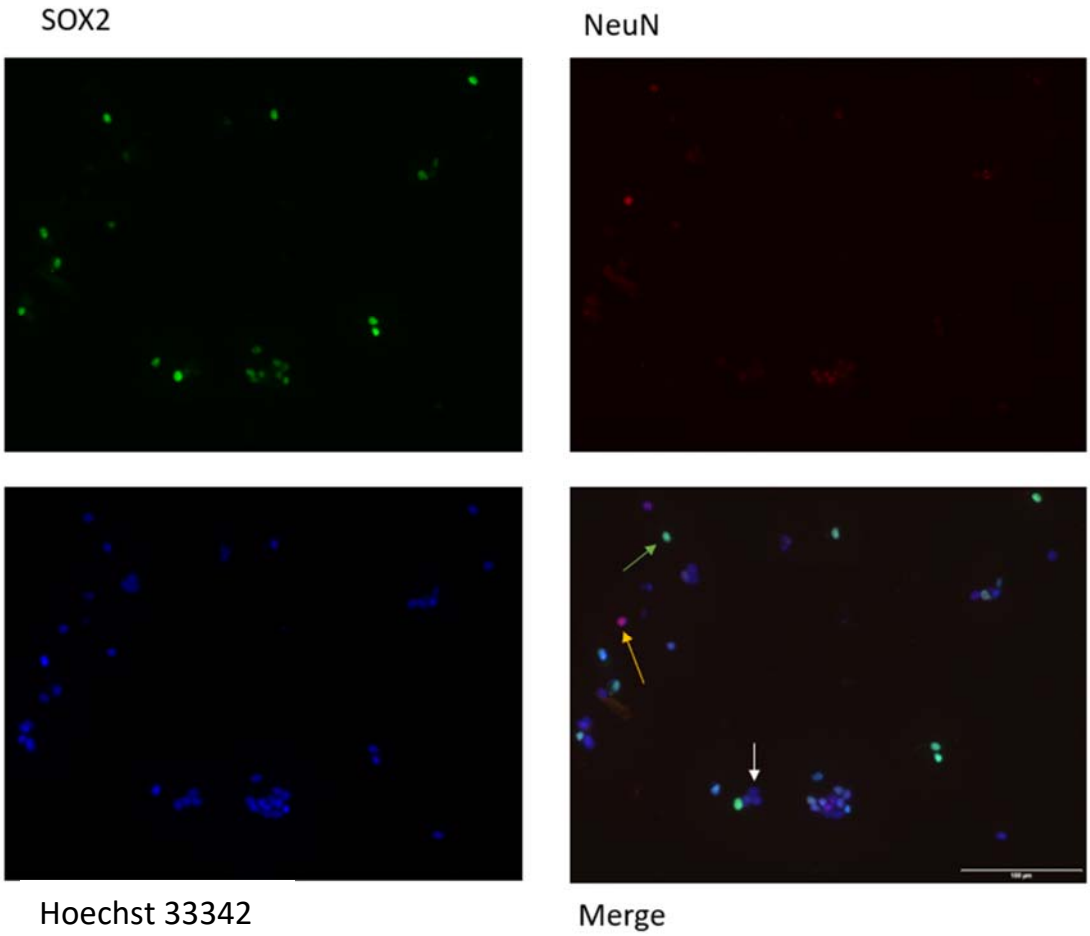

Figure 17: Double-staining of P6 opossum cortex with the IFR method. Homogenized cell nuclei were stained for SOX2 (green) and NeuN (red). Cell nuclei were stained with Hoechst 33342 (blue). Images were acquired with 20x 0.5 NA objective. Images are a projection of 10 µm z-stack acquired with 0.5 µm steps. Examples of neural stem cell (SOX2+/NeuN-, green arrow), neuron (SOX2-/NeuN+, yellow arrow) and non-neuronal cell (SOX2-/NeuN-, white arrow) are shown. Scale bar: 100 µm.

In total, 828 Hoechst 33342-positive cells were counted within experiments using both anti-SOX2 and anti-NeuN antibodies, out of which 63.94% ± 21.44% were SOX2-positive, 78.49% ± 10.58% were NeuN-positive, while 49.64% ± 9.77% were both SOX2- and NeuN-positive cells (Table 9).

Out of a total of 869 cells counted within experiments combining anti-SOX2 and anti-SOX9 antibodies, 64.02% ± 24.89% were SOX2-positive, 47.93% ± 34.02% were SOX9-positive, while 39.01% ± 15.01% were simultaneously SOX2- and SOX9-positive cells (Table 9). The ratio of single markers in double-staining experiments correlates well with their respective values obtained with single staining shown in Table 8, further demonstrating correct experimental settings.

Double-staining experiments allowed additional calculation relative to neuronal cell population. Out of the overall NeuN-positive cell population (n=653), 62.94% were also positive for SOX2. Similarly, inside the SOX9-positive cell population (n=405), 83.7% were also positive for SOX2 (Table 9).

Table 9: Percentage of double-positive cells counted from IFR experiments involving respective marker combinations in relation to cells stained with Hoechst 33342 (n) for opossum P5-6.

Marker combination	**Percentage in relation to Hoechst 33342 staining**
SOX2+/NeuN+	49.64% ± 9.77% (n=828)
SOX2+/SOX9+	39.01% ± 15.01% (n=869)
	Percentage of double-positive cells in a pool of NeuN and SOX9, respectively
(SOX2+/NeuN+)/NeuN+	62.94% (n=653)
(SOX2+/SOX9+)/SOX9+	83.7% (n=405)

SOX2 and NeuN are considered markers for opposite processes inside a cell. The former is a marker of proliferative pluri- and multipotent stem cells, and the latter a marker of differentiation. For them to coexist inside the same cell population came as a surprise. The existence of SOX2 in neurons was previously reported and will be discussed in chapter 5.6[54].

The (co)expression pattern for SOX9 was, in contrast, expected, since it is known that neural stem cells (both during developing as well as in adult life inside neurogenic niches) express glial cell markers such as SOX9 or GFAP[54]. It was important to confirm their coexpression in opossum since there were no previous reports of SOX2 and SOX9 expression in developing opossum cortex.

However, it also gave us several new subpopulations of cells to characterize and categorize!

SOX2+/NeuN+ should correspond to the subpopulation of "young" neurons, as they have expressed the marker for differentiated neurons, but still harbour the residual marker of proliferation. SOX2+/SOX9+ cells most probably correspond to the population of neural stem/progenitor cells since gliogenesis in opossum should start around P18[12,17]. Additionally, double-staining experiments allowed us to characterize the percentage of these immature (SOX2+/NeuN+) neurons inside the overall neuron population (NeuN+), which is described as the subpopulation of cells expressing both SOX2 and NeuN markers, inside the cell population expressing NeuN[96] (Table 9). Since we detected around 63% of NeuN-positive neurons being SOX2/NeuN double-positive, we can conclude that at this developmental stage the majority of neurons are newborn/immature cell population, which is in agreement with IHC data analysing markers for cortical neurogenesis described in work of Puzzolo and Mallamaci[12]. Following the same principle, we were able to characterize the percentage of the subpopulation of cells expressing both SOX2 and SOX9 markers, inside the cell population expressing SOX9 (Table 9). The observed result indicates that 83.7% of the SOX9-positive cells also express SOX2, which is expected since both are markers of neural stem cells.

According to our measurements, almost half (49.64%) of cells were positive for both SOX2 and NeuN, labelling "young" neuronal population and emphasizing the all-encompassing period of rapid differentiation at this postnatal period. Much less, but still a significant amount (39.01%) of cells were positive for both SOX2 and SOX9, indicating a neurogenic pool of stem/progenitor cells, rather than astrocytes (which should appear during the third postnatal week).

A more comprehensive way of visualizing the subpopulations of cells is through a doughnut chart, where each end of the double positive cell population annulus concurs with a different

cell line characterized with a single cell marker, visualizing both the percentage of overlap, but also the excess (Figures 18 and 19).

Since the SOX2+/NeuN- cells accounts for approximately 15% (the “excess” in the percentage of SOX2+, if we exclude double-positive cells), we can also conclude that this cell population are the “true” neural stem cells.

The combination of SOX2 and SOX9 does not allow similar extrapolation since neither of the two markers is exclusive for one cell type (unlike NeuN which is generally considered to be neuron-specific). However, we cannot completely exclude opossum-specific, transient, or prolonged (co)expression of all considered markers and their combinations during cortical histogenesis.

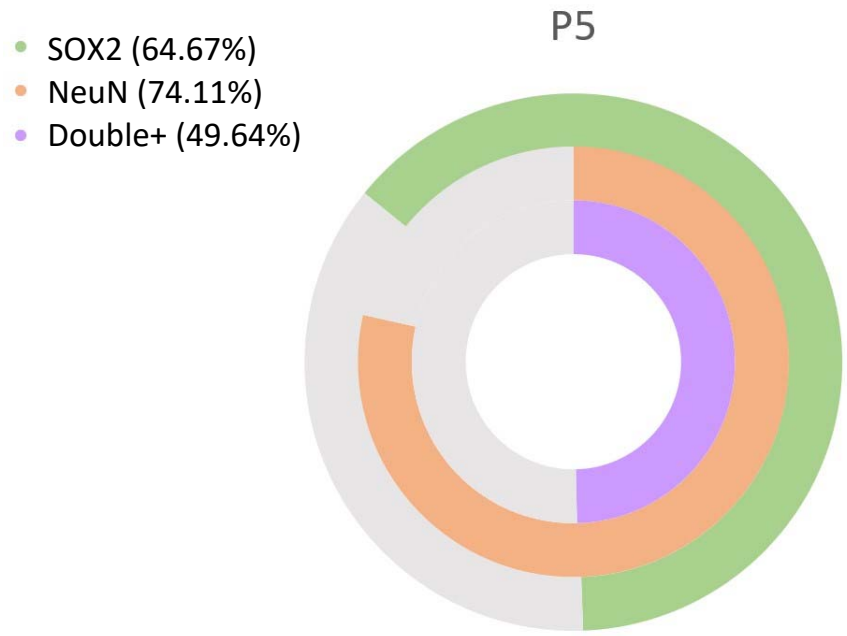

Figure 18: Visualization of different cell subpopulations in P5-6 opossum cortex. Green: SOX2, 64.67% ± 9.9% (n=1387), p<0.05; orange: NeuN, 74.11% ± 2.93% (n=645), p<0.05; Purple: SOX2+/NeuN+ double-positive cells, 49.64% ± 9.77% (n=828), p<0.05. The percentages represent the amount of respective cell populations in the whole opossum cortex. There is a subpopulation of SOX2+ cells that is not positive for NeuN, and a population of NeuN+ cells not positive for SOX2. Both cell subpopulations are visible as the green and orange part of the annulus not concentric with the purple part of the annulus, respectively.

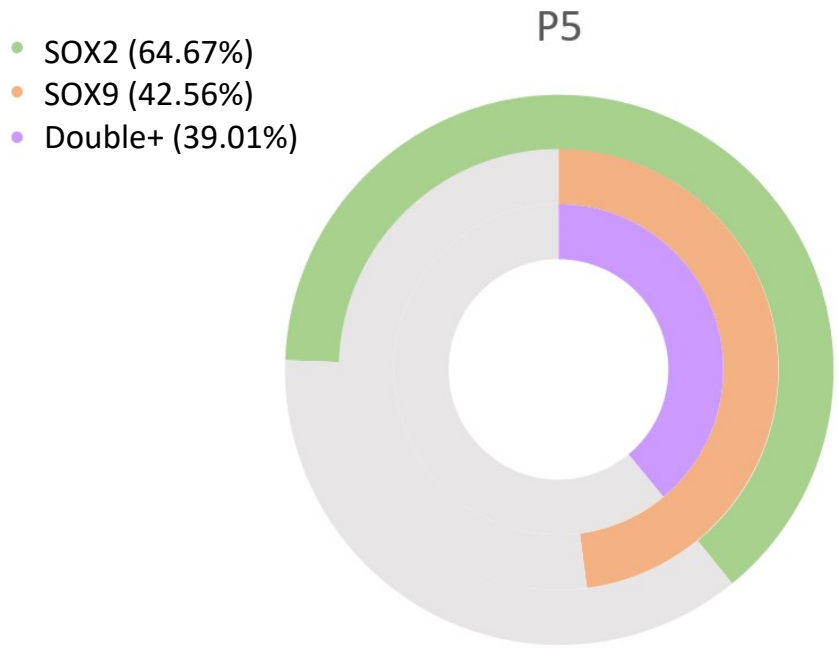

Figure 19: Visualization of different cell subpopulations in P5-6 opossum cortex. Green: SOX2, 64.67% ± 9.9% (n=1387), p<0.05; orange: SOX9, 42.56% ± 17.56% (n=733), p<0.05; Purple: SOX2+/SOX9+ double-positive cells, 39.01% ± 15.01% (n=869), p<0.05. The percentages represent the amount of respective cell populations in the whole opossum cortex. There is a subpopulation of SOX2+ cells that is not positive for SOX9, and a population of SOX9+ cells not positive for SOX2. Both cell subpopulations are visible as the green and orange part of the annulus not concentric with the purple part of the annulus, respectively.

4.3.1.4. IHC analysis on tissue slices from P6 opossum cortex

To further verify the presence of SOX2+/NeuN+ as well as SOX2+/SOX9+ double-positive cell population, we performed IHC analysis on tissue slices obtained from P6 opossum cortex. Immunohistochemistry was performed as described in Materials and Methods. These experiments allowed the reconstruction of the *in vivo* architecture of the developing opossum cortex. Using the same combination of antibodies used for IFR double-stain experiments, we were able to detect the proliferative, ventricular zone containing SOX2- and SOX9- positive cells, as well as NeuN-positive neurons distributed across the entire cortical section, from ventricular layers towards the pial surface (at this stage upper cortical layers are just about to form in opossum, Figure 11), as shown in Figure 20 and Figure 21. Most importantly, double-positive SOX2+/NeuN+ (Figure 20) as well as SOX2+/SOX9+ (Figure 21) were clearly identified (indicated with arrowheads).

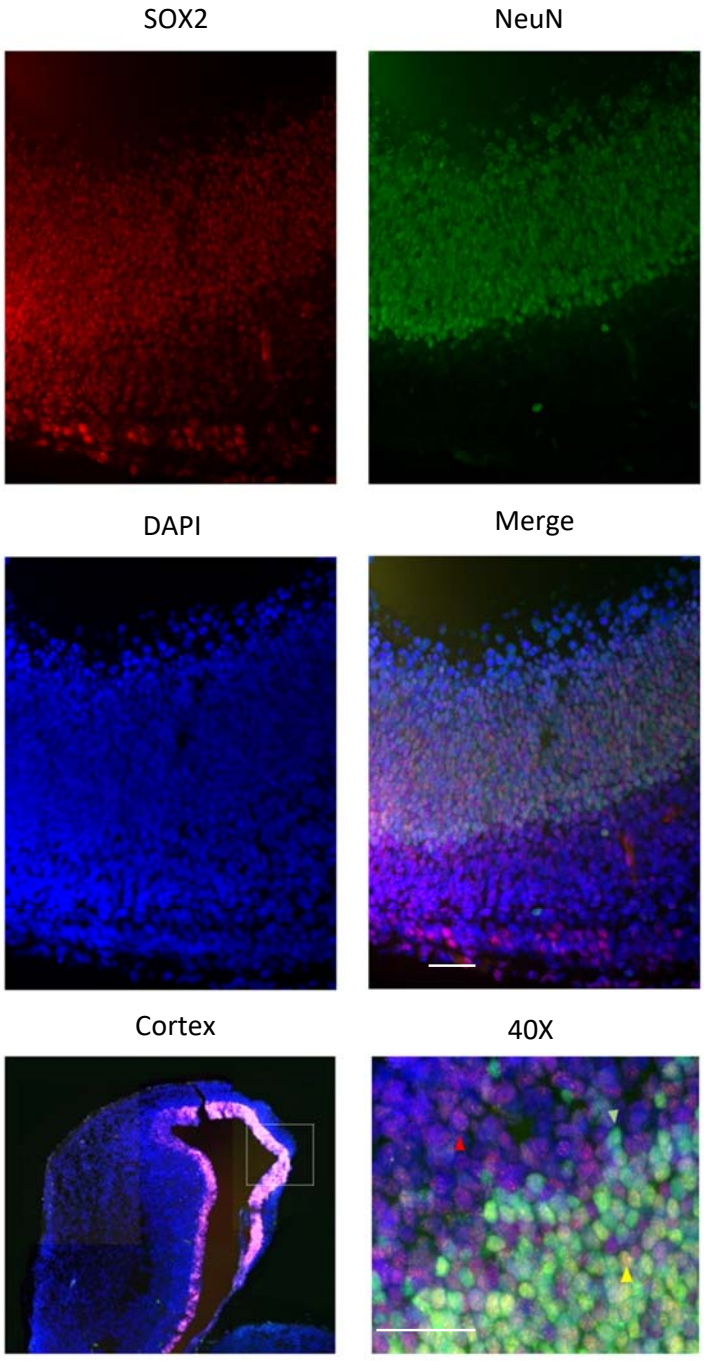

Figure 20: IHC of P6 opossum cortex. Cells were stained with anti-NeuN antibody (NeuN, red), anti-SOX2 antibody (SOX2, green), and DAPI was used for labelling cell nuclei (DAPI, blue). Merged panel shows the overlap of antibodies (Merge), while panel Cortex indicates the region of the opossum P6 cortex analysed in this experiment (obtained by stitching of several images to reconstruct the entire cortical hemisphere). Magnification: 10x, 0.5 NA. Panel 40X represents an image taken with 40x, 0.5 NA oil immersion objective of the same area, with SOX2-positive cell indicated with a green arrowhead, NeuN-positive cell indicated with a red arrowhead, and double-positive cell indicated with a yellow arrowhead. Scale bars: 50 µm.

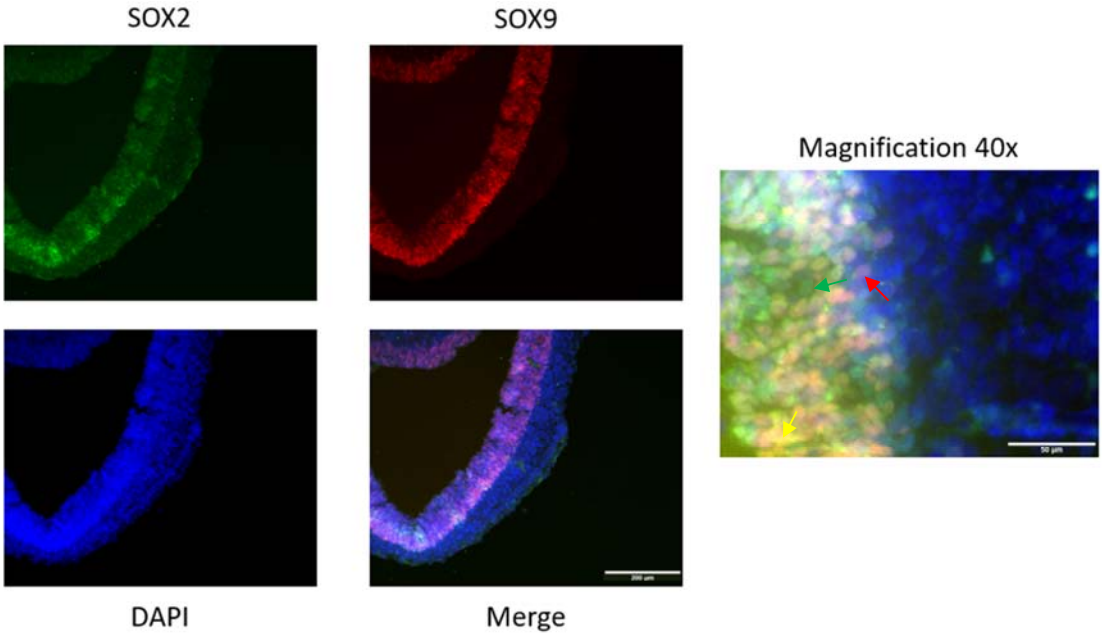

Figure 21: IHC of P6 opossum cortex. Cells were stained with anti-SOX2 antibody, anti-SOX9 antibody, and DAPI was used for labelling cell nuclei. Merged panel shows the overlap of antibodies. Magnification: 10x, 0.5 NA. Scale bar: 200 µm. Higher, 40x, 0.5 NA magnification of the same area shows the position of different cells, with SOX2-positive cell indicated with a green arrow, NeuN-positive cell indicated with a red arrow, and double-positive cell indicated with a yellow arrow. Scale bar: 50 µm.

Finally, the existence of differentiated neurons coexpressing SOX2 was observed also on primary dissociated cortical cultures of P4 opossum cortex at days *in vitro* (DIV) 1 (Figure 22). The cell cultures were prepared as described in Methods section using protocol for recently established opossum-derived cortical cultures[34]. In this case, the most widely used marker for post-mitotic neurons (β-tubulin III or TUJ1) was used in combination with SOX2, clearly showing the presence of double-positive cells.

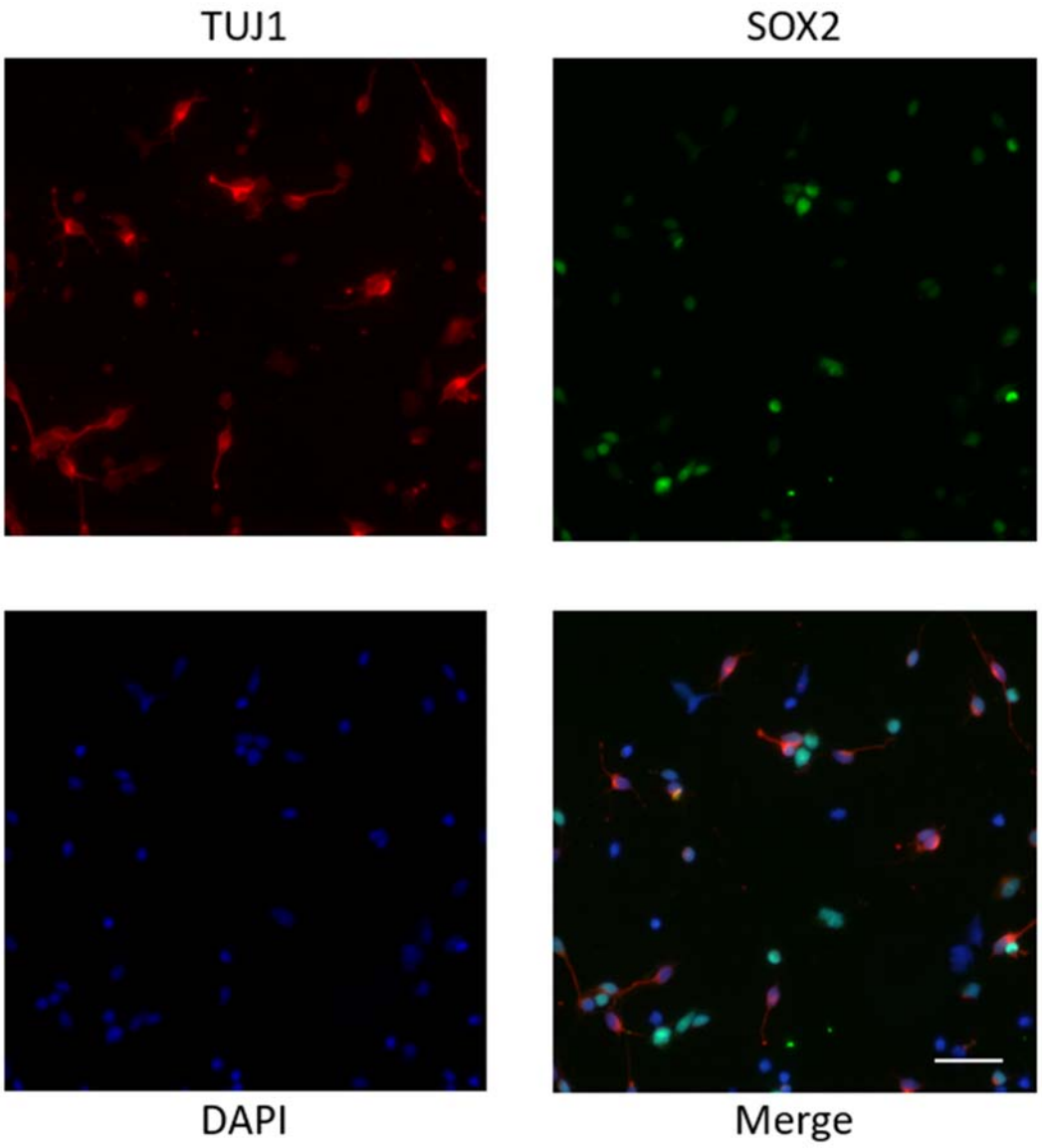

Figure 22. Primary cultures of P4 opossum cortex at DIV1. Cells were fixed 24 h after plating and stained for β-tubulin III (TUJ1, red), SOX2 (green) and DAPI nuclear stain (blue). The last panel shows merged staining. Scale bar, 20µm.

In conclusion, SOX2-expressing neurons were identified using IFR, IHC on cortical tissue slices as well as immunofluorescence on primary dissociated cultures of P5-6 opossum cortex.

4.3.2. Cellular composition in P16-18 opossum cortex

The same procedure in ascertaining the cellular composition of P5-6 opossum cortex has been used in P16-18. Both absolute and relative cell counts were calculated using the same approach.

4.3.2.1. Absolute cell count in P16-18 opossum cortex

Two separate experiments per each homogenized opossum cortex obtained from four opossum from two different litters were made to strengthen the statistical significance of these results (refer to Chapter 4.3.1.1 for a more comprehensive explanation of absolute cell count). Each experiment counted the number of cells in each of the four corner squares of the Neubauer chamber in the haemocytometer, and all the counted squares were averaged. As per the formula for determining the number of cells in a suspension, the average was multiplied by 10 000 due to the volume of the final suspension being double the size of P5-6 opossum cortex. The example of such experiment is shown in Table 10.

Table 10: Example of the acquisition of the absolute number of cells from IFR experiments counted on a haemocytometer in P16-18 opossum cortex.

	Number of cells per square
Square 1	1151
Square 2	1100
Square 3	1055
Square 4	1125
Average	1107.75
Total number (x10 000)	11 077 500

According to our measurements performed in a series of independent IFR experiments, a P16-18 opossum cortex has, on average, approximately 12, 717, 500 ± 1, 185,271 cells.

In the span of ten days, the number of cells in the opossum cortex increases by a factor of 2.5. It is important to note the only other reported source of the number of cells in the P18 opossum cortex is again by Seelke *et al*. They report 1, 637, 000 ± 58, 000 cells in the opossum cortex, out of which 60.55%, or 985, 000 are neurons, and 653, 000 are non-neurons[17]. The difference in the obtained results, including the discrepancies reported by Dos Santos et al will be further discussed in the Discussion.

4.3.2.2. Relative cell count in P16-18 opossum cortex

The relative cell count for P16-18 opossum cortex was obtained by counting experiments from seven different animals, each from a different litter.

In total, 2685 Hoechst 33342-positive cells were counted within experiments using anti-SOX2 antibody, out of which 41.38% ± 5.03%, were SOX2-positive cells. 1400 cells were counted within experiments using anti-NeuN antibody, with 46.5% ± 8.25%, being NeuN-positive, and 1285 cells were counted within experiments using anti-SOX9 antibody, 24.28% ± 3.13% being SOX9-positive (Table 11).

Table 11: Percentage of cells counted from IFR experiments involving respective markers in relation to total cells stained with Hoechst 33342 (n) for opossum P16-18.

Antibody	Percentage
SOX2	41.38% ± 5.03% (n=2685)
NeuN	46.5 % ± 8.25% (n=1400)
SOX9	24.28% ± 3.13 (n=1285)

To our knowledge, this is the first report using SOX2 and SOX9 as markers with IFR on P16-18 opossum.

The cellular composition of P16-18 opossum cortex differs drastically from its counterpart at P5-6. At this point in the development of the opossum cortex (illustrated in Figure 11), the SVZ harbours an abundance of proliferative cells, and the SP thickens to become the widest layer in the telencephalic wall, with IZ following closely behind, while the VZ diminishes. The MZ remains an unchanged layer a few cells thick.

The percentage of SOX2-positive cells diminishes between P5-6 and P16-18 opossum cortex, signifying maturation of the overall cortex. However, around 40% of cells are still SOX2-positive, meaning that the period of proliferation and differentiation is still ongoing.

Conversely, the lower percentage of NeuN-positive cells in P16-18 than in P5-6 correlates with the expansion of the non-neural cell population and subsequent neural pruning, which happens in mice shortly after birth, a time period comparable to, or shortly before P16-18 in the opossum[6,7].

The overall number of SOX9-positive cells decreases between P5-6 and P16-18: only 24% of cells are SOX9-positive cells at this developmental period, halving the percentage from the P5-6 (~48%). At this stage, in accordance with the onset of astrogenesis in the opossum cortex[12], SOX9 marks both the newborn astrocytes as well as neural stem/progenitor cells. This significant decrease in SOX9-positive cells could reflect the different expression pattern of radial glia cell population, given their heterogeneity and gradual disappearance in postnatal development[5].

Two explanations for this overall decrease in specific cell population percentages, but increase in cell number, are the differentiation of neurons and astrocytes, where less cells can be stained with two markers, and the higher number of non-neuronal cell types, including microglia (identified at this stage by IHC, unpublished data).

From the relative and absolute number of cells, we can also calculate the number of neurons and non-neuronal cells in P16-18 opossum cortices. The average opossum cortex of that age has 5.9 million neurons and 6.8 million non-neuronal cells.

4.3.2.3. Double-staining experiments in P16-18 opossum cortex

After the successful method setting described in Chapter 4.3.1.3, we proceeded with double-staining experiments for P16-18 opossum cortex and subsequently for P30. Four different litters containing four different animals were used to count cells containing both SOX2 and NeuN. In total, 1224 Hoechst 33342-positive cells were counted within experiments using both anti-SOX2 and anti-NeuN antibodies, out of which 43.92% ± 0.82% were SOX2-positive and 52.06% ± 7.07% were NeuN-positive. Out of 1169 Hoechst 33342-positive cells, 33.88% ± 5.93% were both SOX2- and NeuN-positive cells (Table 12).

Three different litters, as well as three different animals were used to identify the percentage of cells positive for both SOX2 and SOX9. Out of a total of 967 cells counted within experiments combining anti-SOX2 and anti-SOX9 antibodies, 41.1% ± 6.56% were SOX2-positive and 24.27% ± 1.38% were SOX9-positive. Out of 1285 Hoechst 33342-positive cells, 21.48% ± 3.01% were simultaneously SOX2- and SOX9-positive cells (Table 12).

Out of the NeuN-positive cell population, 60.83% were also positive for SOX2 (n=651), and inside the SOX9-positive cell population, 88.46% were also positive for SOX2 (n=312, Table 12).

Table 12: Percentage of double-positive cells counted from IFR experiments involving respective marker combinations in relation to cells stained with Hoechst 33342 (n) for opossum cortex P16-18.

Antibody	**Percentage**
SOX2+/NeuN+	33.88% ± 5.93% (n=1169)
SOX2+/SOX9 +	21.48% ± 3.01% (n=1285)
	Percentage of double-positive cells in a pool of NeuN and SOX9, respectively
(SOX2+/NeuN+)/NeuN+	60.83% (n=651)
(SOX2/SOX9)/SOX9	88.46% (n=312)

The percentage of SOX2+/NeuN+, as well as SOX2+/SOX9+ cells decreased between P5-6 and P16-18, further indicating maturation of the overall opossum cortex. An alternative explanation could be the increase of other non-neural cells, such as microglia. However, the percentages of both cell populations ((SOX2+/NeuN+)/NeuN+ and (SOX2+/SOX9+)/SOX9+) stayed the same, despite the drastic increase in the overall cell count (5.2 million cells in P5-6 versus 12.7 million cells in P16-18). This points to a continuous, even more rapid production of both cell populations in P16-18. This is visually summarized in Figures 23 and 24.

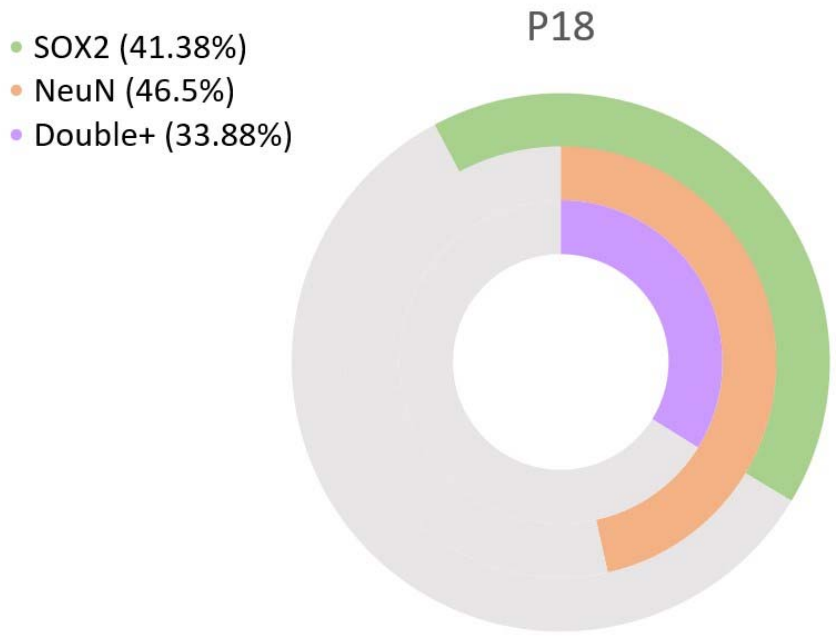

Figure 23: Visualization of different cell subpopulations in P16-18 opossum cortex. Green: SOX2, 41.38% ± 5.03% (n=2685), p<0.05; orange: NeuN, 46.5 % ± 8.25% (n=1400), p<0.05; Purple: SOX2+/NeuN+ double-positive cells, 33.88% ± 5.93% (n=1169), p<0.05. The percentages represent the amount of respective cell populations in the whole opossum cortex. There is a subpopulation of SOX2+ cells that is not positive for NeuN, and a population of NeuN+ cells not positive for SOX2. Both cell subpopulations are visible as the green and orange part of the annulus not concentric with the purple part of the annulus, respectively.

We can also assume that after we exclude the double-positive cells, the remaining 7,5% of SOX2+/NeuN- cells could correspond to neural stem cells and that this population of cells is decreasing with respect to the P5-6 (15%, Figure 18).

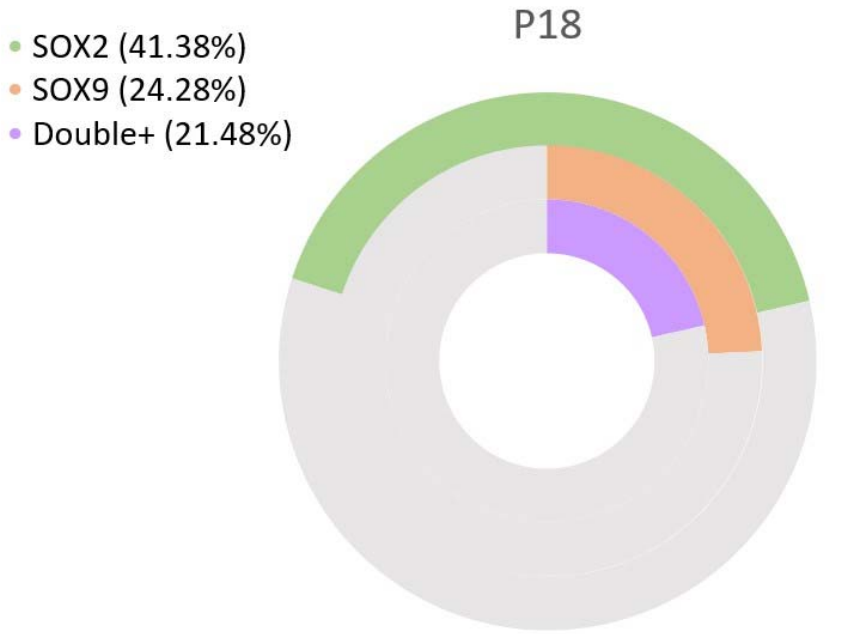

Figure 24: Visualization of different cell subpopulations in P16-18 opossum cortex. Green: SOX2, 41.38% ± 5.03% (n=2685), p<0.05; orange: SOX9, 24.28% ± 3.13 (n=1285), p<0.05; Purple: SOX2+/SOX9+ double-positive cells, 21.48% ± 3.01% (n=1285), p<0.05. The percentages represent the amount of respective cell populations in the whole opossum cortex. There is a subpopulation of SOX2+ cells that is not positive for SOX9, and a population of SOX9+ cells not positive for SOX2. Both cell subpopulations are visible as the green and orange part of the annulus not concentric with the purple part of the annulus, respectively.

4.3.3. Cellular composition in P30 opossum cortex

The same procedure in ascertaining the cellular composition of P5-6 and P16-18 opossum cortices has been used in P30. Both absolute and relative cell counts were calculated using the same approach.

4.3.3.1. Absolute cell count in P30 opossum cortex

Two separate experiments per homogenized opossum cortex obtained from opossum from different litters were made to strengthen the statistical significance of these results (refer to Chapter 4.3.1.1 for a more comprehensive explanation of absolute cell count). Each experiment counted the number of cells in each of the four corner squares of the Neubauer chamber in the haemocytometer. All the counted squares were averaged. As per the formula for determining the number of cells in a suspension, the average was multiplied by 20 000 due to the volume of the final suspension being double the size of that in P16-18 and four times as big as in P5-6 (Table 13).

Table 13: Example of the acquisition of the absolute number of cells from IFR experiments counted on a haemocytometer in P30 opossum cortex.

	Number of cells per square
Square 1	969
Square 2	1117
Square 3	1154
Square 4	1206
Average	1111.5
Total number (X20 000)	22, 230, 000

According to our measurements, a P30 opossum cortex has, on average, approximately 21, 797, 500 ± 996, 145 cells.

Between P16-18 and P30, the opossum again almost doubles the number of cells in the cortex. The rate of cell addition is slowing down (4.2 million in P5-6, 12.7 million in P16-18 and 21.8 million in P30), however, the P30 opossum is still a rapidly developing pup.

4.3.3.2. Relative cell count in P30 opossum cortex

The relative cell count for P30 opossum cortex was obtained by counting experiments from six different litters and six different animals from those litters. In total, 4562 cells were counted from experiments containing SOX2, out of which 40.79% ± 5.09%, were SOX2-positive. 1459 cells were counted with experiments containing NeuN, with 49.35% ± 4.94%, being NeuN-positive, and 3103 cells were counted within experiments containing SOX9, with 26.81% ± 5.89% being SOX9-positive (Table 14).

Table 14: Percentage of cells counted from IFR experiments involving respective markers in relation to total cells stained with Hoechst 33342 (n) for opossum P30.

Marker	Percentage
SOX2	40.79% ± 5.09% (n=4562)
NeuN	49.35% ± 4.94% (n=1459)
SOX9	26.81% ± 5.89% (n=3103)

To our knowledge, this is the first count of SOX2- and SOX9-stained cells with IFR on P30 opossum cortex.

From the relative and absolute number of cells, we can also calculate the number of neurons and non-neuronal cells in P30 opossum cortex. The average opossum of that age has 10.8 million neurons and 11 million non-neuronal cells, suggesting that at this developmental stage non-neuronal cells are more numerous than neurons.

The architectural development of the opossum cortex is at P30 more like its adult version. The VZ is diminished to a narrow strip of cells, while both the SVZ and MZ remain unchanged. However, the CP, SP and IZ all continue to grow. At this point, neurogenesis is at its peak, both in number and in density[17].

There is still a large percentage of SOX2+ cells present in the P30 opossum cortex comparable to that of P16-18, which confirms the prolonged period of neurogenesis in the postnatal opossum. It also indicates that the total number of SOX2+ cells has doubled in comparison to the P16-18 opossum cortex, because the overall number of cells in the P30 cortex doubled, and their percentage stayed the same. The same is true for the NeuN+ and SOX9+ cells as well.

The trend of NeuN+ cells in the P30 opossum cortex correlates with the work of Bandeira *et al*., if we normalize the P30 opossum as P10 rat (from Cardoso-Moreira *et al*., where developmental correspondence of P30 opossums is between P3 and P14 mouse or rat)[6,7]. The neuron to non-neuron ratio is more akin to a P10 rat, indicating the similar onset of gliogenesis between the two species.-We can conclude that P30 is still a period of planar and relatively equal growth for each of the cell populations.

4.3.3.3. Double-staining experiments in P30 opossum cortex

Three different litters containing three different animals were used to count cells containing both SOX2 and NeuN. In total, 1182 Hoechst 33342-positive cells were counted within experiments using both anti-SOX2 and anti-NeuN antibodies, out of which 52.58% ± 4.28% were SOX2-positive and 51.83% ± 4.66% were NeuN-positive. Out of 1459 Hoechst 33342-positive cells, 34.68% ± 6.13% were both SOX2- and NeuN-positive cells (Table 15).

Three different litters, as well as three different animals were used to identify the percentage of cells positive for both SOX2 and SOX9. Out of a total of 1965 cells counted within experiments combining anti-SOX2 and anti-SOX9 antibodies, 36.28% ± 2.1% were SOX2-positive and 30.19% ± 6.02% were SOX9-positive. Out of 3103 Hoechst 33342-positive cells, 21.98% ± 5.15% were simultaneously SOX2- and SOX9-positive cells (Table 15).

Table 15: Percentage of double-positive cells counted from IFR experiments involving respective marker combinations in relation to cells stained with Hoechst 33342 (n) for opossum P30.

Antibody	Percentage
SOX2+/NeuN+	34.68% ± 6.13% (n=1459)
SOX2+/SOX9 +	21.98% ± 5.15% (n=3103)
	Percentage of double-positive cells in a pool of NeuN and SOX9, respectively
(SOX2+/NeuN+)/NeuN+	70.28% (n=720)
(SOX2/SOX9)/SOX9	81.97% (n=828)

Further confirming the findings from the previous chapter are the double-positive cell populations, SOX2+/NeuN+ and SOX2+/SOX9+, both of which have relatively equal percentages between P16-18 and P30. The difference is the percentage of the immature neurons inside the neural population, which increased compared to P16-18, meaning that the production of newborn neurons continues at P30. This result differs from the work of Seelke *et al*., who claim peak cortical neurogenesis happens around P18, extending from P14 to P24[17]. The results obtained on P30 opossum cortex are visually summarized in Figures 25 and 26.

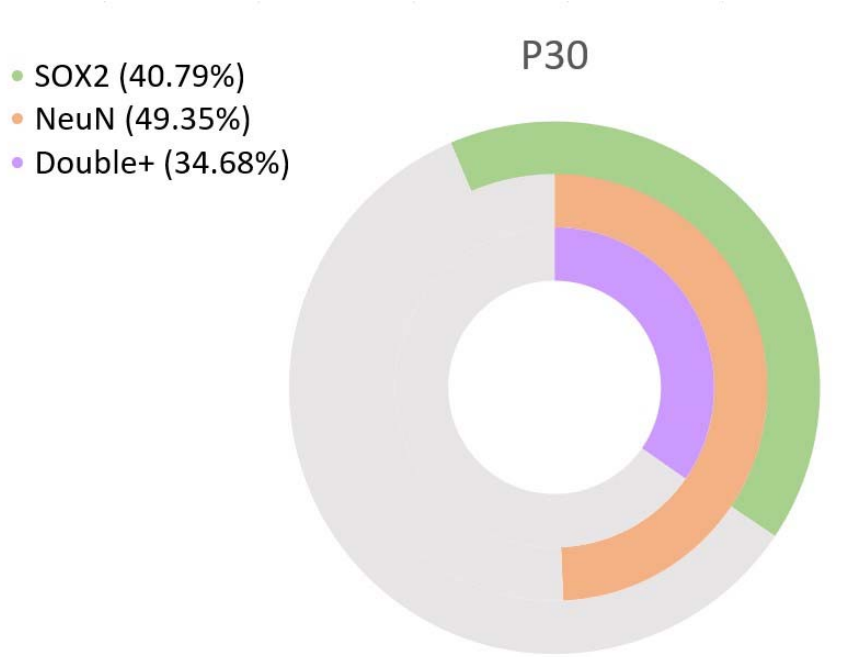

Figure 25: Visualization of different cell subpopulations in P30 opossum cortex. Green: SOX2, 40.79% ± 5.09% (n=4562), p<0.05; orange: NeuN, 49.35% ± 4.94% (n=1459), p<0.05; Purple: SOX2+/NeuN+ double-positive cells, 34.68% ± 6.13% (n=1459), p<0.05. The percentages represent the amount of respective cell populations in the whole opossum cortex. There is a subpopulation of SOX2+ cells that is not positive for SOX9, and a population of SOX9+ cells not positive for SOX2. Both cell subpopulations are visible as the green and orange part of the annulus not concentric with the purple part of the annulus, respectively.

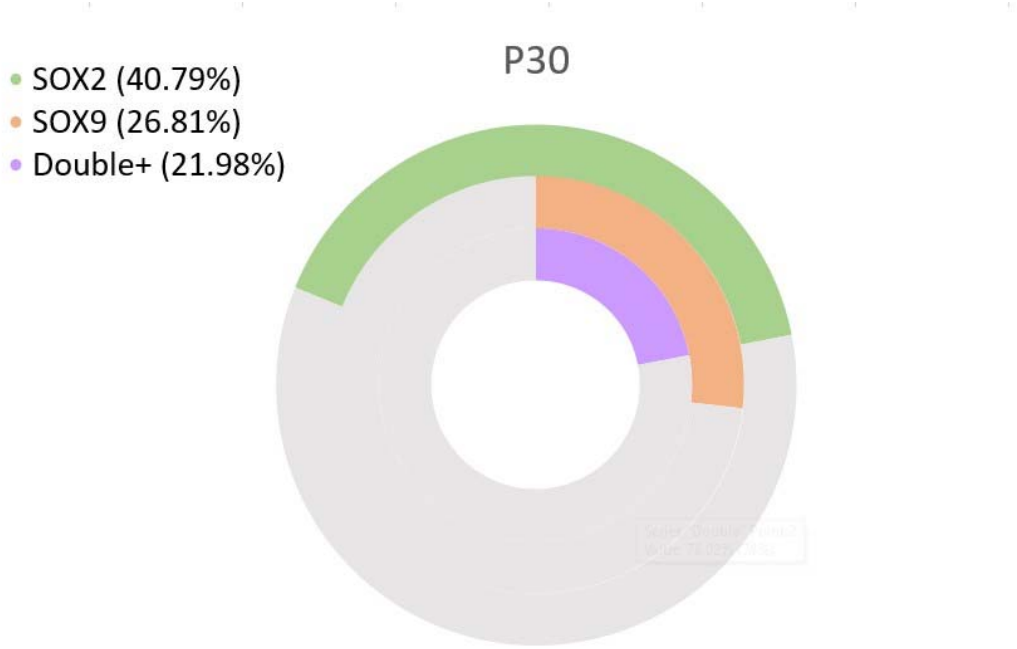

Figure 26: Visualization of different cell subpopulations in P30 opossum cortex. Green: SOX2, 40.79% ± 5.09% (n=4562), p<0.05; orange: SOX9, 26.81 % ± 5.89% (n=3103), p<0.05; Purple: SOX2+/SOX9+ double-positive cells, 21.98% ± 5.15% (n=3103), p<0.05. The percentages represent the amount of respective cell populations in the whole opossum cortex. There is a subpopulation of SOX2+ cells that is not positive for SOX9, and a population of SOX9+ cells not positive for SOX2. Both cell subpopulations are visible as the green and orange part of the annulus not concentric with the purple part of the annulus, respectively.

5. Discussion

5.1. Lack of data and literature references in early developmental traits of opossum and rodent CNS

Despite being the most prominent laboratory animal for more than a century[97] , mice are lacking in data when it comes to the quantification of their embryonic and early postnatal development. Despite well defined cortical layers and its architecture throughout the development of both mice and rats, they both lack the number of neuronal and non-neuronal cells in key embryonic days. Moreover, that lack of information persists even throughout their postnatal days (except for Bandeira *et al*. where the rat brains from various postnatal ages, spanning from P0 to P90 was characterized with IFR[6]), with the adult specimen having a clearly defined range of specific cell lines. Without such a groundwork to compare the opossum to the most prominent laboratory animals, it became increasingly difficult to devise a starting point for our experiments and their comparative value.

As was the case with literature concerning the number of cells in the embryonal and early postnatal development in mice and rats, only a handful of papers with opossum as their laboratory animal of interest were available at the start of this project. The majority of the literature was contained in the previous works of Puzzolo and Mallamaci[12], Seelke *et al*.[17] and Majka *et al*[33], all of which sprung from much older works of Saunders *et al*.[31], VanDerBerg *et al*.[15], Varga *et al*. [26], and Nicholls[13,29]. Those pioneer works were more focused on spinal cord regeneration after injury while the regenerative potential of the opossum brain related to their postnatal development remained largely unexplored.

It was not until the Cardoso-Moreira *et al*.[7] paper published in 2019 that we could compare the opossum developmental phases with that of mice and rats. This paper, together with collected information from the aforementioned literature gave us extremely useful coordinates of opossum development. This is partially the reason why every step of this journey had to be rigorously checked and defined, as literature data was so lacking. Additionally, the only other two papers on opossum postnatal development were published

by Seelke *et al*. in 2013 and 2014, which were already excluded from the research done by Dos Santos *et al*. due to inconsistencies with the number of cells in the opossum cortex and the number of neurons expected for opossum body mass[32]. Moreover, this discrepancy was also noticed in comparison to other marsupials. In fact, the authors reported that using the same method, the total number of neurons is about one order of magnitude smaller than expected for its body mass. We also report a discrepancy both in body weight and the number of cells in specific postnatal days (Table 4, Table 9, Figure 27, summarized in Table 16).

Table 16: Discrepancy between the number of cells in opossum cortex and their mass between our work and that of Seelke et al., for the two comparable timepoints[17].

	Our work		**Seelke *et al*.**	
Postnatal day	P18	P30	P18	P35
Body size (in g)	1.71 ± 0.11	5.02 ± 0.13	2.5 ± 0.5	7 ± 1.1
Number of cells (in millions)	12.71 ± 1.2	21.8 ± 1	1.637 ± 0.058	1.580 ± 0.141

As is evident, their opossum are more massive than ours, and have a much lower number of cells in the cortex, which was also noticed by Dos Santos *et al*.[17,32].

5.2. Protocol modifications for the inverted microscope

Having access only to inverted microscopes, the original protocol for IFR had to be adapted to the inverted microscope, resulting in several benefits.

The original protocol used upright microscopes and relied on absolute number counts as its primary data output. We used different microscopes for counting the absolute and the relative number of cells (see 3.1.4 for more detail) due to the thickness of the haemocytometer glass and the working distance associated with the objective used. The working distance for this setup needs to be much wider than for counting the relative number of cells, as the latter uses only a thin coverslip glass. Moreover, the light passing through the haemocytometer allowed visualization and counting of Hoechst 33342-labelled nuclei only since the red-staining used for NeuN in combination gave too low of an intensity of fluorescence output.

Counting of the relative number of cells using additional markers opened up an additional avenue of tissue content analysis. With this upgrade it became possible not only to compare the number of cells between different time points, but also to distinguish particular cell lines in each of the time points of interest, which significantly improved our understanding of the opossum cortical growth and its inner workings. The possibility to use different markers in addition, and in combination with NeuN opens a great opportunity for future research, applicable on virtually any brain sample, invertebrates included[98].

Additionally, improvements in the method allow for long-term storage of coverslips and acquired data for future analyses. In the original method, the content is counted by hand, and the samples are discarded afterwards leaving no material for further analysis. In the case of our method, the evidence remains in the form of both pictures and coverslips, which can be stored at -20°C or -80°C for over a year, with minimal degradation and information loss (except for the unavoidable decay over time of some fluorophores such as Alexa Fluor 488). More advanced, but also much more expensive methods based on flow cytometry such as Fluorescence-activated cell sorting (FACS) were proposed as reliable semi-automatized cell counting[54,89].

5.3. IFR and immunocytochemistry

Isotropic fractionator, a key method in this research, has been proposed and validated by Suzana Herculano-Houzel and Roberto Lent in 2005[82]. Although this, and subsequent papers reference a variety of animal species on which a successful brain fractionation has been performed, only two papers by Seelke *et al* [17,89] used opossum tissues in this way, but on P18 or older postnatal ages, with already mentioned discrepancies in obtained results compared with other marsupial species [32].

We had to consider key factors while modifying the procedure: the age of the sampled animals, the anatomy of their brain, the total volume of biomass available, and the stiffness of the fractionated tissue.

Three opossum ages were chosen for their key anatomical and biological features. The youngest age was chosen to be P5-6, due to its ability to regenerate CNS tissue[12,20,29,34], but also because younger opossum brains are too small and underdeveloped and are difficult to work with. The second age was P17-18, chosen as the counterpart to the first age: the brain is still not fully developed, but the regenerative abilities have ceased to exist. This age group also correlates well with the onset of astrocytogenesis, as first GFAP-positive cells with branched morphology typical for astrocytes were reported at P16 by IHC[12]. The third age was chosen to be P30, as an additional way to verify the more mature point of opossum cortical neuro- and astrocytogenesis, while the onset and completion of oligodendrocytogenesis differs between the prior literature sources. Puzzolo and Mallamaci place the onset of oligodendrocytogenesis around P40[12,17]. Unfortunately, we were not able to verify this point using OLIG2 as a marker. It was however very useful still to confirm the presence of SOX2/NeuN and in particular SOX2/SOX9 coexpression at P30, given the known role of SOX9 in oligodendrocytogenesis as well (see section 5.6.3).

As previously mentioned, neonatal opossum brains have an underdeveloped cortical structure, to the point where the neocortex is comprised of only two of the usual six layers, with most of the cortical architecture missing, including the cerebellum[12,13]. Even the older

timepoints of P17-18 and P30 still have a significantly different brain anatomy than their rat counterparts, with all the main cellular components being present just at P30 or later timepoints.

Conversely, the size of the available biomass is significantly lower in developing opossum brains than in adult rat brains. Another point to consider was that opossum cortex mass varies greatly between time points, which meant adjusting the method for both the experiment preparation portion and the final immunochemistry part.

The age of the brain also plays a key role on the amount of extracellular matrix and connective tissue present. There is a major difference in tissue stiffness even between opossum of different postnatal ages.

The range of tissues tested both in our research and previously reported shows the flexibility and robustness of IFR: it is fast, reliable, and doable in most working conditions. It can be adapted to a variety of tissues, with slight modifications to the protocol, bearing in mind the rigidity and stiffness of the chosen tissue. The less connective tissue is present, the easier will it be to dissociate it into a cell suspension. The brain being one of the softest tissues in our body is advantageous. Additionally, the destructive nature of the protocol for all but the cell nuclei can also be seen as an advantage, as it leaves the nuclei both intact and exposed for immunostaining analyses.

Not having an outer layer of biological matter to penetrate, the antibodies are free to bind to their targets in the nucleus much faster than their counterparts in regular immunocytochemistry. The removal of extracellular matrix and other cellular components additionally reduces background signal. This can be exploited to drastically shorten the incubation duration of both the primary and secondary antibody, completing the whole immunocytochemistry (ICC) process in one working day.

However, the same destructive nature of IFR has its downsides. The protocol demands the destruction of the three-dimensional cortical structure and its dissociation, which deprives us from the exact spatial distribution of analysed cells in the given region or tissue. IHC on cortical tissue slices can be used both to observe the spatial positioning of the markers of interest, and to strengthen and complement the results obtained with IFR.

Similarly, as the protocol for IFR demands all but the cell nuclei to be degraded and discarded, only nuclear markers could be used, which limited our options to a few well known markers, and also prompted us to research other available markers.

Despite the ability of our microscopes to simultaneously and without interference detect four different and distinct antibodies via four mirror units (see chapter 3.1.3 for details), we only performed triple immunocytochemistry staining due to possible spectral overlap with the addition of far-red Alexa Fluor 633 fluorophore. The only part of the cell remaining in our experiments is the nucleus, and having three different antibodies potentially competing for space, together with the DNA intercalator Hoechst 33342, could lead to signal overlap and/or antibody crosstalk.

5.4. Commercially available primary antibodies applied to opossum

It is important to keep in mind the markers' initial purpose, which might, but does not have to coincide with the researchers' needs. In most cases the marker of interest is specific for most, but not all cells of a certain type (e.g., NeuN is expressed in most, but not all neurons).

We tested a variety of primary antibodies to serve as markers for specific cell lines (Table 5). Due to the lack of protocols specifically developed for opossum, and the general lack of data regarding opossum as laboratory animals, we compared the protein sequence similarity between each of the referent immunogen used to produce the primary antibody and the whole corresponding protein sequence in the opossum. The alignment was done with UniProt Align function, which found high similarity (in almost all of the tested antibodies) in accordance with data obtained from *M. domestica* genome sequencing[35], as described by Mikkelsen *et al*.[10].

Firstly, the markers of interest (SOX2, and SOX9 in particular) are well preserved throughout evolution[9,10,38,40,55]. Moreover, both the previous work in our laboratory and that of several others has already used a palette of markers with various imaging methods and on postnatal ages of *M. domestica*. Calretinin, Tbr1, Tbr2, Cux1, Foxp2, Pax6, Tle4, GFAP, O4, S100β GABA, GAD, Tuj1 and pH3 have been used on opossum cortical slices by Puzzolo and Mallamaci[12]. Additionally, NeuN has previously been used on the *M. domestica* cortex[17,89,91,99], the cerebellum[90], and the spinal cord[85] by IHC. Seelke and coworkers used NeuN with IFR on postnatal ages P18, P35 and older, while Bartkowska and coworkers immunostained opossum cortex and cerebellum tissue slices for TrkB, TrkC, Olig2, HuD, Ki67, Tle4, TUJ1 and GFAP[90,91,99]. Altogether, these markers were analysed on opossum of various postnatal ages, ranging from P1 to P60. To the best of our knowledge, none of the antibodies used in these works were custom made (i.e., developed using opossum protein as an immunogen).

Previous research done in our laboratory shows the expression of following markers tested on recently established primary dissociated cortical cell cultures derived from P3-5 and P16-

18 opossum pups: TUJ1, MAP2, NeuN, Synapsin 1, GAD65, VGLUT2, GFAP, Vimentin, Iba1, Pax2, ATF3, SOX2 and BLBP[34,100]

In conclusion, literature has provided us with data from opossum tissues and primary cell cultures researched on various opossum postnatal ages and on various parts of the CNS (cortex, cerebellum, and spinal cord). However, this body of knowledge regarding the postnatal opossum is still incomplete. Ideally, antibody specificity should be further confirmed with specific tests and reproduced by different laboratories to get the complete expression map for each marker.

5.4.1. SOX2

The well-defined properties of transcription factor SOX2, a member of the SOXB1 subgroup, coincides with the characteristics of a neural progenitor/stem cell. It serves as a proliferative and pluripotency marker, and the protein sequence similarity between opossum and human is higher than 91.7%. It has been found to greatly influence the reprogramming capabilities of differentiated cells into their embryonic precursor, and disappears with the onset of cell differentiation[101].

We found that this disappearance in the opossum follows a gradual decline in expression, rather than a steep cut-off, suggesting lingering activity for a time period after cell differentiation. This can be observed as different intensities of SOX2 staining in cells transitioning into their differentiated state. Further supporting this claim are our unpublished results on primary dissociated neuronal cultures, showing a higher intensity of SOX2 in non-neuronal (β-tubulin III-negative) cells, compared to double positive β-tubulin III/SOX2 cells. It is to be expected that a member of what has been defined as “one of the most important developmental regulatory groups of transcription factors“ would have a prolonged, albeit decreasing role to play even after cell differentiation[42].

As SOX2 is associated with the progenitor cells' multipotency, it is also possible that its gradual loss narrows down cell fate until it takes on a differentiated role, induced by the complementary marker(s) of differentiation. Indeed, recent evidences confirm this “novel“

functional role of SOX2 in differentiated neurons in mice, while molecular mechanisms and targets mediating SOX2 function are currently being explored[44,102].

5.4.2. NeuN

NeuN is the nuclear marker of choice when it comes to labelling postmitotic, terminally differentiated neurons, with the exception of cerebellar Purkinje cells, mitral cells of the olfactory bulb and retinal photoreceptors. It also fails to label layer Vila cells in the neocortex and non-granulated cell interneurons in the cerebellum of mice[56,103]. As this study is focused on the opossum cortex, only layer Vila cells, cerebellar Purkinje cells and granulated cell interneurons could be a potential concern for an incorrect count of overall neurons with the IFR. However, the overall percentage of Purkinje cells has been reported to be less than 0.2% in adult human and less than 2% in adult rat brain[104]. Given all the developmental evidence, it is safe to conclude similar or even lower numbers of Purkinje cells in the developing opossum brain[7]. The opossum cerebellum is lacking at P0, which it develops in the first two postnatal weeks. Moreover, rat Purkinje cells mature around rat P12, which is roughly equivalent to opossum P30, meaning their number, while important to note, should not impact the importance of this study[7,105].

Another potential concern of NeuN labelling is its species-dependant expression in some specific cell subpopulations. For example, substantia nigra pars reticulata neurons in gerbil lack NeuN labelling, whereas it is present in rats[68]. As previously described, opossum are the closest (metatherian) outgroup to the eutherian lineage (Figure 5), and have a high degree of synteny with mice, rats and humans[9]. These facts do not exclude opossum-specific patterns of NeuN expression in specific cell subpopulations but make it very unlikely.

The appearance of NeuN occurs gradually as the cell differentiates, which is indicative of the cells' physiological status. This is evident as different intensity staining of cells just entering their differentiated state. Interestingly, NeuN stains the opossum nuclei in a specific pattern. Rather than a unified stain across the nucleus (as it is the case with SOX2), it clusters, most probably due to its reciprocal proportion to chromatin concentration, as reported in mice[57]. Our recent work on primary opossum dissociated cultures derived from the neonatal

opossum cortex (P3-5) also confirmed the early expression of NeuN (already at DIV1), in correspondence with other neuronal markers, including β-tubulin III and microtubule associated protein 2 (MAP2)[34].

There is a significant number of NeuN-positive neurons (around 37%) in P5-6 that are SOX2-negative, indicating they could have differentiated earlier (i.e. several days prior). We hypothesize that these can be the pool of neuronal networks with already downregulated SOX2, developed during the late embryonic period to allow suckling, breathing, and grabbing at birth (in coordination with other CNS structures). Moreover, they could correspond to neurons already migrated away from VZ towards pial surface at this developmental stage (Figure 11). Accordingly, the rest of the neurons are the population of newborn, less mature neurons, amounting to 62.94%.

It would be interesting to include prior timepoints into further research to differentiate between embryonal and postnatal neurogenesis, however, the extraction and preparation of opossum cortex prior to P6 becomes exponentially more difficult due to their extremely small size and tissue fragility.

5.4.3. SOX9

Sun *et al*. report SOX9 as an astrocyte-specific marker in the adult brain, the exception being the neurogenic regions. However, as the SOX family performs a variety of functions throughout the developing body, it can also be found in other places at different postnatal days[54,106]. It is expressed in developing chondrocytes and drives chondrogenesis and sex determination[38]. It is also a myocard modulator, preventing the onset of myotubes. However, the interesting properties for this study are its ability to suppress neural cell fate, while promoting astrocytic properties, especially in the neural crest[48,107]. Outside of mature astrocytes, SOX9 is present in developing oligodendrocytic lineages and in the neurogenic regions, more specifically in the neural stem/progenitor cells, where it suppresses the aforementioned neural cell fate even after the appearance of adult neuron-specific markers such as NeuN[108].

Oligodendrocytogenesis is reported to start after P40 in opossum, according to Puzzolo and Malamacci, a time point beyond the postnatal ages considered in this study[12]. However, the expression of SOX9 in neural stem/progenitor cells is evident at P6, where they are believed to be the main contributor of the SOX9-positive cell population. The amount of SOX9-positive stem cells which differentiate into neurons (if any) is still unknown due to the inability to perform combined SOX9/NeuN staining with available antibodies (both developed in rabbit). However, the immunofluorescence stains performed on primary neuronal cultures (derived from both P3-5, as well as P16-18 opossum cortex) suggest the exclusive coexpression of SOX9 with astrocytic markers such as vimentin and GFAP, while double-positive β-tubulin III/SOX9 cells were never observed[109].

5.4.4. Other tested markers

Several other markers of interest were tested to broaden the expression profile of developing cortical cell populations. As previously, for each marker, protein sequence similarity was checked before performing immunofluorescence experiments (Appendix 5).

Although PAX6 has been shown to have 100% homology between opossum and rabbit (Table 5), it is reportedly not expressed in all of the cortical neurons[68]. Immunostaining on P16-18 opossum cortical cells was not specific enough and the background was relatively high, in particular in cell clusters. PAX6 is known to recruit neural stem cells into neurons for developing the visual and the olfactory systems, but not all the cortical neurons express PAX6. Although it can be a potent tool in olfactory and visual studies, it is lacking in range for our own study.

Although PAX2 can be used as a marker of GABAergic neurons, its role in the developing brain is reported to be manyfold, from dorsal-ventral brain segmentation and subsequent radial cortical layer segregation, to GABAergic neuron characterization[63,65,66,110]. With opossum cortical development being shifted into the postnatal period, it would be unwise to limit PAX2's influence on only GABAergic neurons without further study.

BLBP is another example of an extremely important developmental marker without a clear and uniform expression pattern/role[60,61]. It is expressed in both young astrocytes and young neurons, but also in radial glia, before their differentiation[58,59,62]. Moreover, it persists into adulthood and, although intriguing and important, would open more questions than give answers in this study. Finally, given both the nuclear and cytoplasmic staining observed in P4 and P17 opossum primary cortical cultures[100], it was not a suitable choice for IFR and cell classification.

Ki67 was one of the first antibodies considered in this study, as it is both well established and widely used as a clinical marker of cell proliferation. However, its protein sequence similarity has been determined to be only 55.97% between opossum and rabbit, and 49.63% between opossum and mouse (Table 5). This has also been confirmed by immunostaining experiments, where the Ki-67 antibody presented a strong background noise, even after BSA saturation treatment and antigen retrieval process.

5.4.5. Cell lines and populations corresponding to markers and their combination

By choosing well-defined expressional markers we were able to track the specific cell population throughout the developing opossum brain. SOX2 marks the presence of multipotent neural progenitor/stem cells. NeuN corresponds to the population of adult, postmitotic neurons. SOX9 marks astrocytes in the adult opossum brain as well as multipotent neural stem cells, while also being crucial for the neuron-glia fate switch in the developing brain. By combining these markers, we can further dissect and follow the cell populations of interest, and their fluctuations through time. Cells expressing both SOX2 and NeuN can be considered immature/newborn postmitotic neurons that still have not fully lost their multipotent expression pattern and are in the process of maturation. It is important to note that this combination of markers has already been observed, although in much smaller percentages, in the spinal cord of E15.5 and E18.5 mice[46]. Although they should not be able

to further differentiate into cells other than neurons due to the presence of NeuN, the persistence of SOX2 in them is certainly significant. It opens the discussion about the potential role of SOX2 and other proliferative/stem cell markers in a newly differentiated cell, as there seem to be no clean cutoff between the two states, but rather a gradient where the proliferative markers (in this example SOX2) gradually diminishes, and is substituted by a growing amounts of differentiation markers (NeuN for neurons or SOX9 for astrocytes)[42]. How long SOX2 lingers in the newly differentiated cells is unclear, and could lead to interesting new conclusions, once researched. Their counterpart, the SOX2/NeuN double-negative cells could be oligodendrocytes (at later developmental stages) or astrocytes, microglia, or even fibroblasts or endothelial cells (remnants of meningeal blood vessels). Endothelial cells could be recognized by their typical elongated nuclear shape and were easily disregarded. We tested nuclear microglial marker PU1, without success (Appendix4).

Cells expressing only SOX2, but not NeuN, are therefore “true“ progenitor cells capable of differentiating into all neural cell lines, while cells expressing NeuN without SOX2 indicate more mature neurons. They become mature, or fully formed neurons after myelinization of their axons.

The coexpression of markers SOX2 and SOX9 marks the transition between progenitor cells and astrocytic lineage. As astrocytogenesis is believed to start around P18 in opossum, cells expressing both SOX2 and SOX9 are, prior to P18, considered to be radial glia-like neural stem/progenitor cells, due to the ability of SOX9 to suppresses the neural cell fate[12], and considering the morphology of GFAP-positive cells analysed by IHC on P8 and P12 opossum cortical tissue slices[12]. After P18, the population of SOX2+/SOX9+ double-positive cells contain both the young astrocytes and the neural stem/progenitor cells. The use of quadruple immunocytochemistry could give a more precise diversification of those cell lineages. However, its disadvantages have already been discussed in Chapter 5.5.

The cells negative to either SOX2, NeuN or SOX9 are expected to be oligodendrocytes (only in opossum older than P30), microglia, or even fibroblasts or remnants of meningeal blood vessels. However, more precise cell-specific markers are required to completely describe the population of the “non-neuronal“ cells.

5.5. Temporal characterization

To research the regenerative capabilities and the developmental stages of the postnatal opossum cortex, we have selected three timepoints as our research focus. These were selected in accordance with previous work done on the opossum spinal cord, with a substantial margin for error. The opossum spinal cord loses its regenerative capabilities rather abruptly, between P9 and P12, starting with the most mature part, the cervical region and continuing towards the lumbar region, which matures the slowest[20,26,29]. To capture the regenerative capabilities in the brain, P5-6 has been selected as the first timepoint of interest. While a full 24 hours in a rapidly developing opossum brain can make a rather big difference, the exact time of opossums' birth is seldom known. Due to this and other logistical reasons such as transport and availability, a timeframe, rather than a specific timepoint, has been chosen.

The same is true for the second timepoint, P16-18, which is well outside the regenerative time period of the opossum spinal cord, but the cortical structure is still developing. P30 has been chosen as the third timepoint in which the cortical structures have been fully established, as the majority of non-neuronal cells emerge between P18 and P35[17]. However, oligodendrocytogenesis has been reported to start after P40, according to Puzzolo and Mallamaci[12].

In conclusion, we managed to cover the postnatal period that comprises neurogenesis (almost completely, including all the three postnatal age groups considered), astrocytogenesis (from P18 and P30) and possibly the onset of oligodendrocytogenesis (P30).

It is important to note the only other reported source of the number of cells in the P18 opossum cortex is again by Seelke *et al*. They report 1, 637, 000 ± 58, 000 cells in the opossum cortex, out of which 60.55%, or 985, 000 are neurons, and 653, 000 are non-neurons (Figure 27). An unbiased, automated method of cell counting, such as artificial intelligence-based programs, possibly combined with flow cytometry would greatly benefit further such research and alleviate the conflicting results.

Age	% Neurons	# cells (in millions)	# neurons (in millions)	# non-neurons (in millions)
P18	60.55 ± 9.44	1.637 ± .058	.985 ± .139	.653 ± .163
P35	44.44 ± 9.21	1.580 ±.141	.743 ± .093	.836 ± .093

Figure 27: Number and percentage of neurons and non-neurons in P18 and P35 opossum cortex, as reported by Seelke et al.

Another useful way of interpreting the results of opossum temporal characterization is as a temporal dynamic of individual markers. This gives an overall view on marker maturation throughout the timepoints of interest, rather than the overall cortical tissue status at those same timepoints (Figures 28 and 29).

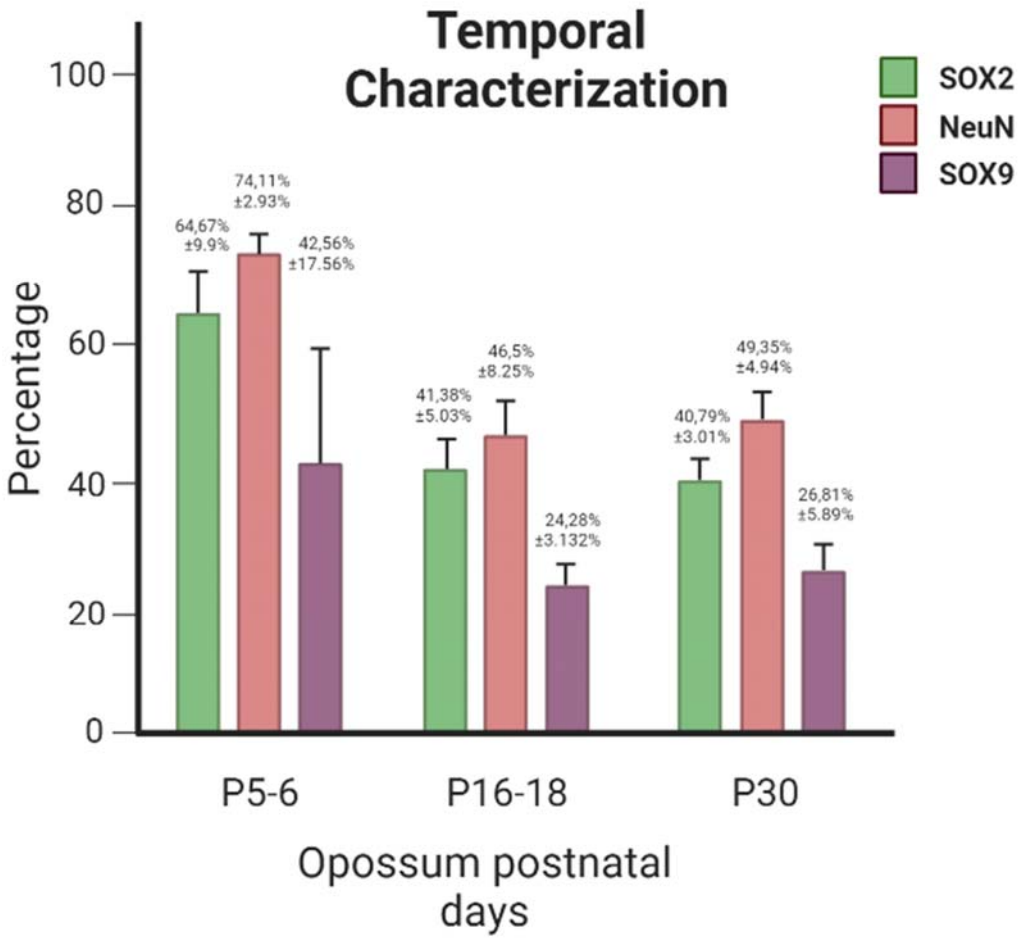

Figure 28: Temporal characterization of markers throughout the opossum cortex at postnatal days of interest. Y-axis: percentage of cells labelled with specific antibodies; X-axis: opossum postnatal days of interest with corresponding percentages and standard errors; SOX2: green; NeuN: red; SOX9: purple. Error bars and the number of experiments for each postnatal day and marker are explained in their respective tables (Tables 8, 11 and 14).

There is a clear trend with a decrease in all three markers from P5-6 towards P30 (exception being SOX9 in P5-6 due to its high standard error, addressed in Chapter 4.3.1.2). As the opossum matures and grows, the proliferative marker SOX2 diminishes in percentage. However, the differentiation markers SOX9 and NeuN also diminish in their percentage. This can be explained by the influx of other non-neuronal cells, but also by the diminishing double-positive cell percentages (Figure 29), which were the major pool of all three individual markers. Less cells accounting for more cell populations means lesser percentages of those respective markers in general.

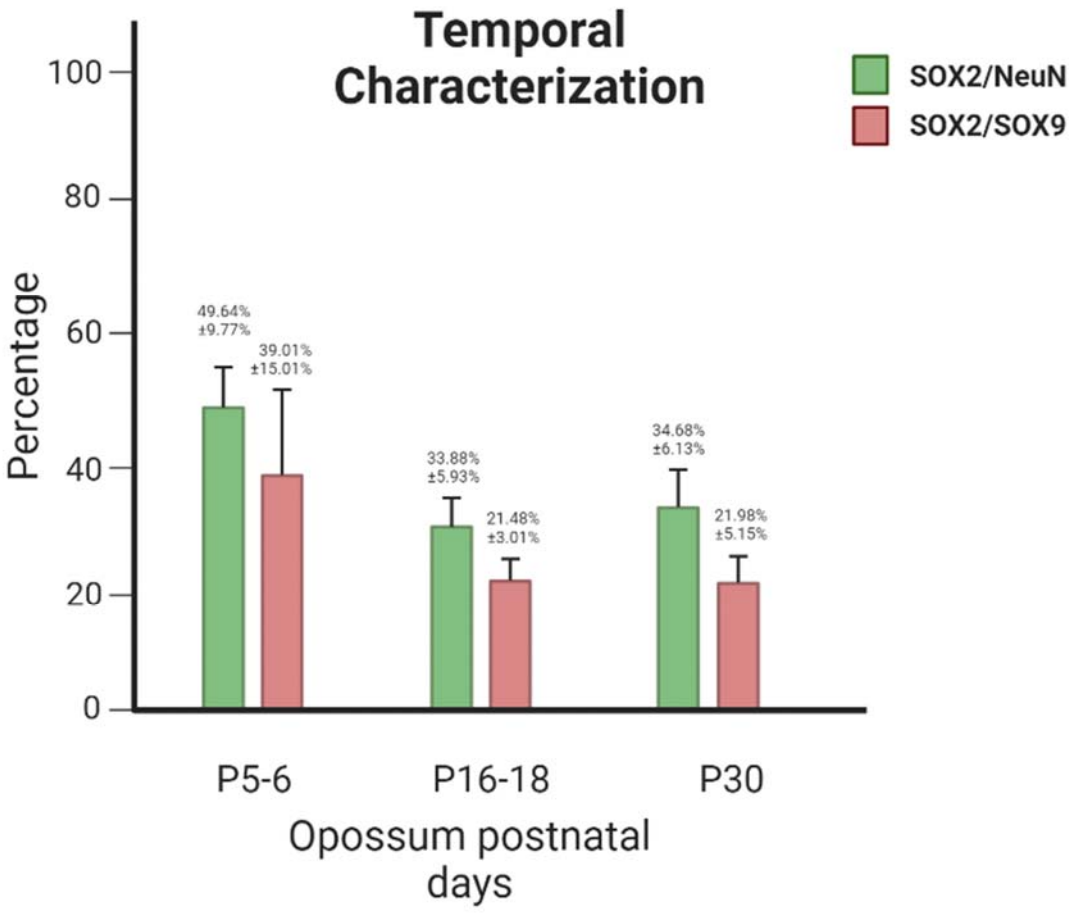

Figure 29: Temporal characterization of marker pairs throughout the opossum cortex at postnatal days of interest. Y-axis: percentage of cells labelled with specific antibody pairs; X-axis: opossum postnatal days of interest with corresponding percentages and standard errors; Green: SOX2/NeuN; Red: SOX2/SOX9.

Marker segregation into more narrow and defined cell populations is another strong indicator of cortical maturation. And while the difference in percentage of cell lines defined by the intersection of these marker pairs does lower throughout the development of the postnatal opossum cortex, their presence in the P30 opossum must also be noted. Both immature neurons and neural stem/progenitor cells as well as astrocytes, noted by the green bar and the red bar respectively, have a large presence in P30, which also indicates that the growth and development of opossum is far from over. Further evidence comes from the population

of “young” neurons and astrocytes in their respective cell pools, which changes only marginally throughout all three timepoints (Figure 30).

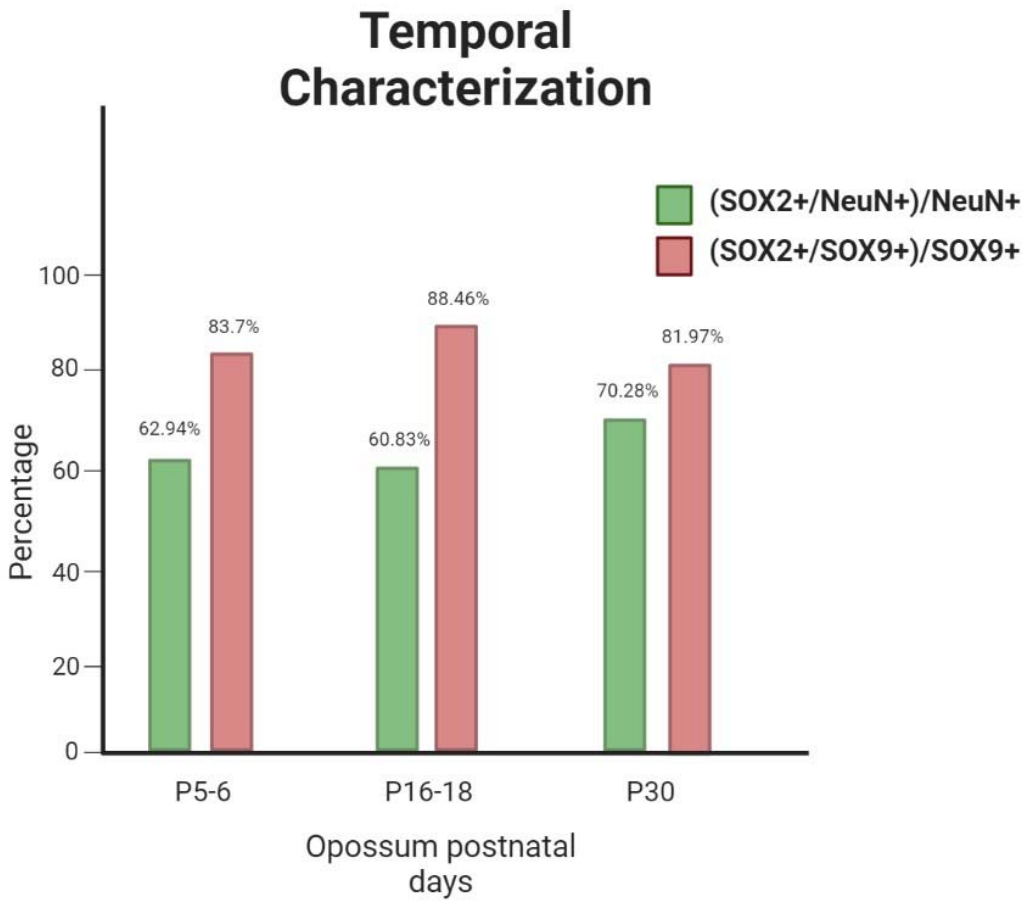

Figure 30: Temporal characterization of marker pairs throughout opossum cortex at postnatal days of interest. Y-axis: percentage of specific cell populations; X-axis: opossum postnatal days of interest with corresponding percentages and standard errors; Green: (SOX+2/NeuN+)/NeuN+, which corresponds with the population of young neurons in the overall neural population; Red: (SOX2+/SOX9+)/SOX9+, which corresponds with the population of young astrocytes, or the neural stem/progenitor cells in P5-6.

5.6. Opossum on the evolutionary scale

Our laboratory's previous and ongoing work has provided interesting evidence of CNS regeneration in opossum. Pioneering work[10,13,14,26] has well documented the cessation period of the regenerative potential following injury during the postnatal development of *M. domestica*. To do so*, in vivo* or *in vitro* injury on isolated spinal cord was performed. Our laboratory has expanded upon their work with an *in vitro* experimental platform for regenerative studies by establishing primary dissociated cortical[34,100] as well as spinal cord cultures (unpublished data). Moreover, proteomic analysis identified proteins and their distribution unique to intact opossum spinal tissue of different ages and regenerative capabilities[35]. It has identified a total of 4735 proteins involved in various cellular processes, from proliferation and differentiation to cell signalling and growth. Most notably, several proteins related to various neurodegenerative diseases have been discovered, that change in the opossum spinal cord during the period critical for neuroregeneration, among them amyloid proteins and presenilin related to Alzheimer's disease, Rab GTPases linked to Parkinson's disease, and huntingtin and huntingtin interacting protein 1 related to Huntington's disease.

The primary neuronal spinal cell cultures from neonatal opossum of different ages (P5 and P18 opossum spinal cord) confirmed their varying degree of regenerative capacity, and consequently the possibility to successfully establish their respective primary cell cultures, with limited regenerative potential in cultures prepared from opossum older than two weeks.

Spinal cord primary cell cultures are more challenging to obtain and to maintain, and less frequently used[86]. It was therefore not surprising that cortical cell cultures were easier to establish for both postnatal ages (P3-5 as well as P16-18), which already indicated a higher degree of cortical plasticity compared to the spinal cord tissue of the same age (in terms of cell survival and regeneration).

The most curious observation was the surprisingly high longevity and regenerative capacity of cortical cell cultures following injury after *in vitro* regeneration tests (so-called scratch test, or the wound healing assay). This was confirmed on cell cultures at DIV30 and older, which is

significant in terms of higher regenerative capacity than primary cell cultures obtained from rodents[100].

In conclusion, *in vitro* results confirm higher regenerative potential of cortex vs. spinal cord as well as opossum vs. rodents (of comparable age). The presence of SOX2+/NeuN+, as well as SOX2+/SOX9+ double-positive cells in opossum cortex of all observed ages further emphasises their higher degree of plasticity over spinal cord tissue, as well as over rodents.

As regenerative capabilities are often attributed to invertebrates and lower vertebrates, colloquially dubbed “more primitive”, the same could be said for the *M. domestica*. However, it is precisely due to their long period of postnatal regenerative capabilities that their metatherian ancestry should be considered “not as primitive as expected”[32].

Future studies using additional markers and their more insightful combinations (OLIG2, BLBP, and NeuN in conjunction with SOX9, for example) await new fundings and projects. Additionally, the IFR method, with its almost limitless application potential is to be explored as well. Together, and coupled with other tests and imaging methods they are ready to reveal the nature of the yet unexplored parts of human and animal development.

These relatively undemanding and “simple” techniques used in this work are nevertheless able to give insight into some of the fundamental questions in neurobiology, such as the development of the cortex and its substructures, and the neuroregenerative capacity of the CNS.

6. Conclusion

- We investigated physical characteristics of opossum, mainly their size and weight throughout their developing postnatal days. They develop quickly, growing in mass by a factor of 22 between P3 and P30, and in size by a factor of 4.
- We developed and optimized the IFR for opossum tissues (mainly cortices) of different postnatal ages and size and introduced modifications to the original protocol which allowed its use on an inverted microscope. Several parameters, such as volume, buffers, number and duration of washes, incubation times and others (including microscope configuration and upgrades) were tested for each of the ages of interest, before the optimal conditions were reached.
- We tested different experimental conditions and homogenization times due to different stiffness and prevalence of extracellular matrix in different postnatal ages, different fixation durations, centrifuge settings, antigen retrieval, washing steps, specificity of different antibodies, various concentrations of primary antibodies, their incubation period, and mounting procedures.
- We introduced relative number counting, where different cell lines (e.g., neurons, neural stem cells and astrocytes) were labelled with different antibodies.
- We compared the similarity of each immunogen used to produce primary antibodies with opossum protein sequence.
- We applied commercially available cell markers SOX2, NeuN and SOX9 to all three postnatal ages of interest and confirmed their expression patterns with available literature, primary dissociated cell cultures and cortical slices.
- To the best of our knowledge, while NeuN has been used on dozens of different animal species, humans included, SOX2 has never been used as a marker with the IFR method, while SOX9 has been used only on adult mouse brain.
- We measured the relative and absolute number of cells in P5-6, P16-18 and P30 opossum cortex. We also measured the combination of markers available to see how exclusive they were, and we also identified double-positive cell populations (SOX2+/NeuN+ as well as SOX2+/SOX9+).

- The relative cell count was obtained by performing the IFR immunostaining protocol with modifications to the original protocol which offered several advantages: reduced photobleaching; long-term (weeks or months) storage and imaging on both upright or inverted fluorescence microscopes (including widefield and confocal microscopy); increased signal to noise ratio and image quality (when using oil-immersion objectives with higher numerical aperture); finally, the use of additional markers, i.e. cell-specific antibodies increases the versatility of this method (counting of different cell types, not just neurons). None of this is possible with samples loaded on haemocytometer.
- We used an inverted microscope equipped with 20x dry objective with long working distance to count the total number of cells in a fraction and ultimately in the whole brain. In this way, we visualized fluorescently labelled cell nuclei with light passing from below through the semi-transparent chamber (haemocytometer). UV excitation for Hoechst 33342 allowed for correct focusing, counting as well as imaging.
- To verify the presence of SOX2+/NeuN+ as well as SOX2+/SOX9+ double-positive cell population, we performed IHC analysis on tissue slices obtained from P6, P17 and P30 opossum cortex and confirmed the existence of double-positive cells.
- We confirmed the overlap of SOX9 with SOX2 in progenitor cells, and that SOX9 can be used as a reliable marker for differentiated astrocytes in P16-18 and P30.
- We confirmed SOX2 as a marker for stem/progenitor cells in all ages considered, however, we also found its overlap in neurons where it gradually diminishes.
- The existence of differentiated neurons coexpressing SOX2in P5-6 opossum cortex was observed also on primary dissociated cortical cultures of P4 opossum cortex at days *in vitro* (DIV) 1.

7. Literature

1. Agirman, G., Broix, L. & Nguyen, L. Cerebral cortex development: an outside-in perspective. *FEBS Lett* **591**, 3978–3992 (2017).
2. De Juan Romero, C. & Borrell, V. Coevolution of radial glial cells and the cerebral cortex. *Glia* **63**, 1303–1319 (2015).
3. Geschwind, D. H. & Rakic, P. Cortical evolution: judge the brain by its cover. *Neuron* **80**, 633–647 (2013).
4. Kriegstein, A., Noctor, S. & Martínez-Cerdeño, V. Patterns of neural stem and progenitor cell division may underlie evolutionary cortical expansion. *Nat Rev Neurosci* **7**, 883–890 (2006).
5. Malatesta, P., Appolloni, I. & Calzolari, F. Radial glia and neural stem cells. *Cell Tissue Res.* **331**, 165–178 (2008).
6. Bandeira, F., Lent, R. & Herculano-Houzel, S. Changing numbers of neuronal and non-neuronal cells underlie postnatal brain growth in the rat. *Proc. Natl. Acad. Sci. U.S.A.* **106**, 14108–14113 (2009).
7. Cardoso-Moreira, M. *et al.* Gene expression across mammalian organ development. *Nature* **571**, 505–509 (2019).
8. Neuronal, neural stem cell and glial cell markers | Abcam. https://www.abcam.com/neuroscience/neural-markers-guide.
9. Samollow, P. B. The opossum genome: insights and opportunities from an alternative mammal. *Genome Res* **18**, 1199–1215 (2008).
10. Mikkelsen, T. S. *et al.* Genome of the marsupial Monodelphis domestica reveals innovation in non-coding sequences. *Nature* **447**, 167–177 (2007).
11. Abbot, P. & Capra, J. A. What is a placental mammal anyway? *eLife* **6**, e30994 (2017).
12. Puzzolo, E. & Mallamaci, A. Cortico-cerebral histogenesis in the opossum Monodelphis domestica: generation of a hexalaminar neocortex in the absence of a basal proliferative compartment. *Neural Dev* **5**, 8 (2010).

13. Nicholls, J. G., Stewart, R. R., Erulkar, S. D. & Saunders, N. R. Reflexes, fictive respiration and cell division in the brain and spinal cord of the newborn opossum, Monodelphis domestica, isolated and maintained in vitro. *Journal of Experimental Biology* **152**, 1–15 (1990).
14. Saunders, N. R., Adam, E., Reader, M. & Møllgård, K. Monodelphis domestica (grey short-tailed opossum): an accessible model for studies of early neocortical development. *Anat Embryol (Berl)* **180**, 227–236 (1989).
15. VandeBerg, J. L. & Robinson, E. S. The Laboratory Opossum (Monodelphis Domestica) in Laboratory Research. *ILAR J* **38**, 4–12 (1997).
16. Belle, E. M. S., Duret, L., Galtier, N. & Eyre-Walker, A. The decline of isochores in mammals: an assessment of the GC content variation along the mammalian phylogeny. *J Mol Evol* **58**, 653–660 (2004).
17. Seelke, A. M. H., Dooley, J. C. & Krubitzer, L. A. Differential changes in the cellular composition of the developing marsupial brain. *J. Comp. Neurol.* **521**, 2602–2620 (2013).
18. Bartkowska, K., Gajerska, M., Turlejski, K. & Djavadian, R. L. Expression of TrkC Receptors in the Developing Brain of the Monodelphis opossum and Its Effect on the Development of Cortical Cells. *PLOS ONE* **8**, e74346 (2013).
19. Cheung, A. F. P. *et al.* The Subventricular Zone Is the Developmental Milestone of a 6-Layered Neocortex: Comparisons in Metatherian and Eutherian Mammals. *Cerebral Cortex* **20**, 1071–1081 (2010).
20. Mladinic, M., Muller, K. J. & Nicholls, J. G. Central nervous system regeneration: from leech to opossum. *J. Physiol. (Lond.)* **587**, 2775–2782 (2009).
21. Tanaka, E. M. & Ferretti, P. Considering the evolution of regeneration in the central nervous system. *Nat Rev Neurosci* **10**, 713–723 (2009).
22. Varadarajan, S. G., Hunyara, J. L., Hamilton, N. R., Kolodkin, A. L. & Huberman, A. D. Central nervous system regeneration. *Cell* **185**, 77–94 (2022).

23. Ban, J. & Mladinic, M. Monodelphis domestica: a new source of mammalian primary neurons in vitro. *Neural Regen Res* **17**, 1726–1727 (2022).
24. Mladinic, M. *et al.* Differential expression of genes at stages when regeneration can and cannot occur after injury to immature mammalian spinal cord. *Cell. Mol. Neurobiol.* **25**, 407–426 (2005).
25. The Principles of Humane Experimental Technique. *Medical Journal of Australia* **1**, 500–500 (1960).
26. Varga, Z. M., Bandtlow, C. E., Erulkar, S. D., Schwab, M. E. & Nicholls, J. G. The critical period for repair of CNS of neonatal opossum (Monodelphis domestica) in culture: correlation with development of glial cells, myelin and growth-inhibitory molecules. *Eur J Neurosci* **7**, 2119–2129 (1995).
27. Kawaguchi, S., Iseda, T. & Nishio, T. Effects of an embryonic repair graft on recovery from spinal cord injury. *Prog Brain Res* **143**, 155–162 (2004).
28. Becker, C. G. & Diez Del Corral, R. Neural development and regeneration: it's all in your spinal cord. *Development* **142**, 811–816 (2015).
29. Nicholls, J. & Saunders, N. Regeneration of immature mammalian spinal cord after injury. *Trends Neurosci.* **19**, 229–234 (1996).
30. Kalil, K. & Reh, T. Regrowth of severed axons in the neonatal central nervous system: establishment of normal connections. *Science* **205**, 1158–1161 (1979).
31. Saunders, N. R. *et al.* Growth of axons through a lesion in the intact CNS of fetal rat maintained in long-term culture. *Proc Biol Sci* **250**, 171–180 (1992).
32. Dos Santos, S. E. *et al.* Cellular Scaling Rules for the Brains of Marsupials: Not as 'Primitive' as Expected. *Brain Behav Evol* **89**, 48–63 (2017).
33. Majka, P. *et al.* A three-dimensional stereotaxic atlas of the gray short-tailed opossum (Monodelphis domestica) brain. *Brain Struct Funct* **223**, 1779–1795 (2018).
34. Petrović, A. *et al.* Establishment of Long-Term Primary Cortical Neuronal Cultures From Neonatal Opossum Monodelphis domestica. *Front Cell Neurosci* **15**, 661492 (2021).

35. Tomljanović, I., Petrović, A., Ban, J. & Mladinic, M. Proteomic analysis of opossum Monodelphis domestica spinal cord reveals the changes of proteins related to neurodegenerative diseases during developmental period when neuroregeneration stops being possible. *Biochem Biophys Res Commun* **587**, 85–91 (2022).
36. Herculano-Houzel, S. Mammalian neurobiology: The elephant (brain) in the room. *Current Biology* **32**, R176–R178 (2022).
37. Bonfanti, L. & Peretto, P. Adult neurogenesis in mammals – a theme with many variations. *Eur J of Neuroscience* **34**, 930–950 (2011).
38. Bowles, J., Schepers, G. & Koopman, P. Phylogeny of the SOX family of developmental transcription factors based on sequence and structural indicators. *Dev Biol* **227**, 239–255 (2000).
39. Chew, L.-J. & Gallo, V. The Yin and Yang of Sox proteins: Activation and repression in development and disease. *J Neurosci Res* **87**, 3277–3287 (2009).
40. Graham, V., Khudyakov, J., Ellis, P. & Pevny, L. SOX2 Functions to Maintain Neural Progenitor Identity. *Neuron* **39**, 749–765 (2003).
41. Ellis, P. *et al.* SOX2, a Persistent Marker for Multipotential Neural Stem Cells Derived from Embryonic Stem Cells, the Embryo or the Adult. *Developmental Neuroscience* **26**, 148–165 (2005).
42. Sarkar, A. & Hochedlinger, K. The Sox Family of Transcription Factors: Versatile Regulators of Stem and Progenitor Cell Fate. *Cell Stem Cell* **12**, 15–30 (2013).
43. Takahashi, K. & Yamanaka, S. Induction of Pluripotent Stem Cells from Mouse Embryonic and Adult Fibroblast Cultures by Defined Factors. *Cell* **126**, 663–676 (2006).
44. Mercurio, S. *et al.* Sox2 Acts in Thalamic Neurons to Control the Development of Retina-Thalamus-Cortex Connectivity. *iScience* **15**, 257–273 (2019).
45. Cavallaro, M. *et al.* Impaired generation of mature neurons by neural stem cells from hypomorphic Sox2 mutants. *Development* **135**, 541–557 (2008).

46. Hoffmann, S. A. *et al.* Stem cell factor Sox2 and its close relative Sox3 have differentiation functions in oligodendrocytes. *Development* **141**, 39–50 (2014).

47. Zhang, S. *et al.* Sox2 Is Essential for Oligodendroglial Proliferation and Differentiation during Postnatal Brain Myelination and CNS Remyelination. *J Neurosci* **38**, 1802–1820 (2018).

48. Pevny, L. & Placzek, M. SOX genes and neural progenitor identity. *Curr Opin Neurobiol* **15**, 7–13 (2005).

49. Wegner, M. All purpose Sox: The many roles of Sox proteins in gene expression. *Int. J. Biochem. Cell Biol.* **42**, 381–390 (2010).

50. Harley, V. R., Lovell-Badge, R. & Goodfellow, P. N. Definition of a consensus DNA binding site for SRY. *Nucleic Acids Res* **22**, 1500–1501 (1994).

51. Peirano, R. I. & Wegner, M. The glial transcription factor Sox10 binds to DNA both as monomer and dimer with different functional consequences. *Nucleic Acids Res* **28**, 3047–3055 (2000).

52. Rau, M. J., Fischer, S. & Neumann, C. J. Zebrafish Trap230/Med12 is required as a coactivator for Sox9-dependent neural crest, cartilage and ear development. *Dev Biol* **296**, 83–93 (2006).

53. Akiyama, H., Chaboissier, M.-C., Martin, J. F., Schedl, A. & de Crombrugghe, B. The transcription factor Sox9 has essential roles in successive steps of the chondrocyte differentiation pathway and is required for expression of Sox5 and Sox6. *Genes Dev* **16**, 2813–2828 (2002).

54. Sun, W. *et al.* SOX9 Is an Astrocyte-Specific Nuclear Marker in the Adult Brain Outside the Neurogenic Regions. *J. Neurosci.* **37**, 4493–4507 (2017).

55. Mullen, R. J., Buck, C. R. & Smith, A. M. NeuN, a neuronal specific nuclear protein in vertebrates. *Development* **116**, 201–211 (1992).

56. Weyer, A. & Schilling, K. Developmental and cell type-specific expression of the neuronal marker NeuN in the murine cerebellum. *Journal of Neuroscience Research* **73**, 400–409 (2003).

57. Lind, D., Franken, S., Kappler, J., Jankowski, J. & Schilling, K. Characterization of the neuronal marker NeuN as a multiply phosphorylated antigen with discrete subcellular localization. *J Neurosci Res* **79**, 295–302 (2005).

58. Ebrahimi, M. *et al.* Astrocyte-expressed FABP7 regulates dendritic morphology and excitatory synaptic function of cortical neurons. *Glia* **64**, 48–62 (2016).

59. Anthony, T. E., Mason, H. A., Gridley, T., Fishell, G. & Heintz, N. Brain lipid-binding protein is a direct target of Notch signaling in radial glial cells. *Genes Dev* **19**, 1028–1033 (2005).

60. Arai, Y. *et al.* Role of Fabp7, a downstream gene of Pax6, in the maintenance of neuroepithelial cells during early embryonic development of the rat cortex. *J Neurosci* **25**, 9752–9761 (2005).

61. Owada, Y. Fatty acid binding protein: localization and functional significance in the brain. *Tohoku J Exp Med* **214**, 213–220 (2008).

62. Feng, L., Hatten, M. E. & Heintz, N. Brain lipid-binding protein (BLBP): a novel signaling system in the developing mammalian CNS. *Neuron* **12**, 895–908 (1994).

63. Namm, A., Arend, A. & Aunapuu, M. Pax proteins in embryogenesis and their role in nervous system development. *Papers on Anthropology* **22**, 133–142 (2013).

64. Burrill, J. D., Moran, L., Goulding, M. D. & Saueressig, H. PAX2 is expressed in multiple spinal cord interneurons, including a population of EN1+ interneurons that require PAX6 for their development. *Development* **124**, 4493–4503 (1997).

65. Batista, M. F. & Lewis, K. E. Pax2/8 act redundantly to specify glycinergic and GABAergic fates of multiple spinal interneurons. *Dev Biol* **323**, 88–97 (2008).

66. Larsson, M. Pax2 is persistently expressed by GABAergic neurons throughout the adult rat dorsal horn. *Neurosci Lett* **638**, 96–101 (2017).

67. Xu, P. X. *et al.* Regulation of Pax6 expression is conserved between mice and flies. *Development* **126**, 383–395 (1999).

68. Osumi, N., Shinohara, H., Numayama-Tsuruta, K. & Maekawa, M. Concise review: Pax6 transcription factor contributes to both embryonic and adult neurogenesis as a multifunctional regulator. *Stem Cells* **26**, 1663–1672 (2008).

69. Gómez-López, S. *et al.* Sox2 and Pax6 maintain the proliferative and developmental potential of gliogenic neural stem cells In vitro. *Glia* **59**, 1588–1599 (2011).

70. Bel-Vialar, S., Medevielle, F. & Pituello, F. The on/off of Pax6 controls the tempo of neuronal differentiation in the developing spinal cord. *Dev Biol* **305**, 659–673 (2007).

71. Panayiotou, E. *et al.* Pax6 is expressed in subsets of V0 and V2 interneurons in the ventral spinal cord in mice. *Gene Expr Patterns* **13**, 328–334 (2013).

72. Bradshaw, N. J. & Hayashi, M. A. F. NDE1 and NDEL1 from genes to (mal)functions: parallel but distinct roles impacting on neurodevelopmental disorders and psychiatric illness. *Cell. Mol. Life Sci.* **74**, 1191–1210 (2017).

73. Chansard, M., Hong, J.-H., Park, Y.-U., Park, S. K. & Nguyen, M. D. Ndel1, Nudel (Noodle): flexible in the cell? *Cytoskeleton (Hoboken)* **68**, 540–554 (2011).

74. Malatesta, P. *et al.* Neuronal or Glial Progeny: Regional Differences in Radial Glia Fate. *Neuron* **37**, 751–764 (2003).

75. Meijer, D. H. *et al.* Separated at birth? The functional and molecular divergence of OLIG1 and OLIG2. *Nat Rev Neurosci* **13**, 819–831 (2012).

76. Schlüter, C. *et al.* The cell proliferation-associated antigen of antibody Ki-67: a very large, ubiquitous nuclear protein with numerous repeated elements, representing a new kind of cell cycle-maintaining proteins. *J Cell Biol* **123**, 513–522 (1993).

77. Cuylen, S. *et al.* Ki-67 acts as a biological surfactant to disperse mitotic chromosomes. *Nature* **535**, 308–312 (2016).

78. Herculano-Houzel, S. The human brain in numbers: a linearly scaled-up primate brain. *Front Hum Neurosci* **3**, 31 (2009).

79. Azevedo, F. A. C. *et al.* Equal numbers of neuronal and nonneuronal cells make the human brain an isometrically scaled-up primate brain. *J. Comp. Neurol.* **513**, 532–541 (2009).

80. Herculano-Houzel, S. The remarkable, yet not extraordinary, human brain as a scaled-up primate brain and its associated cost. *PNAS* **109**, 10661–10668 (2012).

81. Bahney, J. & von Bartheld, C. S. Validation of the isotropic fractionator: comparison with unbiased stereology and DNA extraction for quantification of glial cells. *J. Neurosci. Methods* **222**, 165–174 (2014).

82. Herculano-Houzel, S. & Lent, R. Isotropic fractionator: a simple, rapid method for the quantification of total cell and neuron numbers in the brain. *J. Neurosci.* **25**, 2518–2521 (2005).

83. Herculano-Houzel, S. *et al.* The elephant brain in numbers. *Front. Neuroanat.* **8**, (2014).

84. Herculano-Houzel, S. & Kaas, J. H. Gorilla and Orangutan Brains Conform to the Primate Cellular Scaling Rules: Implications for Human Evolution. *Brain Behav Evol* **77**, 33–44 (2011).

85. Petrovic, A. *et al.* Loss of inhibitory synapses causes locomotor network dysfunction of the rat spinal cord during prolonged maintenance in vitro. *Brain Res* **1710**, 8–21 (2019).

86. Baričević, Z. *et al.* Label-Free Long-Term Methods for Live Cell Imaging of Neurons: New Opportunities. *Biosensors* **13**, 404 (2023).

87. Kaech, S. & Banker, G. Culturing hippocampal neurons. *Nat Protoc* **1**, 2406–2415 (2006).

88. Beaudoin, G. M. J. *et al.* Culturing pyramidal neurons from the early postnatal mouse hippocampus and cortex. *Nat Protoc* **7**, 1741–1754 (2012).

89. Seelke, A. M. H., Dooley, J. C. & Krubitzer, L. A. The Cellular Composition of the Marsupial Neocortex. *J Comp Neurol* **522**, 2286–2298 (2014).

90. Tepper, B. *et al.* Downregulation of TrkC Receptors Increases Dendritic Arborization of Purkinje Cells in the Developing Cerebellum of the Opossum, Monodelphis domestica. *Front. Neuroanat.* **14**, 56 (2020).

91. Bartkowska, K., Aniszewska, A., Turlejski, K. & Djavadian, R. L. Distribution and function of TrkB receptors in the developing brain of the opossum *Monodelphis domestica*: TrkB in the Developing Opossum Brain. *Devel Neurobio* **74**, 707–722 (2014).

92. Lee, K. E. *et al.* Positive feedback loop between *Sox2* and *Sox6* inhibits neuronal differentiation in the developing central nervous system. *Proc. Natl. Acad. Sci. U.S.A.* **111**, 2794–2799 (2014).

93. Zhang, S. Sox2, a key factor in the regulation of pluripotency and neural differentiation. *WJSC* **6**, 305 (2014).

94. Bylund, M., Andersson, E., Novitch, B. G. & Muhr, J. Vertebrate neurogenesis is counteracted by Sox1–3 activity. *Nat Neurosci* **6**, 1162–1168 (2003).

95. Baričević, Z. *et al. SOX2 and SOX9 Expression in Developing Postnatal Opossum (Monodelphis domestica) Cortex*. https://www.preprints.org/manuscript/202309.0840/v1 (2023) doi:10.20944/preprints202309.0840.v1.

96. Morest, D. K. & Silver, J. Precursors of neurons, neuroglia, and ependymal cells in the CNS: What are they? Where are they from? How do they get where they are going? *Glia* **43**, 6–18 (2003).

97. The Laboratory Mouse - 2nd Edition. https://shop.elsevier.com/books/the-laboratory-mouse/hedrich/978-0-12-382008-2.

98. Godfrey, R. K., Swartzlander, M. & Gronenberg, W. Allometric analysis of brain cell number in Hymenoptera suggests ant brains diverge from general trends. *Proc. R. Soc. B.* **288**, rspb.2021.0199, 20210199 (2021).

99. Bartkowska, K., Gajerska, M., Turlejski, K. & Djavadian, R. L. Expression of TrkC Receptors in the Developing Brain of the Monodelphis opossum and Its Effect on the Development of Cortical Cells. *PLoS ONE* **8**, e74346 (2013).

100. Petrović, A., Ban, J., Ivaničić, M., Tomljanović, I. & Mladinic, M. The Role of ATF3 in Neuronal Differentiation and Development of Neuronal Networks in Opossum Postnatal Cortical Cultures. *IJMS* **23**, 4964 (2022).

101. Yamaguchi, S., Hirano, K., Nagata, S. & Tada, T. Sox2 expression effects on direct reprogramming efficiency as determined by alternative somatic cell fate. *Stem Cell Research* **6**, 177–186 (2011).

102. Mercurio, S., Serra, L. & Nicolis, S. K. More than just Stem Cells: Functional Roles of the Transcription Factor Sox2 in Differentiated Glia and Neurons. *Int J Mol Sci* **20**, 4540 (2019).

103. Lyck, L., Krøigård, T. & Finsen, B. Unbiased cell quantification reveals a continued increase in the number of neocortical neurones during early post-natal development in mice. *Eur J Neurosci* **26**, 1749–1764 (2007).

104. Korbo, L. & Andersen, B. B. The distributions of Purkinje cell perikaryon and nuclear volume in human and rat cerebellum with the nucleator method. *Neuroscience* **69**, 151–158 (1995).

105. McKay, B. E. & Turner, R. W. Physiological and morphological development of the rat cerebellar Purkinje cell. *J Physiol* **567**, 829–850 (2005).

106. Scott, C. E. *et al.* SOX9 induces and maintains neural stem cells. *Nat Neurosci* **13**, 1181–1189 (2010).

107. Martini, S. *et al.* A Critical Role for Sox9 in Notch-Induced Astrogliogenesis and Stem Cell Maintenance. *Stem Cells* **31**, 741–751 (2013).

108. Kang, P. *et al.* Sox9 and NFIA Coordinate a Transcriptional Regulatory Cascade during the Initiation of Gliogenesis. *Neuron* **74**, 79–94 (2012).

109. Pongrac, M. In vitro regeneration of primary cell cultures of cortex from postnatal grey short-tailed opossum Monodelphis domestica. (University of Rijeka, 2021).

110. Namm, A., Arend, A. & Aunapuu, M. Expression of Pax2 protein during the formation of the central nervous system in human embryos. *Folia Morphol* **73**, 272–278 (2014).

8. List of Abbreviations

bHLH – Basic Helix-Loop-Helix

BLBP – Brain Lipid-binding Protein

BME – Basal Medium Eagle

CNS – Central Nervous System

CP – Cortical Plate

DIC – Differential Interference Contrast

DAPI - 4’,6-diamidin-2-fenilindol

DIV – Days In Vitro

DMEM – Dulbecco's Minimum Essential Medium

E – embryonic Day

FABP7 – Fatty Acid Binding Protein 7

FACS – Fluorescence-activated Cell Sorting

FBS – Foetal Bovine Serum

$H3^{+}$ - H3-immunoreactive Mitotic Cells

HBSS – Hank's Balanced Salt Solution

ICC – Immunocytochemistry

IFR – Isotropic Fractionator

Ig - Immunoglobulin

IHC – Immunohystochemistry

IP – Intermediate Progenitor Cell

IZ – Intermediate Zone

MAP2 – Microtubule-associated protein 2

MZ – Marginal Zone

NEC – Neuroepithelial Cell

Ngn – Neurogenin

NGS – Normal Goat Serum

NSC – Neuronal Stem Cell

NudEL, Ndel1 – Nuclear Distribution Element-like 1

P – Postnatal day

PAX2 – Paired Box Protein 2

PAX6 – Paired Box Protein 6

PDGFRα – Platelet-derived Growth Factor Receptor α

PFA - Paraformaldehyde

PP - Preplate

PBS – Phosphate Buffer Solution

RGC – Radial Glia Cell

RT – Room Temperature

SD – Standard Deviation

SOX – SRY-related HMG-box gene

SP – Subplate

SRY – Sex-determining Region Y Protein

SVZ – Subventricular Zone

VZ – Ventricular Zone

WM – White Matter

9. List of Figures

10. List of Tables

11. Appendices

Appendix 1: Fixation period for SOX9 antibody

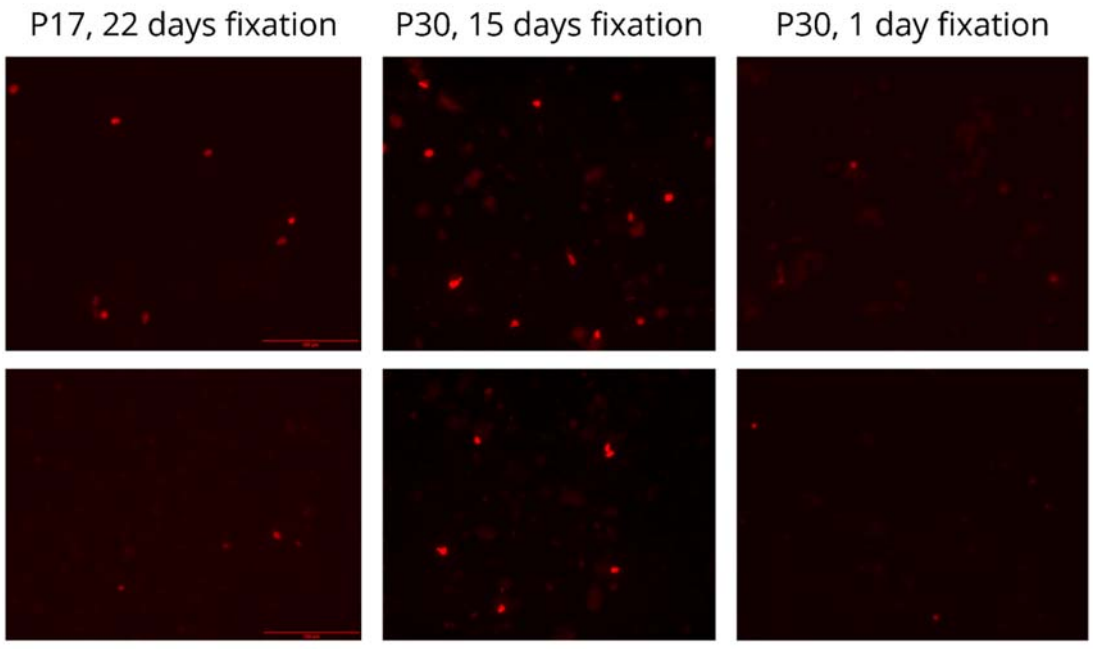

Figure 1 of Appendix 1: State of the SOX9 antibody after different fixation periods. Column 1 represents two experiments made on opossum P17 cortex, both after 22 days of fixation. Column 2 represents two experiments made on opossum P30 cortex, both after 15 days of fixation. Column 3 represents two experiments made on opossum P30 cortex, both after less than 1 day after fixation. Scale bar: 100 µm.

Appendix 2: Microscope configuration analysis

To verify if the appropriate light source, filters and other optical components of the Olympus IX73 and IX83 fluorescence microscopes were used, Fluorescence SpectraViewer (available at https://www.thermofisher.com/order/fluorescence-spectraviewer#!/) was used.

The following parameters were considered and provided to obtain graphs for each Fluorophore and corresponding filter cube:

Fluorophore: **Hoechst 33342**

Light source: Xenon lamp

Excitation filter (wavelength/bandwidth): 365/10

Emission filter (wavelength/bandwidth): 440/40

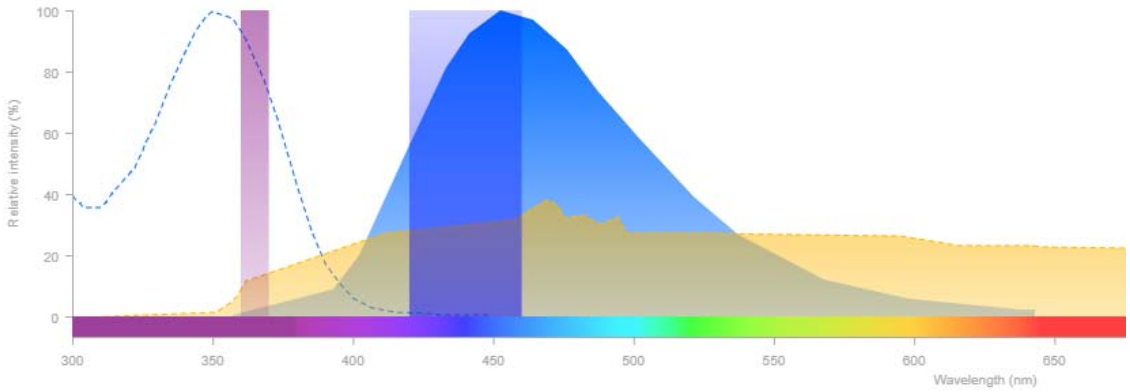

Fluorophore: **Alexa Fluor 488**

Light source: Xenon lamp

Excitation filter: 365/10

Emission filter: 560/100

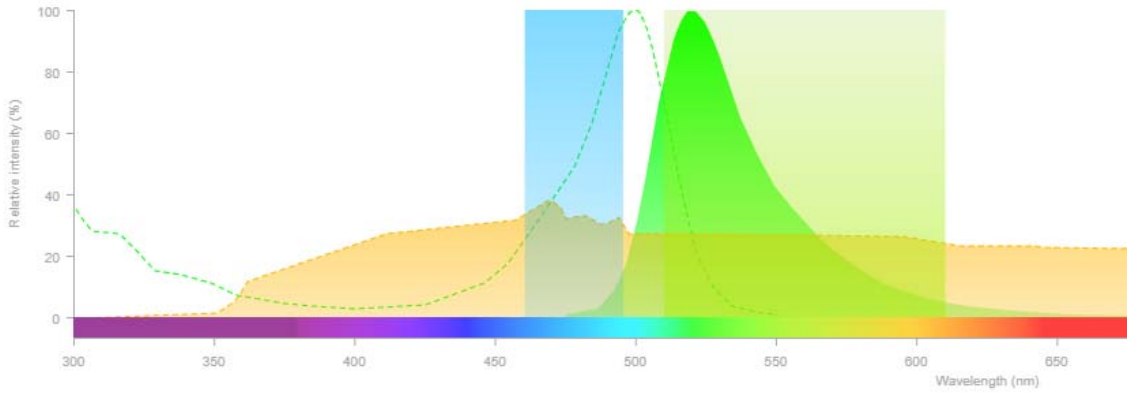

Fluorophore: **Alexa Fluor 555**

Light source: Xenon lamp

Excitation filter: 540/20

Emission filter: 625/100

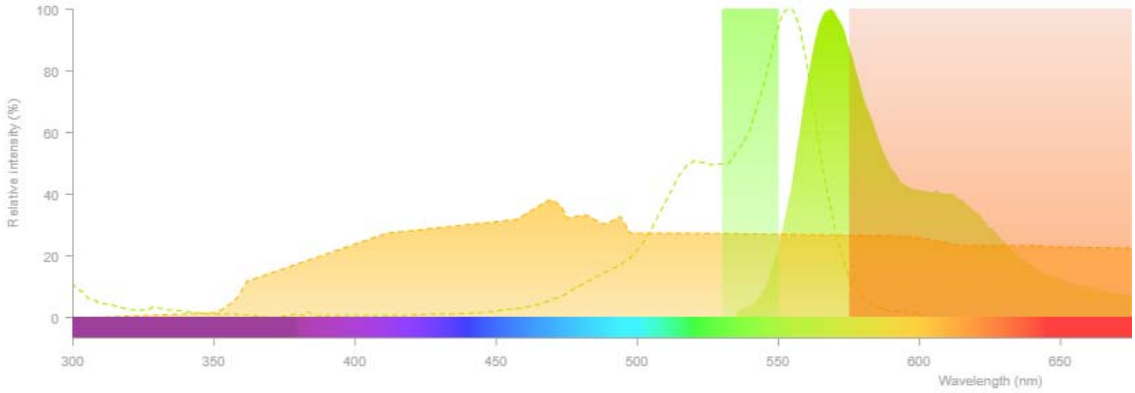

Appendix 3: Omitted primary antibody test

To verify the specificity of secondary antibodies and eliminate the possibility of their unspecific binding, a test with omitted primary antibodies was performed. No unspecific bindings were observed under any of the mirror units.

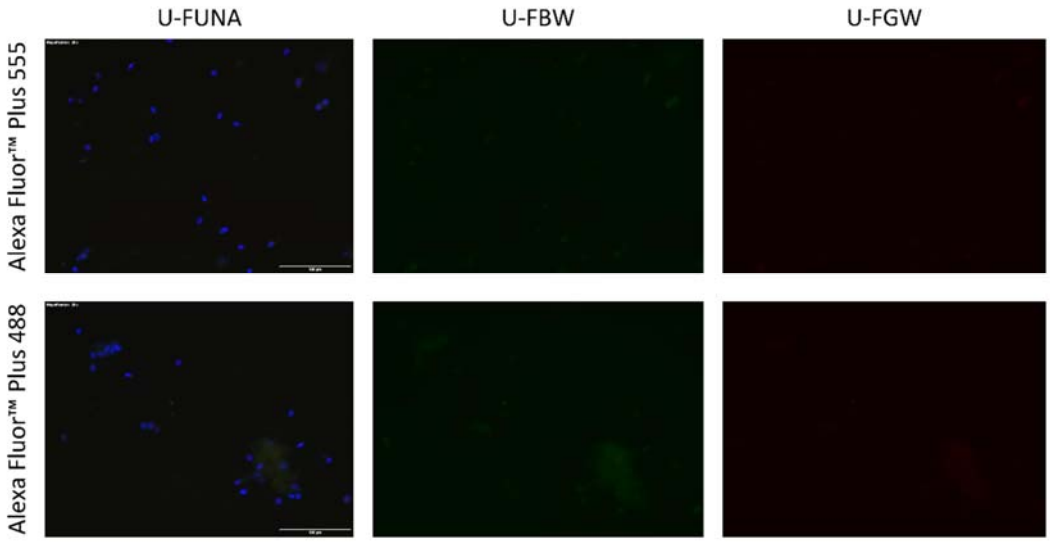

Figure 1 of Appendix 3: Test with omitted primary antibodies. The cell nuclei from P30 opossum, acquired with the same protocol as other experiments were stained with Hoechst 33342 and either Alexa Fluor™ Plus 555 (row 1) or Alexa Fluor™ Plus 555 (row 2) was added, without any primary antibody. They were visualized under different mirror units: U-FUNA (column 1), U-FBW (column 2) and U-FGW (column 3). Scale bar: 100 µm.

Appendix 4: Validation of other primary antibodies

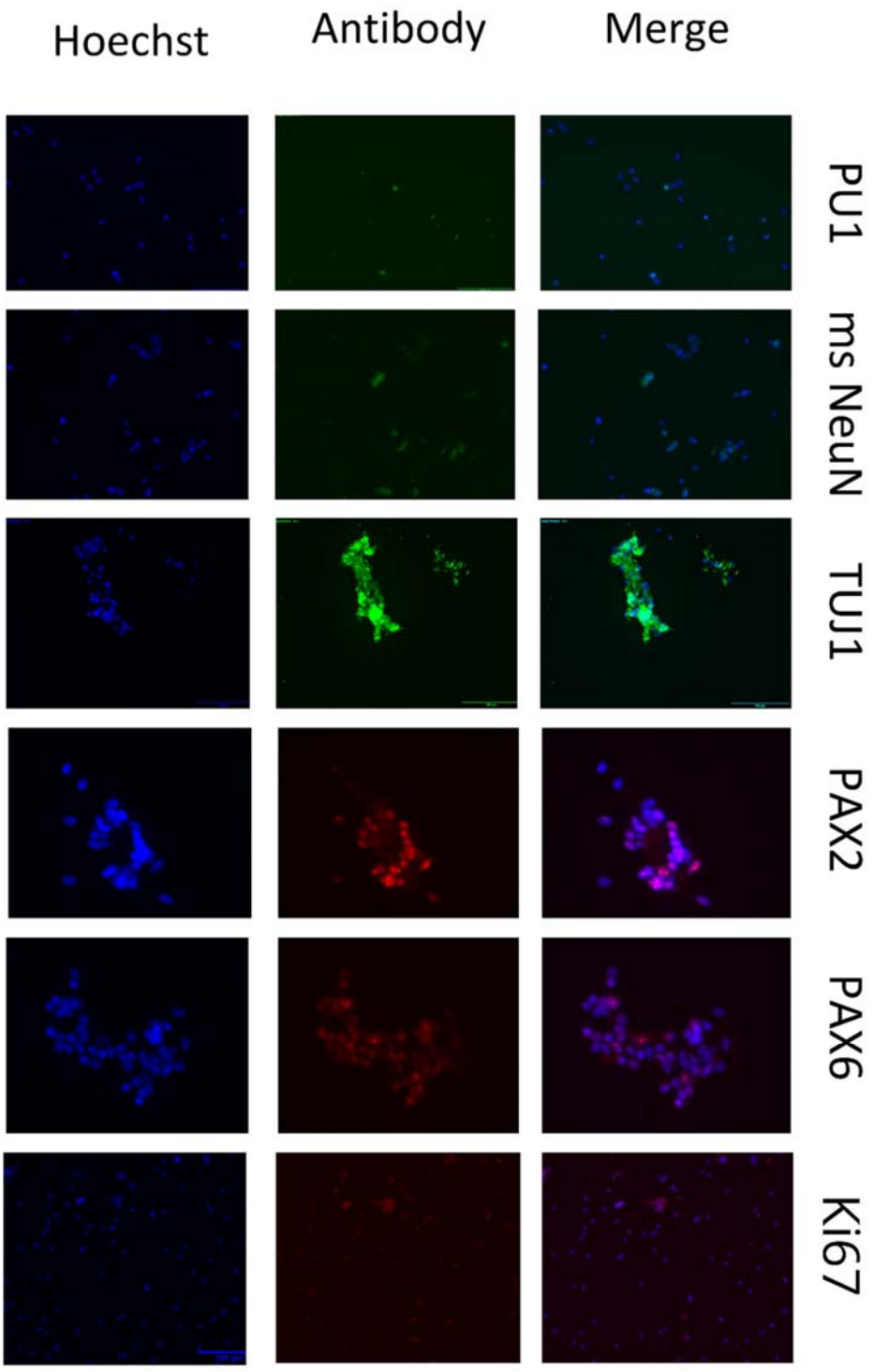

Figure 1 of Appendix 4: Primary antibody validation. Column 1 indicates cells stained with Hoechst 33342, labelling all cell nuclei. Column 2 indicates specific antibody staining of the same cell nuclei, from top to bottom: PU1, ms NeuN, TUJ1, PAX2, PAX6 and Ki67, as indicated in each of their respective rows. Column 3 shows the result of a merged pairs of columns 1 and 2 – the overlap of Hoechst 33342 staining and respective antibodies.

Appendix 5: Immunohistochemical validation of primary antibodies

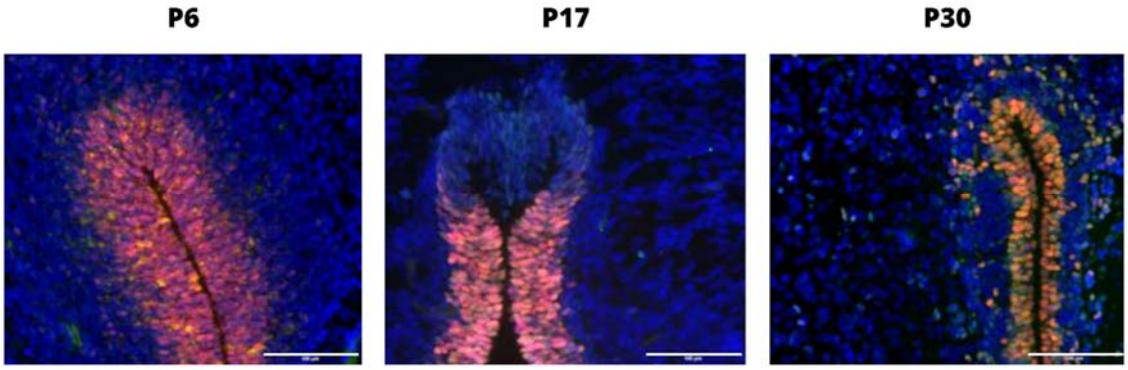

Figure 1 of Appendix 5: Immunohistochemical validation of primary antibodies on opossum tissue. P6, P17 and P30 opossum cortex tissues were stained with a combination of anti-SOX2 (green) and anti-SOX9 (red) antibodies, together with Hoechst 33342 (blue). Scale bar, 100 µm.

12. Biography

ZRINKO BARIČEVIĆ

Home : Tovarnele 18, 53294, Lun, Croatia
Email: zrinko.baricevic@uniri.hr **Phone:** (+385) 0915982451
Gender: Male **Date of birth:** 09/06/1990 **Nationality:** Croatian

WORK EXPERIENCE

[04/04/2019 – 02/09/2023]

PhD laboratory assistant

Odjel za biotehnologiju

City: Rijeka
-Work with laboratory animals
-Designed and held courses and laboratory exercises for undergraduate and graduate students
-Science popularization (Otvoreni dan, Tjedan mozga)

[01/11/2015 – 15/06/2016]

Medical Service Associate

PrimeVigilance

City: Zagreb
- Literature search of drug adverse events on Italian and English pharmacovigilance agencies (AIFA and MHRA)
-Adverse event registration and database filing
-Weekly, monthly and yearly reports for the European Medical Agency (EMA)

[01/04/2015 – 01/11/2015]

Pharmacovigilance Associate

PrimeVigilance

City: Zagreb
-Data entry from post-marketing reports and ICSRs from clinical trials
-Literature search of drug adverse events on Italian and English pharmacovigilance agencies (AIFA and MHRA)
-Adverse event registration and database filing
-Weekly, monthly and yearly reports for the European Medical Agency (EMA)

[01/02/2014 – 30/06/2014]

Solgar product Advisor

Salvus d.o.o.

City: Rijeka
Solgar product advisor for Primorsko-goranska županija
-Diet advisor for nutrition supplements

EDUCATION AND TRAINING

[14/07/2017 – Current]

PhD student

Sveučilište u Rijeci, Odjel za biotehnologiju

City: Rijeka

[01/09/2012 – 01/09/2014] **Master of Biotechnology and Drug Research**

Sveučilište u Rijeci, Odjel za biotehnologiju

City: Rijeka

[01/09/2009 – 01/09/2012] **Baccalaureus of Biotechnology and Drug Research**

Sveučilište u Rijeci, Odjel za biotehnologiju

City: Rijeka

LANGUAGE SKILLS

Mother tongue(s): Hrvatski

Other language(s):

Engleski

LISTENING C2 **READING** C2 **WRITING** C2

SPOKEN PRODUCTION C2 **SPOKEN INTERACTION** C2

German

LISTENING C1 **READING** B2 **WRITING** B2

SPOKEN PRODUCTION C1 **SPOKEN INTERACTION** C1

Italian

LISTENING C1 **READING** C1 **WRITING** B2

SPOKEN PRODUCTION C1 **SPOKEN INTERACTION** C1

Levels: A1 and A2: Basic user; B1 and B2: Independent user; C1 and C2: Proficient user

DIGITAL SKILLS

MS Office (Word Excel PowerPoint) | Figma (Software) | Open Broadcaster Software (OBS) | Photo, video and audio editing skills in Adobe Premiere Pro and Da Vinci | Graphic design online tools (Canva, Inkspace)

HONOURS AND AWARDS

[15/05/2023] **Rector's Award for Excellence in Teaching**

[30/08/2009] **City of Novalja's stipend for academic year 2009/2010**

[30/08/2010] **City of Novalja's stipend for academic year 2010/2011**

[30/08/2011] **City of Novalja's stipend for academic year 2011/2012**

[30/08/2012] **City of Novalja's stipend for academic year 2012/2013**

[30/08/2013] **City of Novalja's stipend for academic year 2013/2014**

[30/08/2014] **City of Novalja's stipend for academic year 2014/2015**

[30/08/2018] **City of Novalja's stipend for academic year 2018/2019**

NETWORKS AND MEMBERSHIPS

[01/09/2019 – Current] **Committee for extracurricular activities** Odjel za biotehnologiju

Extracurricular activities committee member for undergraduate and graduate students at the Department of Biotechnology

[15/07/2019 – Current] **Appealed Disciplinary Committee member** Odjel za biotehnologiju

[10/04/2019 – Current] **President of the Alumni club at the Department of Biotechnology** Odjel za biotehnologiju

[17/07/2020 – Current] **Alumni network member of the University of Rijeka** Sveučilište u Rijeci

[01/06/2018 – 01/04/2023] **Doctoral studies representative at the Department of Biotechnology** Odjel za biotehnologiju

[01/04/2022 – 01/04/2023] **Assistant representative at the Department of Biotechnology** Odjel za biotehnologiju

[01/10/2021 – 30/09/2023] **Member of the Student council at the University of Rijeka** Sveučilište u Rijeci

[01/09/2018 – 01/04/2023] **Department of Biotechnology Council member**

COMMUNICATION AND INTERPERSONAL SKILLS

Brain Awareness Week

I introduced Brain Awareness Week at the Department of Biotechnology, and have been the main organizer for the ones held 16. – 22. 3. 2020, 15. – 21. 3. 2021, 14. – 20. 3. 2022 and 13. – 19. 3. 2023. The manifestation collaborated with MOHO Center from Volosko in 2022, and was held in collaboration with the Medical Faculty in 2023. Every manifestation featured one of my presentations aimed at science popularization for broad public.

Department of Biotechnology Open days

I co-organized Department of Biotechnology's Open Days held under the University of Rijeka's Science Festival on 17. 4. 2019., 13. 10. 2020., 11. 5. 2021., and 3. 5. 2022.

UNIRI Career Days

I co-organized the first UNIRI Career Days, a week-long manifestation for all students from the University of Rijeka, held from 17.-23. 10. 2022.

MANAGEMENT AND LEADERSHIP SKILLS

Master and bachelor thesis mentosrhip

I was a mentor for following Masters theses:
Identification of cortex cells during postnatal development of M. Domestica (P. Š.)
Quantification of expression of markers of the central nervous system of postantal opossums (Monodelphis domestica) (C. M.)
Validation of immunohistochemical markers on Monodelphis domestica cortical tissue cells (H. K.)

I was also a mentor for a bachelor's thesis titled "The roles of epigenetic modifications in embryonic and adult neurogenesis" by K. V.

CONFERENCES AND SEMINARS

[18/05/2021] **3D Cell Culture and Organoids** Berlin, Germany

[04/06/2020] **BIOVIT Kamp; MERCK 3D kulture stanica**

[09/07/2019 – 11/07/2019] **Laboratory animal training**

PUBLICATIONS

[2023]

Label-Free Long-Term Methods for Live Cell Imaging of Neurons: New Opportunities. Baričević, Ayar, Leita, Ban, Fantner, Mladinic. Biosensors 2023, 13, 404.

[2023]

SOX2 and SOX9 Expression in Developing Postnatal Opossum (Monodelphis domestica) Cortex. Baričević, Pongrac, Ivaničić, Hreščak, Tomljanović, Petrović, Cojoc, Mladinic, Ban. Preprints 2023, 2023090840.